AN INVESTIGATION OF THE STRENGTH OF AN AIRCRAFT WING BOLT WITH A CENTRALLY DRILLED HOLE

DANIEL FRANCIS

2000

Submitted in fulfilment of the academic requirements for the degree of Master of Science in the Department of Mechanical Engineering, University of Natal

Abstract

The investigation contained herein is a part of a larger, long-term project: The Development of SMART Aircraft Bolts. Structural failures, at highly stressed components, are common in some of the aircraft used by the South African Air Force. The strength of one such component, the wing bolts on the C-130 aircraft, is analysed and compared to the stress distribution in a bolt which has a small hole drilled through the centre of the bolt (which will be used to insert a sensing device). The results of this analysis will be used as input into further phases of the project, e.g., SMART material selection and the development of sensing devices.

Due to the complex physics of a bolted joint, advanced analysis of the bolt under conservative loading was performed, after conducting thorough research into bolted joint design and analysis methods, in order to provoke the final recommendations.

Acknowledgements

I would like to take this opportunity to thank Professor V. E. Verijenko of the University of Natal, Mechanical Engineering Department, for his support and guidance throughout this project. My sincere thanks is also expressed to Col. Neil Napier of the South African Air Force for arranging visits to the Air Base and for facilitating information transfer.

Dedication

I wish to dedicate this thesis to my parents. I am truly grateful for their sacrificial investment in my education and commitment to my success in life as a whole.

Table of Contents

I. List of Tables and Figures

1. Introduction

This investigation is only a small part of a larger, long-term project: The Development of SMART Aircraft Bolts. A history of structural failure of some of the aircraft used by the South African Air Force (SAAF), such as the C-130 carrier, has been reported. Therefore, development of new and innovative methods of inspecting and tracking the structural integrity of highly-stressed components is required.

The wing bolts which attach the outer wing to the inner wing of the C-130 aircraft were identified as critical components. The larger project consists of research and development of SMART bolts which will be used as sensor elements within the structure to provide local compliance information about critical, highly stressed structural locations and will operate passively to provide peak strain information when interrogated. The interrogation of the bolts requires access to highly-stressed regions of the bolt. As most bolt failures indicate cracking at the first engaged thread, the ideal access would require a small hole drilled through the centre of the bolt through which a sensing device could be inserted.

The main objective of this investigation is to compare the stress distribution in the existing bolt geometry to bolts with different sized holes drilled through the centre. The relative changes in peak stresses are also be determined. The results would be used in further phases of the project to assist with material selection and the development of sensing devices.

The investigation consists of a study of the finite element method, bolt design issues, an overview of transformation-induced plasticity (TRIP) materials (the proposed material for the SMART bolt), finite element analysis of the bolt and recommendations.

This investigation would be used as input to further stages in the project: e.g., material selection, sensing technique, etc. Thus, at the time of this investigation, many assumptions had to be made, and the analysis does not address acceptable strength as the properties of the final material which will be used is not known.

2. Theory of the Finite Element Method

2.1 Historical Background

Advances in aircraft structural analysis resulted in the basic ideas of the Finite Element Analysis. Some of the highlights in the development of the method are listed below:

- *1941:* Hrenikoff offered a solution to elasticity problems using the "framework method".
- *1943:* Courant's paper, which used piecewise polynomial interpolation over triangular sub-regions to model torsion problems, appeared.
- *1955:* A book by Argyris on energy theorems and matrix methods laid a foundation for further developments in finite element studies.
- *1956:* Turner et al. Derived stiffness matrices for truss, beam and other elements.
- *1960:* Clough first used the term FINITE ELEMENT. In the early 1960s, engineers used the method for approximate solution of problems in stress analysis, fluid flow, heat transfer, and other areas.
- *1967:* Zienkiewicz and Chung published the first book on finite elements. In the late 1960s and early 1970s, finite element analysis was applied to non-linear problems and large deformations.
- *1972:* Oden's book on non-linear continua appeared. In the 1970s, the mathematical foundations were laid, including new element development, convergence studies and other related areas.

Today, the Finite Element Method has become one of the most important engineering tools for scientists and engineers alike and is used in a variety of applications,

including static, dynamic and non-linear stress analysis, fluid flow, heat transfer and various other fields, which extend beyond mechanical and civil engineering.

2.2 Mathematics of the Finite Element Method

2.2.1 Stresses and Equilibrium

A three-dimensional body with volume V and surface S is shown in Figure 2.1. Each point in the body is located by x, y, z co-ordinates. Displacement is specified on some region, defining the boundary. A distributed force **T** is applied on part of the boundary.

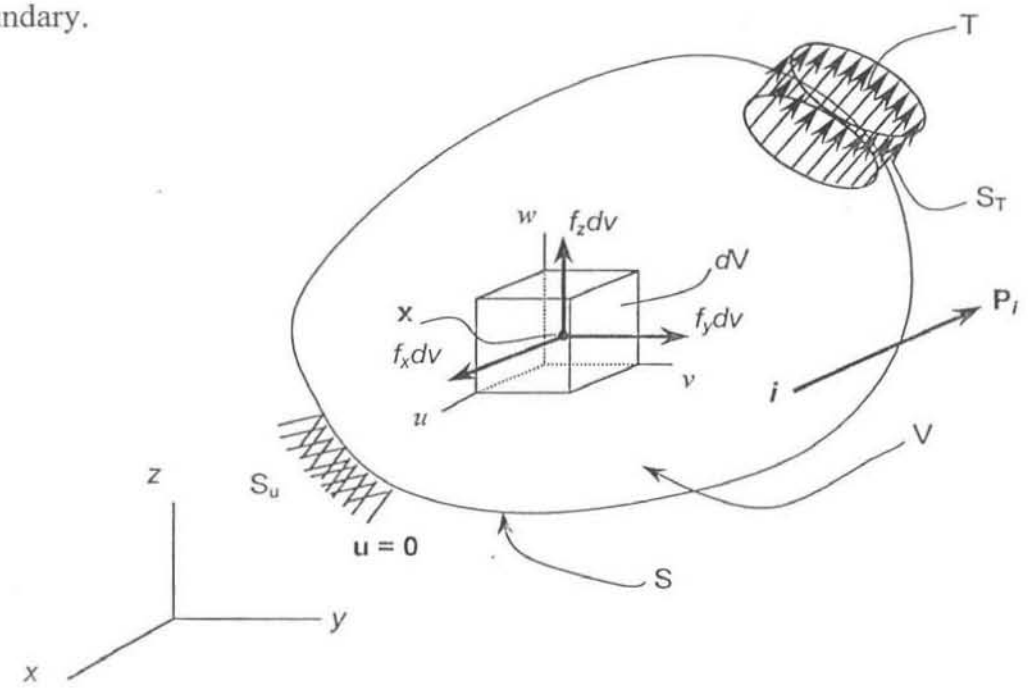

Figure 2.1 – *Three-dimensional body*

The deformation of a point $\mathbf{x} = [x, y, z]^T$ due to the force is given by the three components of its displacement:

$$\mathbf{u} = [u, v, w]^T \tag{2.1}$$

The distributed force per unit volume (e.g. the weight of the volume) is given by the vector **f**:

$$\mathbf{f} = [f_x, f_y, f_z]^T \tag{2.2}$$

The distributed surface force may be given by its components as:

$$\mathbf{T} = [T_x, T_y, T_z]^T \tag{2.3}$$

In addition, a point load **P** acts at a point *i* and is represented by its components as:

$$\mathbf{P}_i = [P_x, P_y, P_z]^T \tag{2.4}$$

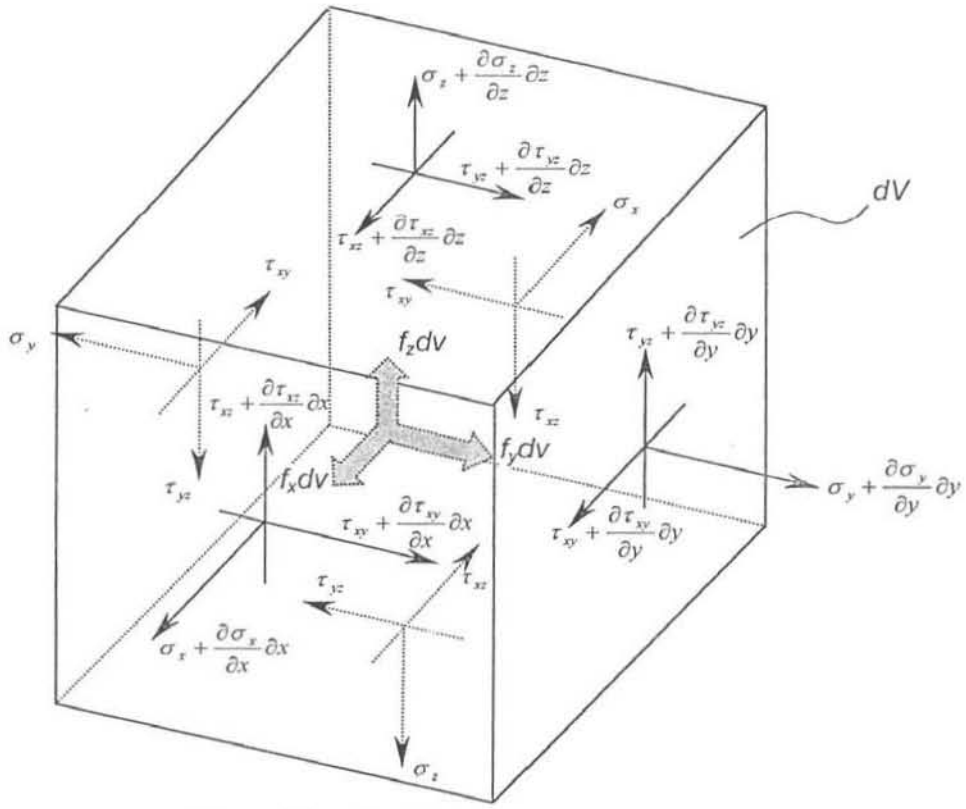

Figure 2.2 – ***Equilibrium of Elemental Volume***

Figure 2.2 shows the stresses acting in the elemental volume *dV*. When the volume *dV* shrinks to a point, the stress tensor is represented by placing its components in a 3x3 symmetric matrix. The stress is represented by the six independent components as follows:

$$\sigma = [\sigma_x, \sigma_y, \sigma_z, \tau_{yz}, \tau_{xz}, \tau_{xy},]^T \tag{2.5}$$

where σ_x, σ_y, σ_z are normal stresses and τ_{yz}, τ_{xz}, τ_{xy} are shear stresses. Considering the equilibrium of the elemental volume, the forces on the faces are obtained first by multiplying the stresses by the corresponding areas. Then, setting $\sum F_x = 0$, $\sum F_y = 0$ and $\sum F_z = 0$, and recognising that $dV = dx\ dy\ dz$, the following equilibrium equations can be written:

$$\frac{\partial \sigma_x}{\partial x}+\frac{\partial \tau_{xy}}{\partial y}+\frac{\partial \tau_{xz}}{\partial z}+f_x=0$$

$$\frac{\partial \tau_{xy}}{\partial x}+\frac{\partial \sigma_y}{\partial y}+\frac{\partial \tau_{xz}}{\partial z}+f_y=0 \qquad (2.6)$$

$$\frac{\partial \tau_{xz}}{\partial x}+\frac{\partial \tau_{yz}}{\partial y}+\frac{\partial \sigma_z}{\partial z}+f_z=0$$

2.2.2 Boundary Conditions

Figure 2.1 shows displacement boundary and surface loading conditions. If **u** is specified on part of the boundary, denoted by S_u, then

$$\mathbf{u} = 0 \text{ on } S_u.$$

The boundary conditions such as **u** = **a**, where **a** is a specified displacement can also be considered.

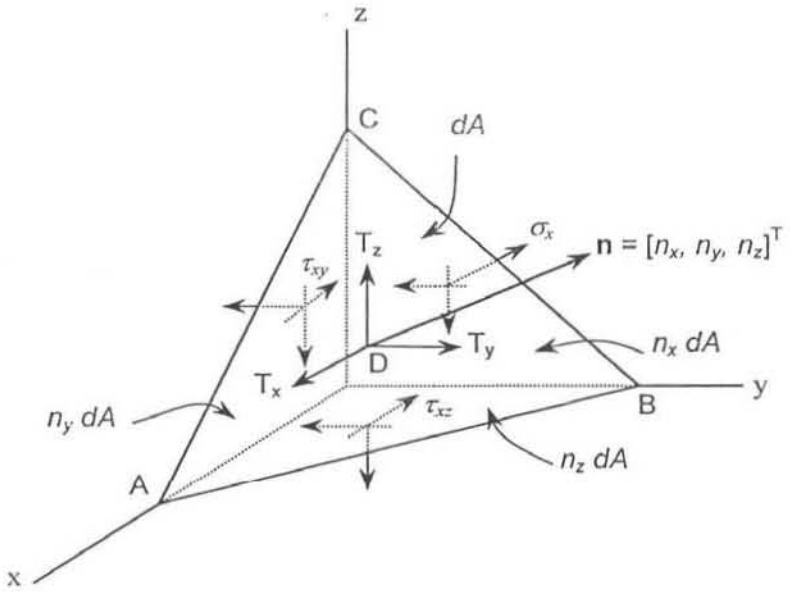

Figure 2.3 – *An Elemental Volume at the Surface*

Now consider the equilibrium of an elemental tetrahedron *ABCD*, shown in Figure 2.3, where *DA*, *DB*, and *DC* are parallel to the *x*, *y*, and *z* axes, respectively, and area *ABC*, denoted by *dA*, lies on the surface. If $\mathbf{n} = [n_x, n_y, n_z]^T$ is the unit normal to *dA*,

then area $BDC = n_x dA$, area $ADC = n_y dA$, and area $ADB = n_z dA$. Equilibrium along the three axes gives:

$$\begin{aligned} \sigma_x n_x + \tau_{xy} n_y + \tau_{xz} n_z &= T_x \\ \tau_{xy} n_x + \sigma_y n_y + \tau_{xz} n_z &= T_y \\ \tau_{xz} n_x + \tau_{yz} n_y + \sigma_z n_z &= T_z \end{aligned} \tag{2.8}$$

These conditions must be satisfied on the boundary, S_T, where the tractions are applied. In this description, the point loads must be treated as loads distributed over small, but finite areas.

2.2.3 Strain-Displacement Relations

Strain can be represented by the following vector:

$$\varepsilon = [\varepsilon_x, \varepsilon_y, \varepsilon_z, \gamma_{yz}, \gamma_{xz}, \gamma_{xy}]^T \tag{2.9}$$

where ε_x, ε_y, and ε_z are normal strains and γ_{yz}, γ_{xz}, and γ_{xy} are the shear strains.

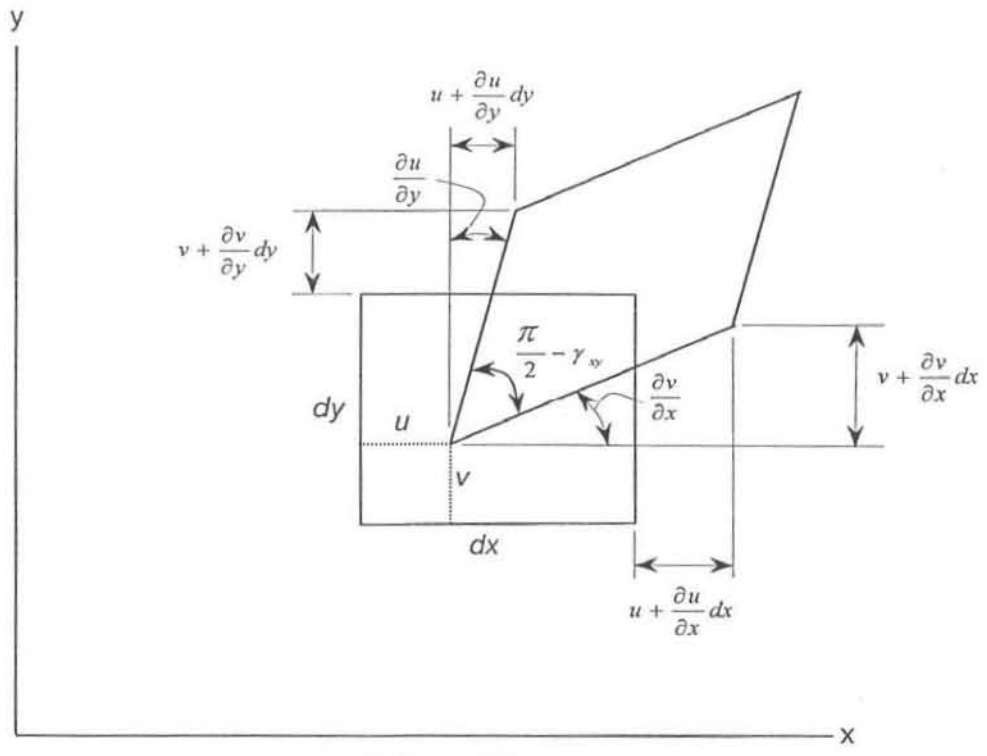

Figure 2.4 – *Deformed Elemental Surface*

Figure 2.4 shows the deformation of the *dx-dy* face for small deformations. Also considering other faces, the following can be written:

$$\varepsilon = \left[\frac{\partial u}{\partial x}, \frac{\partial v}{\partial y}, \frac{\partial w}{\partial z}, \frac{\partial v}{\partial z} + \frac{\partial w}{\partial y}, \frac{\partial u}{\partial z} + \frac{\partial w}{\partial x}, \frac{\partial u}{\partial y} + \frac{\partial v}{\partial x}\right]^T \tag{2.10}$$

2.2.4 Stress-Strain Relations

Considering linear elastic materials, the stress-strain relations come from the generalised Hooke's law. The two material properties for isotropic materials are Young's modulus (i.e. Elastic modulus) E and Poisson's ratio ν. Considering an elemental cube inside the body, Hooke's law gives:

$$\begin{aligned}
\varepsilon_x &= \frac{\sigma_x}{E} - \nu\frac{\sigma_y}{E} - \nu\frac{\sigma_z}{E} \\
\varepsilon_y &= -\nu\frac{\sigma_x}{E} + \frac{\sigma_y}{E} - \nu\frac{\sigma_z}{E} \\
\varepsilon_z &= -\nu\frac{\sigma_x}{E} - \nu\frac{\sigma_y}{E} + \frac{\sigma_z}{E} \\
\gamma_{yz} &= \frac{\tau_{yz}}{G} \\
\gamma_{xz} &= \frac{\tau_{xz}}{G} \\
\gamma_{xy} &= \frac{\tau_{xy}}{G}
\end{aligned} \tag{2.11}$$

The shear modulus (or modulus of rigidity), G, is defined by

$$G = \frac{E}{(1+\nu)(1-2\nu)} \tag{2.12}$$

From Hooke's law,

$$\varepsilon_x + \varepsilon_y + \varepsilon_z = \frac{(1-2\nu)}{E}(\sigma_x + \sigma_y + \sigma_z) \tag{2.13}$$

Substituting for $(\sigma_y + \sigma_z)$ and so on into Equation 2.11, the following inverse relations are obtained:

$$\sigma = \mathbf{D}\varepsilon \tag{2.14}$$

where **D** is the symmetric (6 × 6) material matrix given by

$$\mathbf{D} = \frac{E}{(1+\nu)(1-2\nu)}\begin{bmatrix} 1-\nu & \nu & \nu & 0 & 0 & 0 \\ \nu & 1-\nu & 0 & 0 & 0 & 0 \\ \nu & \nu & 1-\nu & 0 & 0 & 0 \\ 0 & 0 & 0 & 0.5-\nu & 0 & 0 \\ 0 & 0 & 0 & 0 & 0.5-\nu & 0 \\ 0 & 0 & 0 & 0 & 0 & 0.5-\nu \end{bmatrix} \tag{2.15}$$

2.2.5 Potential Energy and Equilibrium

The aim, in solid mechanics, is to determine the displacement **u** of the body shown in Figure 2.1 which satisfies the equilibrium equations 2.6. Stresses are derived from strains, which in turn are derived from displacements. This requires a solution of second-order partial differential equations. Exact solutions to these equations are only available for simple geometries and loading conditions. However, for complex geometries and more general boundary and loading conditions, obtaining an exact solution is an almost impossible task. Approximate solution methods usually employ potential energy (or variational methods) which place less stringent conditions on the functions.

The total **potential energy** Π of an elastic body is defined as the sum of the total strain energy (U) and the work potential (WP):

$$\Pi = \underset{(U)}{\text{Strain energy}} + \underset{(WP)}{\text{Work potential}} \tag{2.16}$$

For linear elastic materials, the strain energy per unit volume in the body is $\frac{1}{2}\sigma^T\varepsilon$. For the elastic body shown in Figure 2.1, the total strain energy U is given by:

$$U = \frac{1}{2}\int_V \sigma^T \varepsilon \, dV \tag{2.17}$$

The work potential WP is given by

$$WP = -\int_V \mathbf{u}^T \mathbf{f} \, dV - \int_V \mathbf{u}^T \mathbf{T} \, dS - \sum_i \mathbf{u}_i^T \mathbf{P}_i \tag{2.18}$$

The total potential for the general elastic body shown in Figure 2.1 is

$$\Pi = \frac{1}{2}\int_V \sigma^T \varepsilon \, dV - \int_V \mathbf{u}^T \mathbf{f} \, dV - \int_V \mathbf{u}^T \mathbf{T} \, dS - \sum_i \mathbf{u}_i^T \mathbf{P}_i \tag{2.19}$$

Because only conservative systems are considered, the work potential is independent of the path taken. In other words, if the system is displaced from a given configuration and brought back to it's initial state, the forces do zero work regardless of the path.

Principle of Minimum Potential Energy

For conservative systems, of all the kinematically admissible displacement fields, those corresponding to equilibrium extremize the total potential energy. If the extremum condition is a minimum, the equilibrium state is stable.

Kinematically admissible displacements are those that satisfy the single-valued nature of displacements (compatibility) and the boundary conditions. In problems where displacements are the unknowns, compatibility is automatically satisfied.

2.2.6 Rayleigh-Ritz Method

The total potential energy Π in equation 2.19 can be used for finding an approximate solution, for continua. The Rayleigh-Ritz method involves the construction of an assumed displacement field:

$$u = \Sigma\, a_i \phi_i(x,y,z) \qquad i = 1 \text{ to } l$$

$$v = \Sigma\, a_j \phi_j(x,y,z) \qquad j = l+1 \text{ to } m \tag{2.20}$$

$$w = \Sigma\, a_k \phi_k(x,y,z) \qquad k = m+1 \text{ to } n$$

$$n > m > l$$

The functions ϕ_i are usually taken as polynomials. Displacements u, v, w must be *kinematically admissible*. In other words, u, v, w must satisfy specified boundary conditions. Introducing stress-strain and strain-displacement relations, and substituting Equation 2.20 into Equation 2.19 gives:

$$\Pi = \Pi(a_1, a_2, \ldots, a_r) \tag{2.21}$$

where r = number of independent unknowns. The extremum with respect to a_i, ($i = 1$ to r) yields the set of r equations:

$$\frac{\partial \Pi}{\partial a_i} = 0 \qquad i = 1, 2, \ldots, r \tag{2.22}$$

See Example B-1 in Appendix B.

2.2.7 Galerkin's Method

Galerkin's method uses the set of governing equations in the development of an integral form. It is also commonly presented as one of the weighted residual methods. Consider a general representation of a governing equation on a region V:

$$Lu = P \tag{2.23}$$

For the one-dimensional rod in Example B-1 in Appendix B, the governing equation is the differential equation:

$$\frac{d}{dx}\left(EA\frac{du}{dx}\right) = 0$$

Consider L as the operator:

$$\frac{d}{dx} EA \frac{d}{dx}(u)$$

operating on u.

The exact solution must satisfy Equation 2.24 at every point x. An approximate solution $\tilde{U}$, introduces an error $\varepsilon(x)$, called the residual:

$$\varepsilon(x) = L\ \tilde{U} - P \tag{2.24}$$

The approximate methods revolve around setting the residual relative to a weighting function W_i, to zero.

$$\int_v W_i(L\ \tilde{U} - P)\, dV = 0 \qquad i = 1 \text{ to } n \tag{2.25}$$

The choice of the weighting function W_i leads to various approximation methods. In the Galerkin method, the weighting functions W_i are chosen from the basis functions used for constructing $\tilde{U}$. Let $\tilde{U}$ be represented by

$$\tilde{U} = \sum_{i=1}^{n} Q_i G_i \tag{2.26}$$

where G_i, $i = 1$ to n, are basis functions (usually polynomials of x, y, z). The weighting functions are chosen to be a linear combination of the basis functions G_i. Specifically, consider an arbitrary function ϕ given by:

$$\phi = \sum_{i=1}^{n} \phi_i G_i \tag{2.27}$$

where the coefficients ϕ_i are arbitrary, except for requiring that ϕ satisfy homogeneous (zero) boundary conditions where $\tilde{U}$ is prescribed.

Galerkin's method can be stated as follows:

Choose basis functions G_i. Determine the coefficients Q_i in $\tilde{U} = \sum_{i=1}^{n} Q_i G_i$ such that

$$\int_v \phi(L\ \tilde{U} - P)\, dV = 0 \qquad (2.28)$$

for every ϕ of the type $\phi = \sum_{i=1}^{n} \phi_i G_i$ where coefficients ϕ_i are arbitrary, except for requiring that ϕ satisfy homogeneous (zero) boundary conditions. The solution of the resulting equations for Q_i then yields the approximate solution $\tilde{U}$.

Usually, in the treatment of Equation 2.28 an integration by parts is involved. The order of the derivatives is reduced and the natural boundary conditions, such as surface force conditions, are introduced.

Galerkin's Method in Elasticity can now be considered in light of the equilibrium Equations 2.6 in elasticity. Galerkin's method requires:

$$\int_V \left[\left(\frac{\partial \sigma_x}{\partial x} + \frac{\partial \tau_{xy}}{\partial y} + \frac{\partial \tau_{xz}}{\partial z} + f_x \right) \phi_x + \left(\frac{\partial \tau_{xy}}{\partial x} + \frac{\partial \sigma_y}{\partial y} + \frac{\partial \tau_{yz}}{\partial z} + f_y \right) \phi_y + \left(\frac{\partial \tau_{xz}}{\partial x} + \frac{\partial \tau_{yz}}{\partial y} + \frac{\partial \sigma_z}{\partial z} + f_z \right) \phi_z \right] dV \qquad (2.29)$$

where,

$$\phi = [\phi_x,\ \phi_y,\ \phi_z]^T$$

is an arbitrary displacement consistent with the boundary conditions of **u**. If $\mathbf{n} = [n_x,\ n_y,\ n_z,]^T$ is a unit normal at a point **x** on the surface, the integration by parts formula is

$$\int_V \frac{\partial \alpha}{\partial x} \theta dV = -\int_V \alpha \frac{\partial \theta}{\partial x} dV + \int_S n_x \alpha \theta dS \qquad (2.30)$$

where α and θ are functions of (x, y, z). For multidimensional problems, Equation 2.30 is usually referred to as the Green-Gauss theorem or the divergence theorem. Using this formula, integrating Equation 2.29 by parts, and rearranging terms, the following can be written:

$$-\int_V \sigma^T \varepsilon(\phi)\, dV + \int_V \phi^T \mathbf{f}\, dV + \int_S [(n_x\sigma_x + n_y\tau_{xy} + n_z\tau_{xz})\phi_x +$$

$$(n_x\tau_{xy} + n_y\sigma_y + n_z\tau_{yz})\phi_y + (n_x\tau_{xz} + n_y\tau_{yz} + n_z\sigma_z)\phi_z]\, dS = 0 \qquad (2.31)$$

where,

$$\varepsilon(\phi) = \left[\frac{\partial\phi_x}{\partial x}, \frac{\partial\phi_y}{\partial y}, \frac{\partial\phi_z}{\partial z}, \frac{\partial\phi_y}{\partial z} + \frac{\partial\phi_z}{\partial y}, \frac{\partial\phi_x}{\partial z} + \frac{\partial\phi_z}{\partial x}, \frac{\partial\phi_x}{\partial y} + \frac{\partial\phi_y}{\partial x}\right] \qquad (2.32)$$

is the strain corresponding to the arbitrary displacement field ϕ.

On the boundary, from Equation 2.8, $(n_x\sigma_x + n_y\tau_{xy} + n_z\tau_{xz}) = T_x$, and so on. At point loads $(n_x\sigma_x + n_y\tau_{xy} + n_z\tau_{xz})dS$ is equivalent to P_x, and so on. These are the natural boundary conditions in the problem. Thus, Equation 2.31 yields the Galerkin's "variational form" or "weak form" for three-dimensional stress analysis:

$$\boxed{\int_V \sigma^T \varepsilon(\phi)\, dV - \int_V \phi^T \mathbf{f}\, dV - \int_S \phi^T \mathbf{T}\, dS - \sum_i \phi^T \mathbf{P} = 0} \qquad (2.33)$$

where ϕ is an arbitrary displacement consistent with the specified boundary conditions of **u**. One may now use Eq. 2.33 to provide an approximate solution.

For problems in linear elasticity, the above equation is precisely the **principle of virtual work**. ϕ is the kinematically admissible virtual displacement. The principle of virtual work may be stated as follows:

Principle of Virtual Work

A body is in equilibrium if the internal virtual work equals the external virtual work for every kinematically admissible displacement field (ϕ, $\varepsilon(\phi)$).

Note that Galerkin's method and the principle of virtual work result in the same set of equations for problems of elasticity when same basis or co-ordinate functions are used. Galerkin's method works directly from the differential equation and is preferred to the Rayleigh-Ritz method for problems where a corresponding function to be minimised is not obtainable.

2.2.8 Saint Venant's Principle

Finite Element Analysts often have to make approximations in order to define boundary conditions at support-structure interfaces. For example, consider a cantilever beam, free at one end and attached to a column with rivets at the other end. Questions arise as to whether the riveted joint is totally rigid or partially rigid, and as to whether each point on the cross section at the fixed end is specified to have the same boundary conditions. Saint Venant considered the effect of different approximations on the solution to the total problem. Saint Venant's principle states that as long as the different approximations are statically equivalent, the resulting solutions will be valid provided the focus is on regions sufficiently far away from the support. That is, the solutions may significantly differ only within the immediate vicinity of the support.

This principle is used to prove convergence of the SmartBolt model.

2.3 Finite Element Modelling

2.3.1 Steps of a Linear Finite Element Analysis

The primary differences between classical methods and finite elements are the way they "view" the structure and the ensuing solution procedure. Classical methods consider the structure as a continuum whose behaviour is governed by partial or ordinary differential equations. The finite element method considers the structure to be an assembly of small finite-sized particles. The behaviour of the particles and the overall structure is obtained by formulating a system of algebraic equations that can be readily solved with a computer.

Typically, a finite element analysis involves seven steps as stated below. Steps 1,2,4,5 and 7 require decisions made by the user of the finite element program. The rest of the steps are automatically performed by the computer program.

Step 1: *Discretize or model the structure:* This step is generally preceded by a CAD (Computer Aided Design) drawing of the structure. The structure is divided into finite elements. Pre-processors help the user to create the finite element mesh. This step is one of the most crucial in determining the solution accuracy of the problem.

Step 2: *Define the element properties:* At this step, the user must define the element properties and select the types of finite elements that are the most suitable to model the physical system.

Step 3: *Assemble the element stiffness matrices:* The stiffness matrix of an element consists of coefficients which can be derived from

equilibrium, a weighted residual, or an energy method. The element stiffness matrix relates the nodal displacements to the applied forces at the nodes. Assembling of the element stiffness matrices implies application of equilibrium for the whole structure.

Step 4: *Apply the loads:* Externally applied concentrated or uniform forces, moments, and ground motions are provided at this step. Loads are not specified on a structure when modal analysis is performed.

Step 5: *Define boundary conditions:* The support conditions must be provided, i.e., several nodal displacements must be set to known values. The use of boundary elements and reaction force processors allow the evaluation of reactions, which otherwise may not be provided as part of the solution output.

Step 6: *Solve the system of linear algebraic equations:* The sequential application of the above steps leads to a system of simultaneous algebraic equations where the nodal displacements are the unknowns.

Step 7: *Calculate stresses:* At the users discretion, finite element programs can also calculate stresses, reactions, mode shapes or other pertinent information. Postprocessors help the user display the output in a graphical form.

In crating a finite element model one should strive for accuracy and computational efficiency. In most cases the use of a complex and very refined model is not justifiable since it most likely provides computational accuracy at the expense of unnecessarily increased processing time. The type and complexity of the model is dependent upon the type of results required. As a general rule, finite element modelling starts with a simple model. The results from the simple model combined with a an understanding of the behaviour of the system helps decide whether and at which part of the model further refinement is needed.

2.3.2 Types of Finite Elements

Depending on their dimensions, basic elements can be divided into three categories: line, area, and volume elements. Truss, beam and boundary elements are line elements. Plane stress, plane strain, axisymmetric and membrane plate and shell are area elements. Solid or brick, tetrahedral, and hexahedral are volume elements. Axisymmetric elements, although two dimensional in geometry, can also be regarded as solid elements as they model the total cross-section of solids with rotational symmetry.

A detailed study of common elements types available in commercial software was conducted. Whereas only the two types of elements used in the SmartBolt analysis are discussed here, a summary of other element types is contained in Appendix C.

Axisymmetric Elements

Problems involving three-dimensional axisymmetric solids or solids of revolution, subjected to axisymmetric loading, reduce to simple two-dimensional problems.

Storage tanks, rotors, shells, nozzles, and nuclear containment vessels are some representative axisymmetric structures. Because of total symmetry about the *z* axis, all deformations and stresses are independent of the rotational angle θ. In order to analyse an axisymmetric structure, such as a cylinder with thickness, t, subjected to uniform internal pressure, p, the intersection of the cylinder with the plane YZ is modelled in the positive quadrant of the XYZ Cartesian system. (The axisymmetric plane may vary from one software package to another.) The loading, p, that is applied to the finite element model corresponds to a slice of the structure defined by rotating a cross-section of the structure about the z-axis by a unit angle θ = 1rad. Axisymmetric quadrilateral and triangular elements have two transitional degrees-of-freedom per node.

Both triangular and quadrilateral elements have proved to be very highly accurate in comparison with classical analytical solutions. The comments made in the discussion on plane stress compatible and incompatible elements are also valid for axisymmetric elements.

Axisymmetric Formulation

Considering the elemental volume shown in Figure 2.5, the potential energy can be written in the form:

$$\Pi = \frac{1}{2}\int_0^{2\pi}\int_A (\sigma^T \varepsilon r)\,dA\,d\theta - \int_0^{2\pi}\int_A (u^T fr)\,dA\,d\theta - \int_0^{2\pi}\int_l (u^T Tr)\,dl\,d\theta - \sum_i u_i^T P_i \qquad (2.34)$$

where r ×dl× d is the elemental surface area, l is the boundary, and $\mathbf{P}_i$ represents a line load distributed around a circle.

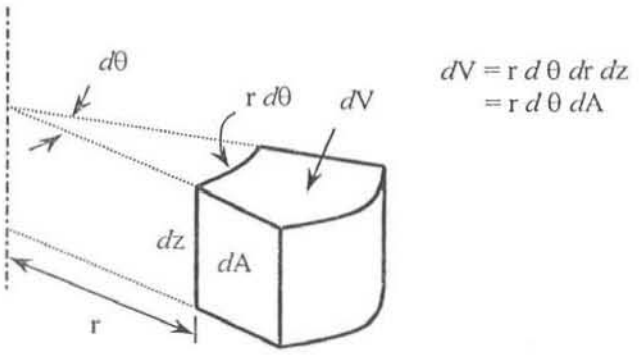

Figure 2.5 – *Elemental Volume*

All variables in the integrals are independent of θ. Thus, Equation 2.34 can be written as:

$$\Pi = 2\pi\left(\frac{1}{2}\int_A (\sigma^T \varepsilon r)dA - \int_A (u^T fr)dA - \int_l (u^T Tr)dl\right) - \sum_i u_i^T P_i \qquad (2.35)$$

where,

$$\mathbf{u} = [u, w]^T \qquad (2.36)$$

$$\mathbf{f} = [f_r, f_z]^T \qquad (2.37)$$

$$\mathbf{T} = [T_r, T_z]^T \qquad (2.38)$$

From Figure 2.6 the following relationship between strains ε and displacements **u** can be written:

$$\varepsilon = [\varepsilon_r, \varepsilon_z, \gamma_{rz}, \varepsilon_\theta]^T \qquad (2.39)$$

$$= \left[\frac{\partial u}{\partial r}, \frac{\partial w}{\partial z}, \frac{\partial u}{\partial z} + \frac{\partial w}{\partial r}, \frac{\partial u}{\partial r}\right]^T \qquad (2.40)$$

The stress vector is correspondingly defined as:

$$\sigma = [\sigma_r, \sigma_r, \tau_{rz}, \sigma_\theta]^T \qquad (2.41)$$

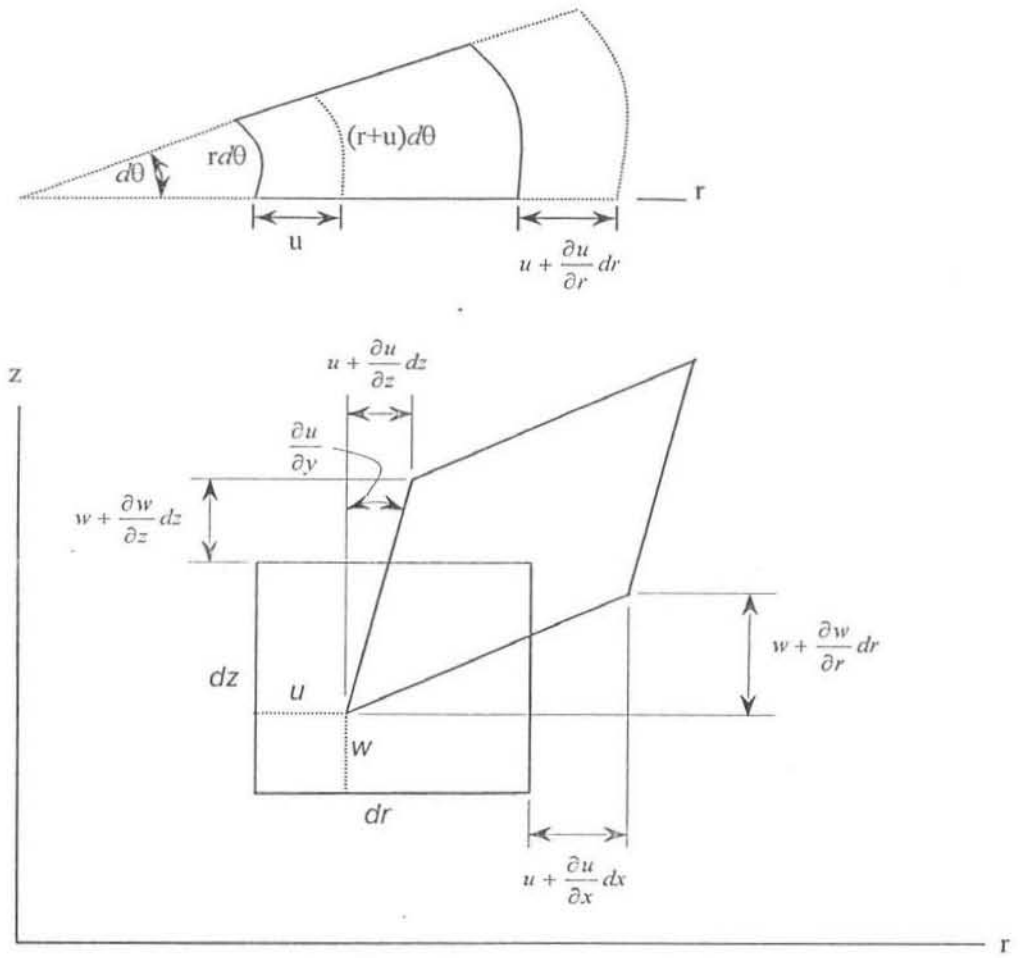

Figure 2.6 – *Deformation of Elemental Volume*

The stress-strain relations are given in the usual form:

$$\sigma = \mathbf{D}\varepsilon$$

where the (4×4) matrix **D** can be written as follows:

$$D = \frac{E(1-\nu}{(1+\nu)(1-2\nu)} \begin{bmatrix} 1 & \frac{\nu}{1-\nu} & 0 & \frac{\nu}{1-\nu} \\ \frac{\nu}{1-\nu} & 1 & 0 & \frac{\nu}{1-\nu} \\ 0 & 0 & \frac{1-2\nu}{2(1-\nu)} & 0 \\ \frac{\nu}{1-\nu} & \frac{\nu}{1-\nu} & 0 & 1 \end{bmatrix} \qquad (2.42)$$

Gap Elements

These elements are used to model cables, gaps between structural components, and gaps between a structure and its supports. Gap elements can be either compressive or tensile. Compressive gap elements become active when compressive forces develop on the boundary element after the gap is closed. Similarly, tensile gap elements (or cable elements) resist tensile forces after the gap is closed (or the cable is extended in tension).

It should be mentioned that most structural problems involving the use of gap elements are non-linear. The nonlinearity is attributed to the change of the system's stiffness which occurs when the gap elements are either activated or deactivated.

2.3.3 Good Practices in Finite Element Modelling

Creating the proper model is the most crucial step in finite element analysis. The goal is to develop the most suitable nodal pattern that provides enough elements to obtain accurate results without wasting data interpretation and processing time. Modelling should always be based on conceptual understanding of the physical system and judgement on the anticipated behaviour of the structure.

The following list of guidelines, accumulated from modelling experience and selected from various sources, can be used as a basis to develop reliable models for static, and to a great extent, for dynamic analysis. The recommendations may not apply to all cases.

a) A finite element mesh should be uniform whenever practical. However, non-uniformity is often required to obtain accurate results in regions of

rapid changes in geometry and loading. Only at those parts of the structure where the geometry, stresses, or loading change dramatically should the mesh be refined.

b) The use of quadrilateral, six-sided solid, and hexahedral elements, should be favoured except where triangular, four-sided solid, and tetrahedral elements are necessary to accommodate irregularities in geometry and loading.

c) When using plate elements to model curved surfaces, a subtended angle of less than 10 degrees should be maintained.

d) A more refined mesh is required to obtain accurate stresses than displacements. A convergence study should be performed, i.e., start with a simple model with a relatively small number of elements and progressively refine the model while observing the change in results.

e) If the stress field has similar gradients in all directions, the analyst should try to maintain an *aspect ratio* of 1. *Aspect ratio* is defined as the ratio between the element's longest and shortest dimensions. Elements with high aspect ratio should be avoided. However, "poor" elements can be used in the analysis provided that they model regions of the structure where the stress gradient varies very gradually along the longest dimension of the elements.

f) For regions with small variation of stresses, the aspect ratio could be as high as 10 to 1 and still yield good results. As a general rule, however, one should keep the element aspect ratios under 10 for deformation analysis and under 3 for stress analysis. It should be noted that in deformation analysis the emphasis is placed on the accurate calculation of

the nodal displacements, while in stress analysis one is interested in an accurate calculation of both the displacements and stresses.

g) Rapid changes in element size should be avoided. When the use of different element sizes is necessary, the transitional parts should be modelled by changing the dimensions of adjacent elements by less than a factor of two.

h) For triangular elements, acute angles less than 30° should be avoided and, for quadrilateral elements obtuse angles greater than 120°. As a general rule, the use of skewed elements is acceptable when the primary interest is displacements. If, however, stresses must be calculated accurately, then less skewing should be incorporated into the model.

i) Holes, cracks, and localised changes in geometry can be characterised as geometric discontinuities. Modelling of geometric discontinuities depends on the interest in the accurate calculation of deformations and stresses in the vicinity of the discontinuity. If deformations and stresses near the discontinuity are not of concern, one can use a global model of the structure that has a coarse mesh around the discontinuity can be used. If the goal is to obtain the response near the discontinuity, a local model should be used. Contrary to the global model, the local model uses a refined mesh in the vicinity of the discontinuity. There are two basic approaches to model holes, cracks and notches:

    - the first one involves the use of a local model with a refined mesh around the discontinuity. This approach usually requires a detailed mesh that can model the region around the discontinuity in very fine detail, or

- if the stress concentration factor, K, is known from handbooks or experimental data, a model that calculates the primary stress around the discontinuity can be used. Such a model is less refined than the one required in the first approach.

Where there are abrupt geometric changes, one should use a more refined mesh in the region where the changes are located.

j) Abrupt changes in material properties can be handled with the approaches suggested for geometric discontinuities, i.e., with the aid of global and local models.

k) For isotropic materials, Poisson's ratio must not be very close to 0.5. Also, for a Poisson's ratio close to zero, the structure may lose almost all its stiffness, and as a consequence, the results could be erroneous.

l) For anisotropic materials, the theoretical limits of Poisson's ratio and Young's modulus along the specified directions must be verified in order to avoid solution of inaccuracies.

m) Models with elements that have stiffnesses differing more than 10^4 should be avoided. Large stiffness variations in a model may lead to singularities and ill-conditioned matrices that cannot be numerically handled by the processor. Large stiffness variations could occur in models that contain very small and very large size elements, in models simulating either soft or stiff structural parts, and in models that include stiff or soft elastic boundary and gap elements. Guidelines for the specific software should be followed for these situations.

n) A refined mesh should be used in the vicinity of abrupt load changes in order to capture the stress variation near the loads. The extent of the region that must be modelled with a fine mesh depends on the attenuation lengths from the points of application of the loads. Various design codes provide attenuation lengths for a variety of engineering applications, e.g. $\sqrt{Rt}$ in ASME Section VIII, where R is the radius and t is the wall thickness of an axisymmetric pressure vessel component.

2.3.4 Elastic Failure Criteria

This discussion assumes elastic behaviour of the structure, i.e., the deformation it experiences is recoverable. In addition, it is also assumed that under the effect of the applied forces, the system experiences small deformations and strains. The word "small" implies infinitesimal changes in geometry of the system. In the elastic state the stresses and strains that develop in a structure are uniquely defined regardless of the spatial and time variation of the applied forces. Once the elastic state is exceeded, even in a small region of the structure, deformation is no longer recoverable and its further development depends on whether the structural material is either ductile or brittle.

For ductile materials, when the magnitude of the external forces is substantial, the structure experiences a permanent deformation known as plastic deformation. Plastic deformations are permanent changes in atomic positions of the structural material. They are irrecoverable and depend on both the spatial and the time variation of the applied forces. Contrary to the elastic state, the plastic state cannot be defined uniquely.

Plastic deformations develop when the combinations of stresses at a region in the structure exceeds a critical value. The critical combination of the stress components, that initiates plastic deformations for ductile materials and cracks for brittle materials, is mathematically expressed as a failure or yield criterion. When regions of a structure are stressed beyond the elastic limit, the results obtained through a linear analysis could be invalid. In linear static and dynamic analysis one does not evaluate deformations in the plastic state. The task of identifying regions that have yielded is accomplished with the aid of failure or yield criteria.

It is pointed out that the word "failure" as used for the failure criteria is rather misleading. The development of either plastic stresses or cracks at a point or section in a structure does not necessarily imply that the structure has failed and cannot carry any further load. It simply means that further analysis using linear elastic theory is no longer valid, at least for the vicinity of the region of the structure that "failed."

Several competing theories propose different failure criteria. In general, all these theories provide fairly similar results. The most widely used failure criteria are the **Tresca** and the **von Mises** for ductile materials, and the maximum normal stress criterion for brittle materials.

In applying the Tresca and von Mises yield criteria the following points are important:

- both the Tresca and von Mises stresses are scalar quantities, and when compared with the yield stress of the structure is stressed beyond the elastic limit.

- yield criteria should be applied with caution in dynamic and fatigue analysis.

Tresca Yield Criterion

The Tresca criterion states that yielding initiates when one-half the largest difference between the principal stresses reaches one-half the yield stress of the structural material under pure tension. Assuming that $\sigma_3<\sigma_2<\sigma_3$ Tresca's yield criterion can be expressed as:

$$\frac{1}{2}(\sigma_1-\sigma_3)=\frac{1}{2}\sigma_y \qquad (2.35)$$

This criterion is not affected by the intermediate principle stress σ_2.

Von Mises Yield Criterion

According to von Mises, plastic deformation at a point initiates when the principal stresses at the point satisfy the relationship:

$$\sqrt{0.5(\sigma_1-\sigma_2)^2+0.5(\sigma_2-\sigma_3)^2+0.5(\sigma_3-\sigma_1)^2}=\sigma_y \qquad (2.36)$$

σ_y is the yield stress of the structural material under uniaxial tension.

Maximum Normal Stress Criterion

For brittle materials, e.g., unreinforced concrete, cast iron and porcelain, the maximum principal stress theory is used to predict brittle fracture. This theory proposes that fracture initiates when the maximum principal stress at a point, if

tensile, is equal to the ultimate stress from a uniaxial tension test and, if compressive, equals the ultimate stress from a uniaxial compression test.

3. Bolted Joints

The purpose of this section is to develop some reasoning of what happens to a bolt during the assembly and loading processes and to identify the factors which contribute to its design. These concepts form the basis of some of the assumptions used in the Smartbolt analysis.

3.1 Basic Concepts

A bolt serves two structural purposes:

- It acts as a pin to keep two or more joint members from slipping relative to each other (resists shear), and/or
- It acts as a heavy spring to clamp two or more pieces together (the bolt is in tension).

In order to perform either of these functions, a bolt must be tightened properly.

When a bolt is tightened (usually by turning the nut or the head of the bolt) the bolt is stretched by a small amount. If the bolt is not stretched, it will not provide a clamping force on the parts being held together. If a bolt is used as a pin, it is still stretched during assembly, because the forces generated by the stretching process hold the nut in place, producing friction between the joined members which contributes to the sliding resistance.

The stretching of the bolt produces tensile stresses, but the turning action during tightening also causes torsional stresses (as a result of friction). Previous research and experiments [1] indicates that these torsional stresses almost completely relax within minutes after tightening. However, it is still a concern during assembly as the combined torsional and tensile stresses could cause bolt failure while tightening.

When a bolt is put into service, it experiences one or more working loads which may put the bolt in any combination of static and cyclic tension and shear loads. The entire joint, i.e. bolt, nut and clamped members, behaves as a system of elastic springs. Thus, in most cases, it is not possible to identify bolt loads exactly, but engineers can only approximate them and introduce a generous safety factor into the design. Generally, the more critical the application, the more complex the bolt analysis is. In some situations, only actual tests of prototype hardware yield reliable results.

The following are some properties of bolted joints which help to predict the joint behaviour:

- Materials
- Bolt geometry
- Function (or service of the joint)
- Working loads
- Working environment

3.2 Bolted Joint Design

3.2.1 Types of Strength

As with all structures, the strength of a bolted joint is determined by the weakest component. In order to design an adequate joint, the following basic "types of strength" must be considered – the designer will identify those which are not applicable in his particular application:

(a) Tensile Strength: Primarily, one should consider the capacity of a bolt to sustain a sufficient tensile force, as this force will be one of the main factors to influence the clamping force between joint members. In most applications, the tensile strength of the bolt at ambient temperature under static loads is the only bolt strength issue of concern.

(b) Thread Stripping Strength: It is necessary to determine whether or not the bolt and nut (or tapped hole) threads will sustain the tensile force in the bolt without shearing (or "stripping"). This is not a concern when standard nuts are used, but the thread stripping strength must be computed for tapped holes.

(c) Shear Strength: In some situations bolts are subjected to loads at right angles to the axis: shear loads. This is especially common in structural applications.

(d) Brittle Fracture Strength: The above types of "normal" strength are the chief factors to consider in "normal" bolts under fairly static loads, at room temperature. However, the bolt behaviour changes, sometimes drastically, when one or more of these qualifications are absent. For example, if the bolt it made of a very hard material it can theoretically support very high tensile loads. If a tiny crack or flaw exists in that bolt's surface, however,

it might fail suddenly and unexpectedly under loads well below its theoretical strength.

(e) Strengths at Extreme Temperatures: This is another deviation from the norm which designers often face. Temperatures that are higher or lower than ambient will alter the tensile and stripping strength of the bolt because of basic changes in the tensile and shear strengths of the material from which the bolt is made.

(f) Fatigue Strength: Cyclic loads lead to entirely different types of failure as opposed to static loads. Materials in cyclic service fail well below their tensile and shear strengths. This is discussed in greater detail later.

(g) Stress Corrosion Cracking Strength: Failure may occur by the simultaneous application of stress and a corrosive environment. The failure of a bolt due to Stress Corrosion Cracking (SCC), or hydrogen embrittlement, can be inversely proportional into its conventional tensile strength (which is related to hardness). Thus, a careful study of the operational environment of the bolt must be conducted.

Although the above are the most common strength factors which influence the integrity of bolted joints, they are not the only ones as different operating environments may have other "side-effects" on joints.

3.2.2 Tensile Strength

If a ductile fastener is placed in a tensile test machine and a pure tension load is gradually applied between the head of the bolt and the nut, a tension versus change-in-length curve such as that shown in Figure 3.1 can be generated.

The proportional limit and the elastic limit are located near each other at the upper end of the elastic region. Repeated loading and unloading of the bolt within the elastic region will never result in a permanent deformation of the bolt, although it may result in fatigue failure.

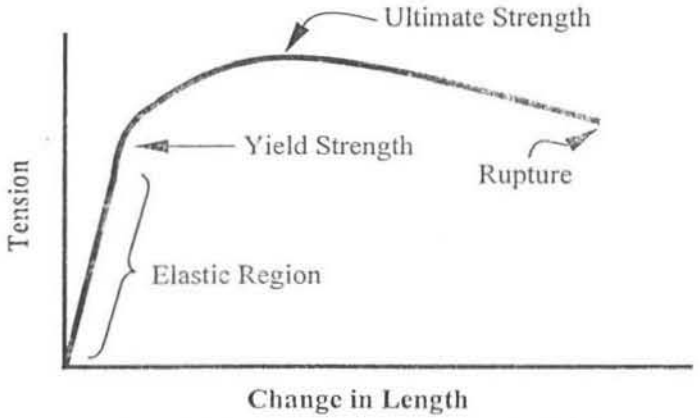

Figure 3.1 – ***Points of interest on the Elastic Curve***

The upper end of the straight line ends at the proportional limit, followed closely by the yield strength point (beyond which tension loads produce some permanent deformation). Loading the fastener to this last point will create a particular amount of deformation – usually chosen as 0.2 or 0.5% of the initial length (proof strength). A definition of this sort is necessary because the point at which an engineering body can be said to have yielded is not obvious. Some portions of the bolt will have yielded long before the body as a whole has been loaded to its yield strength; and other portions of the bolt are not even close to yield when the bolt has deformed permanently by about 0.5%.

Another point of interest is the ultimate strength (often called tensile strength) of the bolt. This is the maximum tension which can be created by a tensile load on the bolt.

It is always greater than the yield strength – sometimes as much as twice yield – but always occurs in the plastic region of the curve, well beyond the point at which the bolt will take a permanent set.

A final point of interest on the elastic curve is the rupture point, where the bolt breaks under the applied load.

If the bolt is loaded well into the plastic region of its curve and then the load is removed, it will behave as suggested in Figure 3.2. Note that it returns to the zero load point along a line that is parallel to the original elastic line, but offset from the original line by an amount determined by the permanent deformation created by the earlier tension load on the bolt.

If the bolt is reloaded, but kept below the initial maximum tensile load applied, the bolt will follow this new straight line and will again function elastically. In face, its behaviour will be elastic well past the tensile load which caused permanent deformation in the first place. The difference between the original yield strength and the new yield strength is a function of the work hardening which has been done on the bolt by taking it past yield on the first cycle, as noted in Figure 3.2. Loading it past this new yield point will create additional permanent deformation; but unless it is taken well past the new yield point the bolt won't be damaged, nor will it break by yielding it a little – in fact it will become a little stronger, at least as far as static loads are concerned.

Many bolt materials can be taken past initial, and new, yield points a number of times before they break. The stronger, more brittle materials, however, can suffer a loss of strength by such treatment [3].

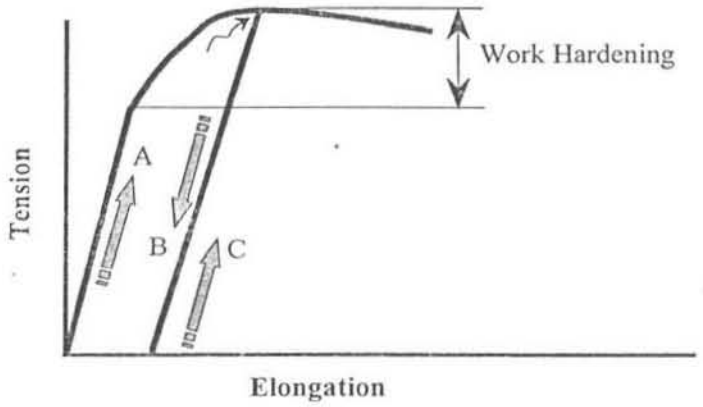

Figure 3.2 – *Work Hardening of a Bolt.* The bolt is loaded (A) to point to M, well past the yield strength, and then unloaded (B) to reveal a permanent deformation. If reloaded, it will follow path (C).

Because the stress distribution in a bolt is complicated, computing strength would be difficult, so engineering societies have devised a way to determine strength experimentally and to base design and manufacturing specifications on the resulting data.

A large number of fasteners, made with well-defined materials and standard thread configurations, were subjected to tensile loads to determine:

- The highest tensile force they could withstand without taking any permanent deformation (called the proof load).
- The tensile force which produces 0.2% or 0.5% permanent deformation (used to define yield strength)
- The highest tensile force they could support prior to rupture (used to define ultimate tensile strength).

The resulting data were then published. One doesn't have to worry about stress magnitudes or variations; the tables tell one the magnitudes of force a fastener of a given shape and material can safely sustain. Fastener manufacturers are required to repeat these tests periodically to make sure that their products meet the original standards.

There was also a need to compute design limits for non-standard-fasteners. Here the path becomes a little more gloomy. The societies which tested the fasteners found, by experiment, that if the load at yield was divided by a cross-sectional area based on the mean of the pitch and minor diameter of the threads, the result was a theoretical tensile stress at yield which agreed closely with the stress at which a cylindrical test coupon of the same material would yield. Similar results for ultimate strength, proof load, etc. were also obtained. The following parameters could then be defined:

- The stress area, A_S of a standard thread, based on the mean of pitch and root diameters (see Figure 3.3)
- The proof strength of a given thread, computed by dividing the experimentally determined proof strength by the stress area
- The ultimate strength and yield strength of a given thread, calculated by dividing the experimentally determined ultimate and yield load, respectively, by the same area.

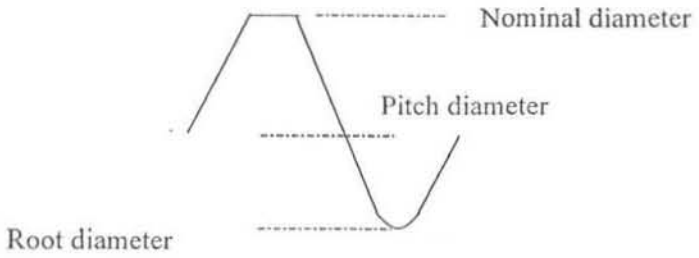

Figure 3.3 – ***The relationship between root diameter, pitch diameter, and outside or nominal diameter.***

The tensile force required to yield or break the bolt is simply,

$$F = \sigma A_S \qquad (3.1)$$

where F = force which will cause the bolt to fail

σ = the ultimate tensile or yield strength of the bolt material

A_S = effective "stress area" of the threads.

3.2.3 Thread Stripping Strength

Another simple equation is used in estimating the static strength of threads:

$$F = S_U A_{TS} \qquad (3.2)$$

where S_U = the ultimate shear strength of the nut or bolt materials

A_{TS} = the cross-sectional area through which the shear occurs. (This is not the cross sectional area of the body.

Failure will occur in either the nut or bolt threads – or in both simultaneously – depending on the relative strengths of the nut and bolt materials. A different expression must be used to compute the shear stress area for each type of failure [4]. The following equations have been derived for standard 60° threads.

Nut Material Stronger than Bolt Material

Failure occurs at the root of bolt threads. The equations for shear area (A_{TS}) and the length of thread engagement (L_e) required to develop full strength of the threads are as follows:

$$A_{TS} = \pi n L_e K_{n\,max}\left[\frac{1}{2n} + 0.57735(E_{S\,min} - K_{n\,max})\right] \tag{3.3}$$

$$L_e = \frac{2A_S}{\pi n K_{n\,max}\left[\left(\frac{1}{2n}\right) + 0.57735(E_{S\,min} - K_{n\,max})\right]} \tag{3.4}$$

where A_{TS} = shear area at root of bolt threads

n = inverse of pitch

A_S = stress area of bolt threads

K_{nmax} = maximum ID of nut

E_{Smin} = minimum PD (pitch diameter) of bolt

Nut Material Weaker than Bolt Material

Failure occurs at the root of the nut threads. The equations are:

$$A_{TS} = \pi n L_e D_{min}\left[\frac{1}{2n} + 0.57735(D_{s\,min} - K_{n\,max})\right] \tag{3.5}$$

$$L_e = \frac{S_{st}\,2A_S}{S_{nt}\,\pi n D_{s\,min}\left[\left(\frac{1}{2n}\right) + 0.57735(D_{s\,min} - K_{n\,max})\right]} \tag{3.6}$$

where D_{smin} = minimum OD of bolt threads

E_{nmax} = maximum PD of nut

S_{st} = tensile strength of the bolt material

A_{TS} = shear area at root of nut threads

n = inverse of pitch

A_S = stress area of bolt threads

L_e = Length of thread engagement required to develop full strength.

Nut and Bolt of Equal-Strength Materials

Failure occurs simultaneously in both parts, at the pitch line. The equations are:

$$A_{TS} = \pi E_p \frac{L_e}{2} \qquad (3.7)$$

$$L_e = \frac{4A_S}{\pi E_p} \qquad (3.8)$$

where E_p = nominal pitch diameter

A_S = stress area of bolt threads

A_{TS} = shear area at pitch line of both threads

L_e = length of thread engagement required to develop full strength

3.2.4 Shear Strength

Shear loads of the sort shown in Figure 3.4 are often encountered in structural steel applications. There can be either one or several shear planes through a bolt, depending on the nature of the joint and the number of joint members being clamped together. These shear planes could pass either through the body of the bolt or through the threads, or through both.

In order to compute the shear strength of the bolt, the shear strength of the material (S_U) is multiplied by the total cross-sectional area of the shear planes, taking all of

them into account. For shear planes through threads, the equivalent thread stress area (A_S) is used. For example, for the conditions of Figure 3.4(d):

$$F = S_U (2A_B + 2A_S) \qquad (3.9)$$

where A_B is the cross-sectional area of the body.

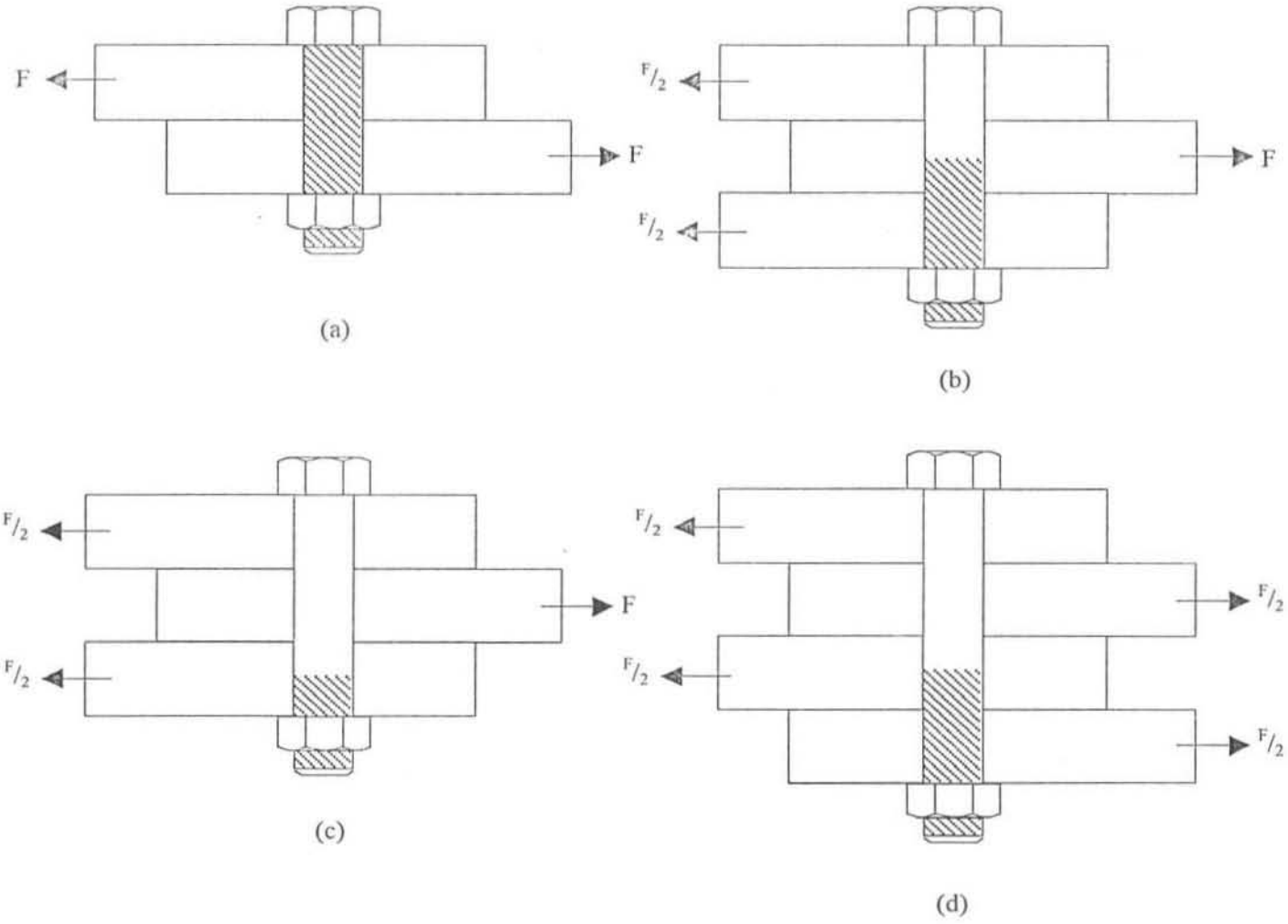

Figure 3.4 – ***Possible shear loading conditions on a bolt in a structural joint***

3.2.5 Torsional Strength

When a nut is tightened, a torsional moment as well as a stretching force is applied to the bolt, as a result of frictional and geometric restraints between the nut and bolt threads. The torsional moment (T_{tor}) applied to the bolt is given by the following expression (assuming that there is no prevailing torque):

$$T_{tor} = F_p\left(\frac{P}{2\pi} + \frac{\mu_t r_t}{\cos\beta}\right) \tag{3.10}$$

where P = thread pitch

μ_t = the coefficient of friction between the threads

r_t = the effective radius of contact between threads

β = the half angle of a tooth

T_{tor} = torsional moment

F_p = preload

Assuming that one can substitute an equivalent cylinder for the fastener, and that the cylinder has a diameter equal to the nominal diameter, D, of the fastener and a length equal to the effective length, L_E, of the fastener (normally approximated as the length of the bolt plus one half of the thickness of the nut, plus one half of the thickness of the head), one can write the following expressions for the angle of twist, θ_{tw} (in radians), the torsional energy, W_{tor}, and the maximum stress, S_{tor}, produced in the outermost fibre of the fastener as follows:

$$\theta_{tw} = \frac{32L_E T_{tor}}{\pi G D^4} \tag{3.11}$$

$$W_{tor} = \frac{1}{2}T_{tor}\theta_{tw} = \frac{1}{2}(T_{tor})^2\left(\frac{32L_E}{\pi G D^4}\right) \tag{3.12}$$

$$S_{tor} = \frac{16T_{tor}}{\pi D^3} \tag{3.13}$$

where G is the shear modulus.

3.2.6 Bending Strength

If the geometry of the joint forces the bolt to bend as it is tightened, it will see additional tensile stress along its outer curved surface and less tensile stress alone the inner curved surface. Assuming that the bolt can be replaced by an equivalent cylinder having an external diameter equal to the nominal diameter of the fastener, D, and a length equal to the fastener's effective length, L_E, the bending moment, M_b, the maximum stress created by pure bending, S_B, and the bending energy, W_{bn}, can be computed as follows:

$$M_b = \frac{IE}{R} = \frac{\pi E D^4}{64R} \tag{3.14}$$

$$S_B = \frac{M_b D}{21} = \frac{ED}{2R} \tag{3.15}$$

$$W_{bn} = \frac{1}{2}\int_0^{L_E} \frac{M_b^2}{EI} dl = \frac{1}{2}\frac{E\pi D^4 L_E}{64R^2} \tag{3.16}$$

where L_E = effective length of the fastener

E = modulus of elasticity

I = moment of inertia

R = radius of curvature

3.2.7 Load Combinations on a Bolt

In most applications a bolt will see a combination of tension, torsion, shear and bending stresses. Exactly which combination will depend on the geometry of the given set of parts and on the coefficient of friction. It is never possible in practice to compute the resulting maximum stresses in a given fastener, because there is never enough information about the variables involved.

An expression for the distribution of energy in a bolted joint – the energy introduced to the joint by the work done in tightening the nut – can be written. Although this equation still involves all the variables encountered in practice, it does show how complex the act of tightening a bolt can be and forces one to keep this fact in mind when dealing with some of the simplified design equations.

Assuming that there is a linear relationship between input torque and turn of the nut, the work into the system, W_{in}, can be defined:

$$W_{in} = \frac{1}{2}\left(T_{in} \times \theta_{in}\right) \qquad (3.17)$$

where T_{in} = the maximum torque applied to the nut

θ_{in} = the total turn applied to the nut (radians) after "snugging".

This is only an approximation, because it assumes a linear relationship. However, this expression describes most of the input work. (In any case, one would probably never have enough information about a fastener to achieve exact solutions.)

When a nut is tightened on a bolt in order to clamp a joint together, work is done on the joint in a number of ways. It is possible to write an expression for each portion of this work and to set their sum equal to the input work. As the assumption of a linear relationship between T_{in} and θ_{in} has been made, the following also assumes a linear build-up in energy stored in each mode.

Work done in stretching of the bolt:

$$W_{ten} = \frac{1}{2}\left(\Delta L \times F_P\right) \qquad (3.18)$$

where ΔL = change in length of the bolt

F_P = preload

Work done in twisting of the bolt:

$$W_{tor} = \frac{1}{2}(T_{tor})^2 \frac{32L_E}{\pi G D^4} \qquad (3.12)$$

Work done against the friction forces between nut and bolt threads:

$$W_{tf} = \frac{1}{2} T_f \times \theta_R = \frac{1}{2} \frac{\mu_t F_P r_t}{\cos\beta} \theta_R \qquad (3.19)$$

where θ_R = the relative turn between nut and bolt.

Work done against friction forces between joint nut and joint members:

$$W_{nf} = \frac{1}{2} T_{nf} \times \theta_{in} = \frac{1}{2} \mu_n F_P r_n \theta_{in} \qquad (3.20)$$

where θ_{in} = total input turn (in radians)

r_n = effective contact radius between nut and joint

μ_n = coefficient of friction between nut and joint

Work done in bending of the bolt:

$$W_{bn} = \frac{1}{2} \frac{\pi E D^4 L_E}{64 R^2} \qquad (3.16)$$

Work done in compressing the joint:

$$W_{jc} = \frac{1}{2}(\Delta T_j \times F_P) \qquad (3.21)$$

where ΔT_j = compression of the joint (deflection)

F_P = preload

Work done in compressing the nut:

$$W_{nc} = \frac{1}{2}(\Delta T_N \times F_P) \tag{3.22}$$

where ΔT_N = compression of the nut (deflection)

F_P = preload

The sum of all these terms can be equated to the input work. Combining these work terms yields the following equation:

$$F_P^2\left[\left(\frac{P}{2\pi}+\frac{\mu_t r_t}{\cos\beta}\right)^2\left(\frac{32L_E}{\pi D^4 G}\right)\right]+F_P\left(\Delta L+\Delta T_j+\Delta T_N+\frac{\mu_t\theta_R r_t}{\cos\beta}+\mu_n\theta_{in}r_n\right) + \left(\frac{E\pi D^4 L_E}{64R^2}-T_{in}\theta_{in}\right)=0 \tag{3.23}$$

This equation involves a number of factors which will be difficult (or impossible) to estimate in a given application – such things as the coefficients of friction, the radius of curvature of the bolt, the relative turn between nut and bolt, and the "deflection" of the nut, for example. The equation also assumes a linear build-up of input torque, T_{in}, which makes it only a rough approximation. This energy equation demonstrates that it is not a trivial matter to predict how much preload is applied to a bolt when torque is applied to the nut.

Designers are interested primarily in the tensile strength of bolts, and less often in the shear strength. The tensile strength determines the amount of preload that can safely be applied to the bolt on tightening, and the amount of tensile working load it can see thereafter. It is important to recognise that the tensile strength of a given fastener is reduced if the fastener also sees torsion or shear loads. In an extreme case, for example, if the nut and bolt threads have galled near the end of the tightening operation, and unusually high level of torsion will result in the bolt. If tension is then

applied, the bolt will break at a tension level well below normal (perhaps even below proof load). The torsion stress has "robbed" part of the total strength of the bolt. Only if the bolt is loaded, statically, in pure tension can it support a proof load without deformation.

Torsion stress will "rob" part of the total strength of the bolt only while the torsion stress is present. As a bolt is torqued, for example, it is subjected to some torsion. Such a bolt will yield at a certain level of tensile stress. After the torque is removed, however, the torsion stress will tend to disappear (as a result of embedment relaxation). If an external tensile load is then applied to the fastener, it will support a higher level of tension than that which caused it to yield in the first place, as suggested in Figure 3.5.

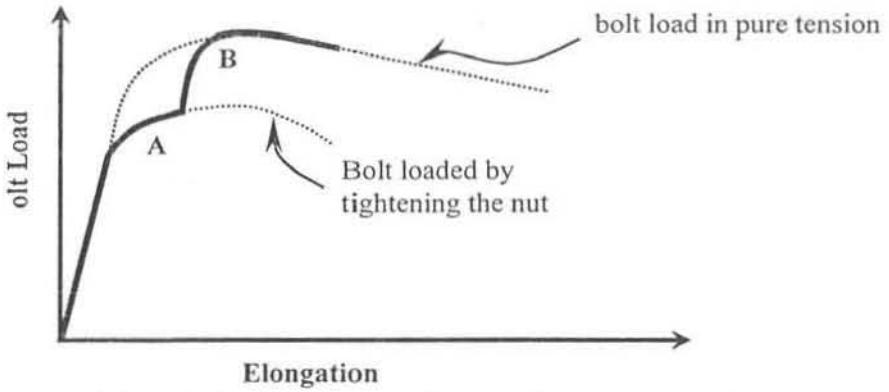

Figure 3.5 – *A Fastener tightened with a Torque tool*
While the bolt is tightened, it is exposed to simultaneous torsion and tension, and will yield at a slightly lower level of tensile stress (A) than a fastener subjected to pure tension. This same fastener however will support a higher tensile stress in service before yielding any further (B), because the torsion stress component will, in general, disappear rather rapidly after initial tightening in most situations.

3.2.8 Prelaod and Torque Control

The main purpose of most bolts is to clamp the joint members together. The clamping force is created when the bolts are tightened during assembly, creating preload (tension) in them.

During initial assembly of an individual bolt there is a linear relationship between the tension in a bolt and its preload. However, the tensile load in a bolt will change as other bolts are tightened and/or the joint is put in service.

Most bolting references use the term "preload" to describe the tension in the bolts at any time, during assembly, in use, etc. It is important to distinguish between the following:

Initial preload: the tension created in a bolt when it is first tightened

Residual preload: the tension remaining in a bolt at the end of the assembly process, after all bolts have been tightened

Tension in a bolt: the tension in a bolt in service.

The tension in a bolt is determined by many factors, each affected by nay subfactors. Preload dominates all other factors in most situations. Correct initial preload is essential.

The easiest and cheapest way to control preload is to control the torque and/or turn, as these are the inputs to the system. Unfortunately, however, the relationship between torque or turn and preload is not as predictable as one would like.

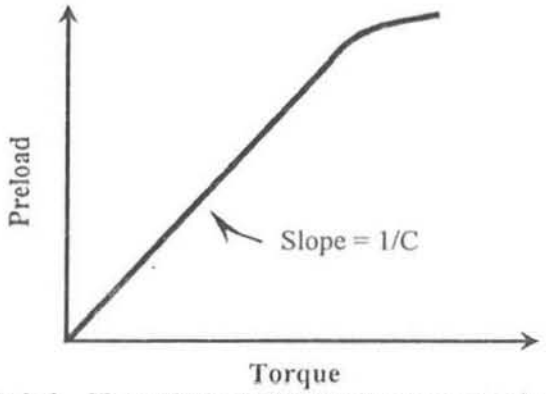

Figure 3.6 – *Normal relationship between applied torque and achieved preload.* The straight line becomes a curve at the top where something (the bolt of joint) starts to yield.

Experience and theoretical analysis indicate that there is usually a linear relationship between the torque applied to a fastener and the preload developed in a given fastener, see Figure 3.6.

torque = Preload x (a constant)

$$T_{in} = F_P \times C \tag{3.24}$$

Deriving the constant, C, has proven to be quite a challenge. A number is equations have been derived which attempt to define it. The following one (known as the long form equation) has been proposed by Motosh [5]:

$$T_{in} = F_P\left(\frac{P}{2\pi} + \frac{\mu_t r_t}{\cos\beta} + \mu_n r_n\right) \tag{3.25}$$

where, T_{in} = torque applied to the fastener

F_P = preload created in the fastener

P = the pitch of the threads

μ_t = the coefficient of friction between nut and bolt threads

r_t = the effective contact radius of the threads

β = the half angle of the threads

μ_n = the coefficient of friction between the face of the nut and the upper surface of the joint

r_n = the effective radius of contact between the nut and joint surface

This equation involves a simplification, and so the "answer" it gives is in error by a small amount. However, it is probably the most revealing of the so-called long-form equations that have been proposed.

The equation shows that the input torque (left side of the equation) is resisted by three reaction torques (three components on the right-hand side). These are:

$F_P \frac{P}{2\pi}$ is produced by the inclined plane action of the nut threads on the bolt threads. This could be called the bolt stretch component of the reaction torque. It also produces the force which compresses the joint and the nut, and it is a part of the torque which twists the body of the bolt.

$F_P \frac{\mu_t r_t}{\cos\beta}$ is a reaction torque created by frictional restraint between nut and bolt threads. It also provides the rest of the torque which twists the bolt (unless there is some prevailing torque which would add a third component to the twist torque).

$F_P \mu_n r_n$ is a reaction torque created by frictional restraint between the face of the nut and the washer or joint.

Using a fastener's dimensions and assuming coefficients of friction and input torque, the magnitude of each of the three reaction components can be computed separately. Experience has shown [1] that the nut friction torque is approximately 50% of the total reaction; thread friction torque is approximately 40% and the so-called bolt stretch component is only 10%.

The coefficient of friction is very difficult to control and virtually impossible to predict. There are more than 30 variables that affect the friction seen in the threaded fastener. These include such things as:

- The hardness of all parts
- Surface finishes
- The type of materials
- The thickness, condition, and type of plating, if present
- The type, amount, condition, method of application, contamination, and temperature of any lubricants involved
- The speed with which the nut is tightened
- The fit between threads
- Hole clearance
- Surface pressures

Many of these factors can be controlled to some degree, but complete control is probably impossible.

Friction is often cited as the only villain in the torque-preload equation, but that is not the case. Although one may think one knows the pitch of threads, the half-angle, or

the effective contact radii between parts, in practice, there are surprising variations in all these factors.

The bolt is not a rigid body. It is a highly stressed component with a very complex shape and severe stress concentrations. The basic deformation is usually elastic, but there are always portions of the bolt (e.g. in the thread roots) which deform plastically, altering the geometric factors r_t and the pitch.

The face of the nut is seldom exactly perpendicular to the axis of the threads. Holes are seldom drilled exactly perpendicular to the surface of the joint, so contact radius r_n is usually unknown. Some experiments indicate that these factors can introduce even more uncertainty than friction does [1].

All of the above variables are at least visible in the long-term equations. There are other sources of error, however, to which this torque-balance equation is blind. When a nut is tightened, work is done on the entire nut-bolt-joint system. Part of the input work ends up as bolt stretch or friction loss, but other portions of the input work end up as bolt twist, a bent shank, nut deformation, and joint deformation. The "true" relationship between input torque and bolt preload, therefore, must take these outputs into account. In one extreme case, for example, if the threads gall and seize, input torque produces just torsional strain and no preload at all. The long-form equation (equation 3.25) would suggest that "all is lost in thread friction torque" for this situation (infinite coefficient of friction in the threads). This isn't true, but thread friction torque is a twist component, so the equation doesn't lie. The result is strain energy, not heat. Although the torque-balance equation does describe the action and reaction torques on the system correctly, it would be incorrect to say, "Every part of

the input energy which is not converted to preload must end up as friction loss because the equation shows only preload or friction terms." The torques are only cam action or friction torques, but what this means from and energy distribution standpoint is not revealed by the torque equation.

Another factor which is not included in the long-form equation is prevailing torque: the torque required to run down a lock nut which has a plastic insert in the threads, for example. The insert creates interference between nut and bolt threads, and thereby helps the fastener resist vibration. The torque required to overcome this interference doesn't contribute to the bolt stretch. It might be considered and addition to the thread friction component of torque, but it is a function of the design of the lock nut, and of the materials used, as well as the geometry, so it is best handled as a separate term, as suggested below:

$$T_{in} = F_p\left(\frac{P}{2\pi} + \frac{\mu_t r_t}{\cos\beta} + \mu_n r_n\right) + T_p \qquad (3.26)$$

where T_P = prevailing torque.

The prevailing torque is not a function of preload, the way all the other terms are. It may also not be a constant; it may change as the lock nut is rather farther down the bolt, or is reused.

The nut used for the Aircraft bolt which is being investigated does contain a plastic insert. The associated prevailing torque is ignored in the analysis of the bolt, as this is a conservative approach.

There is another widely used equation which is probably more useful than the long form. The so-called short-form equation is:

$$T_{in} = F_P(KD) \tag{3.27}$$

where T_{in} = input torque

F_P = achieved preload

D = nominal diameter of the bolt

K = "nut factor" (dimensionless)

If a prevailing torque fastener is used, the equation must be written:

$$T_{in} = F_P(KD) + T_P \tag{3.28}$$

The discussion which follows assumes no prevailing torque, which is usually the case.

Note that the nut factor K is not a coefficient of friction. It is, instead, a general-purpose experimental constant which states that "when this torque is (experimentally) applied to the fastener and the achieved preload is actually measured, it is discovered that the ratio between the torque and preload could be defined by the following expression:

$$\frac{T_{in}}{F_P} = KD \tag{3.29}$$

It is convenient that K summarises anything and everything that has affected the relationship between torque and preload in the experiment: including friction, torsion, bending, plastic deformation of threads, and any other factor that one may or may not have anticipated.

However, the disadvantage of the factor K is that it can only be determined experimentally, and experience has shown that it really has to be redetermined for each new application. Even then, it is not a single number. Experience also shows that for accurate prediction, one has to made a number of experiments to determine the mean K, standard deviation, etc. Having done this, however, one can indeed predict the minimum and maximum preload which one would achieve for a given input torque, at a predictable confidence level. This cannot be done with the long-form equation.

From previous experiments and reports received from field service engineers on maintenance construction sites, the range of K is from 0.15 to 0.25; the mean is 1.99, and the standard deviation is 0.05. [1].

3.2.9 Stiffness and Strain Effects

Consideration of the stiffness and strain effects in a bolt is useful in the definition of bolt behaviour due to external loads.

Consider equal and opposite forces applied to the ends of a rod of non-uniform diameter, as shown in Figure 3.7. If the tension stress created in the rod is below the proportional limit, Hooke's law and the relationship between springs in series can be used to compute the change in length of the rod.

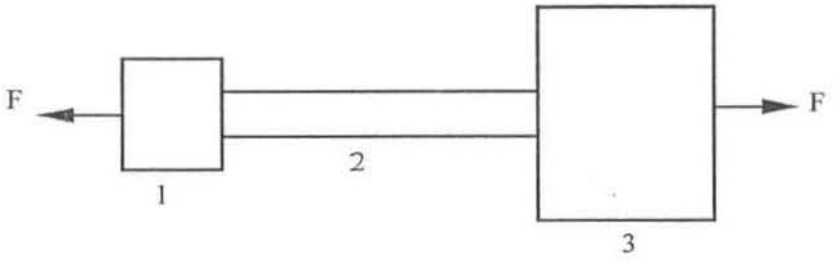

Figure 3.7 – *Rod of Non-uniform Diameter, Loaded in Tension*

The combined change in length of the rod will be equal to the sum of the changes in each section:

$$\Delta L_C = \Delta L_1 + \Delta L_2 + \Delta L_3 \tag{3.30}$$

Hooke's law state that the change in one section will be:

$$\Delta L = \frac{FL}{EA} \tag{3.31}$$

where ΔL = the change in length

A = the cross-sectional area

L = the length of the section

E = the modulus of elasticity

F = the applied tensile force

Since the various sections are connected in series, they each see the same force, so when these two equations are combined, one can write:

$$\Delta L_C = F\left(\frac{L_1}{EA_1} + \frac{L_2}{EA_2} + \frac{L_3}{EA_3}\right) \tag{3.32}$$

The spring constant of a body is defined as:

$$K = \frac{F}{\Delta L} \tag{3.33}$$

where K = the spring constant

ΔL = the change in length of the body under load

F = the applied load

The spring constant of a group of bodies, connected in series, is:

$$\frac{1}{K_T} = \frac{1}{K_1} + \frac{1}{K_2} + \frac{1}{K_3} \tag{3.34}$$

where K_T = the combined spring constant of the group

$K_{1..3}$ = spring constants of individual members of the group

The equation for the spring constant of a body can be rewritten as:

$$\Delta L = \frac{F}{K} \qquad \text{or} \qquad \Delta L = F\left(\frac{1}{K}\right) \tag{3.35}$$

Comparing the equation for the spring constant for a group of bodies to the equation for the stretch or change in length of a group of bodies reveals that:

$$\frac{1}{K_T} = \frac{L_1}{EA_1} + \frac{L_2}{EA_2} + \frac{L_3}{EA_3} \tag{3.36}$$

The stiffness of either a plain or complex body is very much a function of the relation between length and cross-sectional area – it is a function of the shape of the body just as much as it is a function of the material from which the body is made.

The equations used for a rod having several different diameters are basically the equations which would be used for computing the change in length and stiffness of bolts. If one computes or predicts the lengths, cross-sectional areas, and modulus of elasticity of the material, one should be able to compute the deflection under load. As explained below, this is unfortunately not so simple.

Tensile loads are not applied to bolts "from end to end"; they are applied between the inner face of the nut and the under surface of the head. The entire bolt is not loaded,

therefore, the way test rods are. There is zero tensile stress in the free ends, for example.

There is, however, some stress in portions of both the head and threads. One cannot assume that the bolt is merely a cylinder equal in length to the grip length. Instead, one has to make some assumption concerning the stress levels which allow the estimation of an "effective length" for the bolt which is somewhere between the true overall length and the grip length.

Tensile stress in a bolt is maximum near the inner faces of the head and nut, and that tensile stress is zero at the outboard faces of nut and head. Assuming that there is a uniform decrease in stress from inboard to outboard faces of the head, one can make the assumption that the average stress level in the head of the bolt is one-half the body stress; or a mathematically equivalent assumption can be made that one-half of the head is uniformly loaded at the body stress level and that the rest of the head sees zero stress. Similarly, it can be stated that one-half of the threads engages by the nut are loaded at the "exposed thread" stress level. It can now be stated that the effective length, L_E, of the fastener is equal to the length of the body, L_B, plus one-half the thickness of the head, T_H, added to the length of the exposed threads, L_T, plus one half the thickness of the nut, T_N, as suggested in Figure 3.8.

Figure 3.8 – ***Illustration of the Actual Bolt Configuration (A) and the Equivalent Configuration (B)***

There is really no simple way one could deal with the true stress distribution unless an advanced analysis is conducted, e.g. Finite Element Analysis. Even this would require simplifications as the model would require more information about the geometry of a particular bolt and joint than could be provided. However, the assumptions made here give reasonable predictions in many applications, because the bulk of the fastener is stressed at, or near, the levels assumed. It is only the surfaces of the fastener that exhibit the maximum deviations from these averages. Also, as the bolt length to diameter ratio decreases (i.e. the bolt becomes stubby), the above assumption for effective length becomes more inaccurate.

Assumptions concerning the cross-sectional areas of the bolt also have to be made when computing the change in length. The body area is no mystery and can be calculated quite easily. For the cross-sectional area of the threads, however, the effective "stress area," A_S (discussed earlier), must be used.

The approximate change in length of the bolt under load can now be computed as follows:

$$\Delta L_C = F_P\left(\frac{L_{be}}{EA_B} + \frac{L_{se}}{EA_S}\right) \qquad (3.37)$$

where L_{be} = the effective length of the body

L_{se} = the effective length of the threads

ΔL_C = combined change in length of all portions

A_S = the effective area of the threads

A_B = the cross-sectional area of the body

E = the modulus of elasticity

F_P = tension in the bolt

Once it is known how to compute the change in length of the fastener, the spring constant or stiffness can also be estimated using the relationship:

$$K_B = \frac{F_P}{\Delta L_C} \tag{3.38}$$

So far only the stiffness of the bolt itself has been considered. The joint is never clamped by a bolt only, however it is clamped by a bolt-and-nut system – or by a bolt-nut-washer system. The stiffness of this combination of parts is found by:

$$\frac{1}{K_T} = \frac{1}{K_B} + \frac{1}{K_N} + \frac{1}{K_W} \tag{3.39}$$

where K_T = total stiffness of the system

K_B = stiffness of the bolt

K_N = stiffness of the nut

K_W = stiffness of the washer

Joint members can also be treated as springs in series when joint stiffness and deflection are computed. The loads, of course, are compressive rather than tensile, but the basic equations are the same. For example, if equal and opposite forces are applied to a pair of blocks as shown in Figure 3.9, the change in thickness, ΔT_J, of the system of blocks and the spring constant, K_J, will be:

$$\Delta T_J = \Delta T_1 + \Delta T_2 = F\left(\frac{T_1}{EA_1} + \frac{T_2}{EA_2}\right) \tag{3.40}$$

and

$$K_J = \frac{F}{\Delta T_J} \tag{3.41}$$

where

$$\frac{1}{K} = \frac{1}{K_1} + \frac{1}{K_2} = \frac{T_2}{EA_1} + \frac{T_2}{EA_2} \tag{3.42}$$

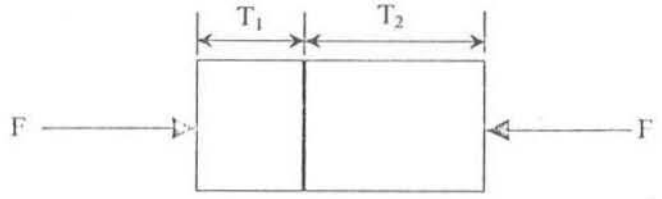

Figure 3.9 – *Two Blocks in Compression*

Theoretically, the relationship between applied compressive force and deflection for the pair of blocks should be linear as long as the force stays within the elastic limit of the material. In practice, however, it is often found that the stiffness of a joint is not linear, and may not be fully elastic.

Just as simplifications were made in assuming an equivalent body shape for a bolt in order to make calculations less complicated, some simplifications need also to be made for the joint.

That portion of the joint which is put in compressive stress by the bolt can be described as a barrel with a hole through the middle. Some researchers have therefore substituted an "equivalent barrel" for the joint, but more common substitutions are hollow cylinders or a pair of frustum cones. A discussion of eight proposed ways to estimate the stiffness of a hard joint is given by Motosh [5]. The equivalent cylinder approach is described at length by Meyer and Strelow [1]. Unfortunately, each of these techniques assumes that:

- Joint behaviour will be linear and fully elastic.
- There is only one bolt in the joint and it passes through the centre of the members being clamped together (this is called a concentric joint).
- The external load applied to the joint is a tension load and it is applied along a line that is concentric with the bolt axis.

Here, the equivalent cylinder approach is demonstrated to estimate stiffness. This involves the general equation:

$$K_J = \frac{EA_C}{T} \qquad (3.43)$$

where K_J = stiffness of the joint

E = modulus of elasticity

A_C = cross-sectional area of the equivalent cylinder used to represent the joint in stiffness calculations

T = total thickness of the joint or grip length

The only difficulty is A_C, the cross-sectional area of the equivalent cylinder. The equations used here for A_C are summarised in Figure 3.10.

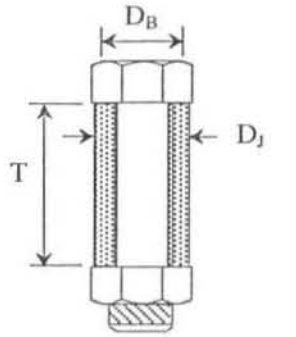

if $D_B \geq D_J$
then

$$A_C = \frac{\pi}{4}\left(D_J^2 - D_H^2\right) \qquad (3.45)$$

D_H is the diameter of the hole in the joint.

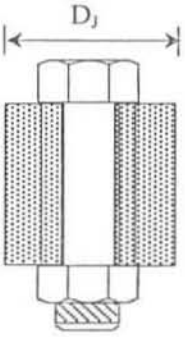

if $D_B < D_J \leq 3D_B$ and $T \leq 8D$
then

$$A_C = \frac{\pi}{4}\left(D_B^2 - D_H^2\right) + \frac{\pi}{8}\left(\frac{D_j}{D_b} - 1\right)\left(\frac{D_B T}{5} + \frac{T^2}{100}\right) \qquad (3.45)$$

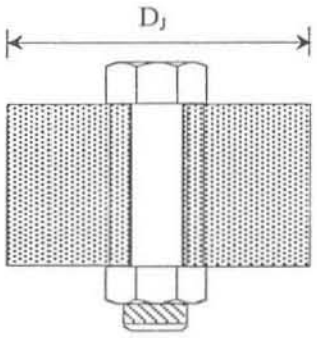

if $D_J \geq 3D_B$ and $T \leq 8D$

$$\text{then } A_C = \frac{\pi}{4}\left[\left(D_B + \frac{T}{10}\right)^2 - D_H^2\right] \qquad (3.46)$$

Figure 3.10 – ***Equations To Compute The Stiffness Of Concentric Joints Using The Equivalent Cylinder Method.***

Note that there are three different equations, depending on the diameter of contact, D_B, between the bolt head (or washer) and the joint, and its relationship to the outside diameter of the joint, D_J [7,8]. If the joint has a square or rectangular cross section, its "diameter" is the length of one side (or of the shortest side of the rectangle). D_H is the diameter of the hole.

Experience shows that the stiffness of a "typical" joint ranges from 3 to 5 times the stiffness of the bolt which would be used in such a joint. Very thin joints, like sheet

metal, will be substantially stiffer, although the stiffness of the bolt will also increase rapidly as it gets shorter.

3.2.10 Theoretical Behaviour of a Joint Under Tensile Loads

In order to understand the working behaviour of a bolted joint, an understanding of the forces and deflection in the joint must first be illustrated. Figure 3.11, greatly exaggerated to illustrate the effects, shows what happens when a bolt is tightened. Tightening the bolt sets up stresses and strain in both the bolt and joint members. The bolt is placed in tension; it gets longer. The joint compresses, at least in the vicinity of the bolt. It always does this, regardless of how stiff it may appear to be.

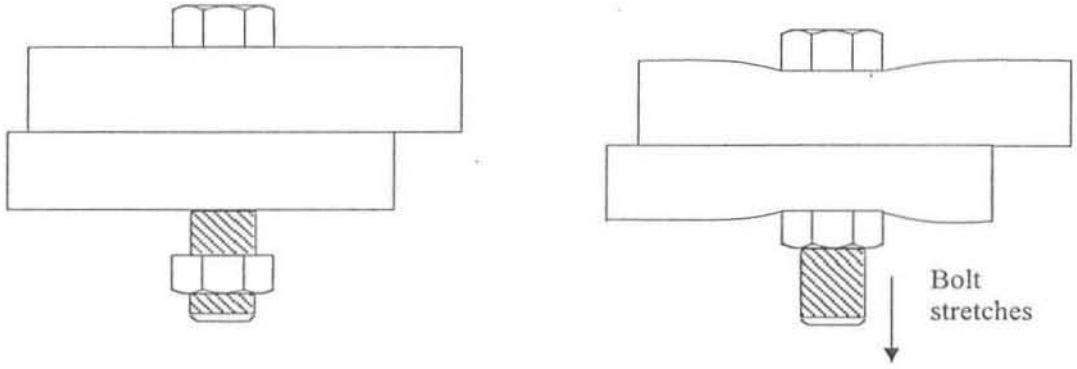

Figure 3.11 – ***Tightening A Bolt Stretches The Bolt And Compresses The Joint***

Separate elastic curves can be plotted for the bolt and joint members (Figure 3.12), plotting the absolute value of the force in each on the vertical axes and the deformation of each (elongation of the bolt and compression of the joint) on the horizontal axes.

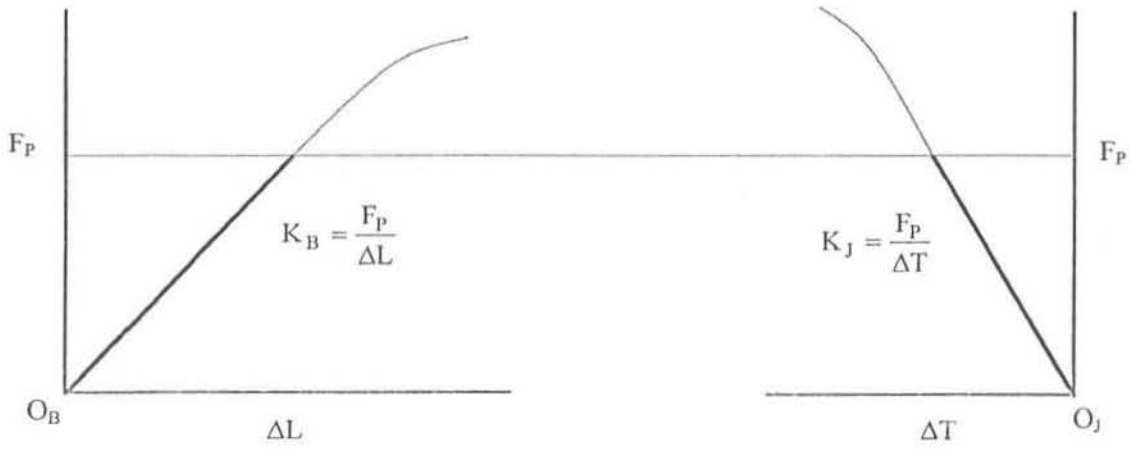

Figure 3.12 – ***Elastic Curves for Bolt and Joint Members***

The following three points should be noted:

1. Typically, the slope, K_B, of the bolt's elastic curve is only one-third to one-fifth of the slope, K_J, of the joint's elastic curve. Another way of stating this is that the stiffness or spring rate of the bolt is only one-third to one-fifth that of the joint.
2. The clamping force exerted by the bolt on the joint is opposed by an equal and opposite force exerted by the joint members on the bolt. The bolt "wants" to shrink back to its original length; the joint "wants" to expand to its original thickness. The bolt stays stretched, however, because the joint is pushing outward on it through the nut and through the head of the bolt.
3. If one continued to tighten the bolt, it (or the joint) would ultimately start to yield plastically. The following discussion assumes that the bolt is operated below the proportional limit of each curve.

The two elastic curves can be combined into what is called a joint diagram, as shown in Figure 3.13. This diagram has proven to be very useful when analysing joint behaviour.

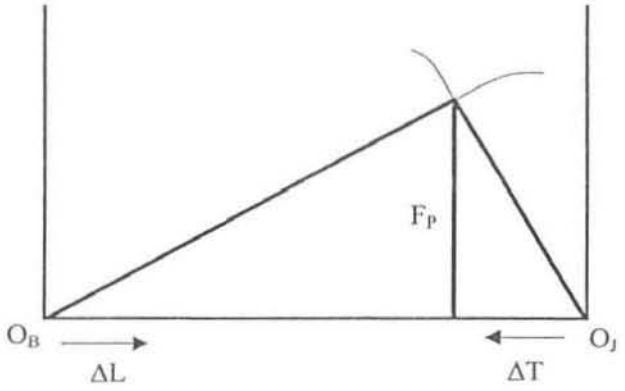

Figure 3.13 – ***The Elastic Curves For Bolt And Joint Combined To Form A Joint Diagram***

The tensile force in the bolt at this point (i.e. the intersection of the elastic curves) is called the "preload" in the bolt – it is equal and opposite to the compressive force in the joint.

Consider now external forces (equal and opposite) applied to the bolt head and the nut. Since the bolt has been tightened, the joint has been pushing outward on the bolt, keeping it in tension. The new external tension load helps the joint support the tension in the bolt. In other words, the new external force partially relieves the joint. See Figure 3.14.

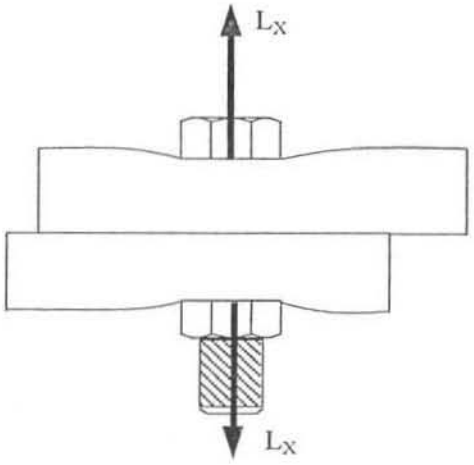

Figure 3.14 – *An External Load, L_X is Applied between the Bolt Head and Nut*

Since the strain (deformation) is proportional to stress (applied force), the partially relieved joint partially returns to its original thickness, moving back down its elastic curve. Simultaneously, the bolt, under the action of the combined joint force and external force, gets longer, following its elastic curve.

Note that the increase in length in the bolt is equal to the increase in thickness (reduction in compression) in the joint. **The joint expands to follow the nut as the bolt lengthens. This is a key to understanding joint behaviour.** See Figure 3.15.

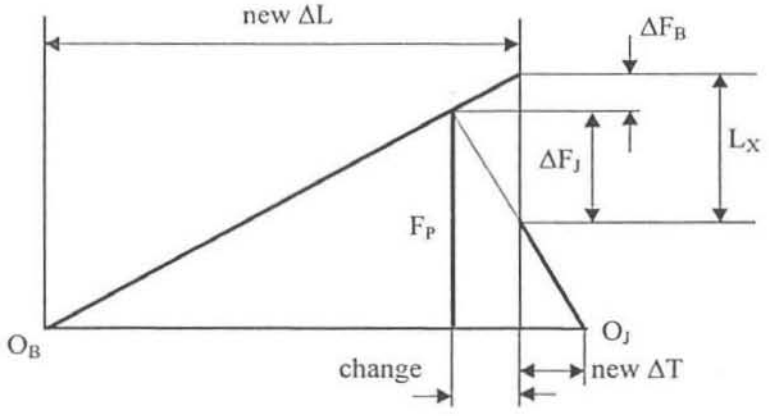

Figure 3.15 – *Joint Diagram with External Loads Applied Between the Bolt Head and Nut*

Recall that the stiffness of the bolt is only one-third to one-fifth that of the joint. This means that for an equal change in deformation (strain), the change in load (force) in the bolt must be only one-third to one-fifth of the change of the load in the joint. See Figure 3.15. The external tension load, L_X, required to produce this change of force and strain in the bolt and joint members is equal to the increase in force on the bolt, ΔF_B, plus the reduction in force in the joint, ΔF_J:

$$L_X = \Delta F_B + \Delta F_J \tag{3.47}$$

Any external tension load, no matter how small, will be partially absorbed as new, added force in the bolt, ΔF_B, and partially absorbed in replacing the reduction in force that the joint originally exerted on the bolt, ΔF_J. The force of the joint on the bolt, plus the external load, equals the new total tension force in the bolt, which is greater than the previous total, but the change in bolt force is less than the external load applied to the bolt.

If the external load continues to increase, a point is reached where the joint members are fully unloaded, as shown in Figure 3.16. This load is called the critical external load. This critical load is not, in general, equal to the original preload in the bolt. However, it is often equal to the preload for several other reasons, for example:

- In many joints the bolt is relatively soft (low spring rate) compared to the joint members. Under these condition s there is a very small difference between the preload in the bolt and the critical external load required to free the joint members.
- Joints almost always relax after they have first been tightened. Relaxation of 10% or 20% of the initial preload is not at all uncommon. If a bolt has

one-fifth the stiffness of the joint (which is also common), then the critical external load required to free the joint members is 20% greater than the residual preload in the bolt when the external load is applied. Under these conditions, the difference between the critical external load and the present preload is just about equal and opposite to the loss in preload that was caused by bolt relaxation. Therefore (by coincidence) the critical external load equals the original preload before bolt relaxation.

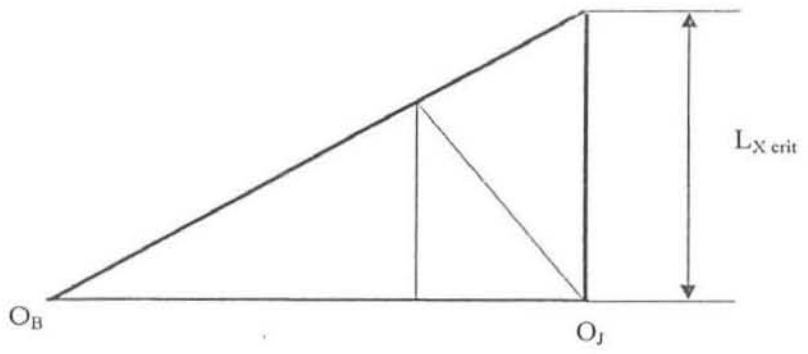

Figure 3.16 – ***The Critical External Load is Reached When ALL the Joint Compression is Relieved***

A derivation of the mathematics of the joint is now presented. Figure 3.17 shows the completed diagram where,

F_P = initial preload

L_X = external tension load

ΔF_B = change in load in bolt

ΔF_J = change in load in joint

ΔL, $\Delta L`$ = elongation of the bolt before and after application of the external load

ΔT, $\Delta T`$ = compression of joint members before and after application of the external load

L_{Xcrit} = external load required to completely unload the joint (not shown on the diagram).

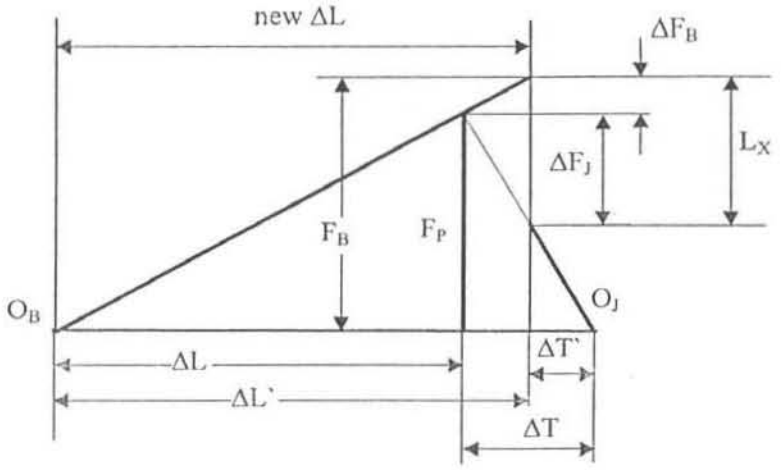

Figure 3.17 – Completed *Joint Diagram*

The spring constants or stiffness of the bolt and joint can be defined as follows:

$$\text{For the bolt:} \quad K_B = \frac{F_P}{\Delta L} \tag{3.48}$$

$$\text{For the joint:} \quad K_J = \frac{F_P}{\Delta T} \tag{3.49}$$

By using trigonometry, and by recognising similar triangles where they occur, the following useful expressions can be derived:

$$\Delta F_B = \left(\frac{K_B}{K_B + K_J} \right) L_X \tag{3.50}$$

until joint separation, after which $\Delta F_B = \Delta L_X$, and

$$L_{Xcrit} = F_P \left(1 + \frac{K_B}{K_J} \right) \tag{3.51}$$

These simple joint diagrams are very basic and very useful, even through they describe the behaviour of the joint under a very uncommon type of loading – a tensile load applied between the bolt head and nut.

Different diagrams must be used if the external load is applied at different planes; but the bolt loads and critical load computed for these situations are only a little different from the loads computed from the diagram already discussed. The first simple diagram, in fact, turns out to be a worst-case situation as far as bolt load calculations are concerned. By using it, a greater-than-actual increase in bolt tension, and a greater-than-actual reduction in interface clamping force in the joint will be predicted. If the design can tolerate the predicted changes it will presumably have no difficulty with the actual changes. As a result, this "classical" joint diagram is often used in joint design and analysis even though it is based on external load application points that will probably never be encountered in practice. For a more thorough understanding, however, one must consider more realistic conditions and the resulting modifications in the joint diagram.

Loads are seldom, if ever, applied to a single "point" in a bolted joint. Loads are created by pressure, weight, shock, inertia, etc., and are transferred to the joint by the connected members. An accurate description of where that load is applied would require a detailed stress analysis (e.g., a Finite Element Analysis). The researchers who developed the classical joint diagram, however, have found a simpler way to "place" the load. They define hypothetical "loading planes," parallel to the joint interface, and located somewhere between the outer and contact surfaces of each joint member. They then assume that the tensile load on the joint is applied to these

loading planes. Joint material between the loading planes will then be, theoretically, unloaded by a tensile load; joint material out of the planes will be "trapped" between plane-of-application of load and the head (or nut) of the fastener.

In the preceding simple joint diagram discussion, these planes coincided with the upper and lower surfaces of the flange or joint. In the following discussion, loading planes will coincide with the interface between upper and lower joint members, as suggested in Figure 3.18.

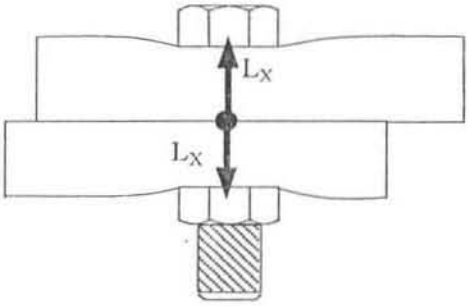

Figure 3.18 – ***An External Load, L_X is at the Joint Interface***

Note that the loading plane is in pure friction. Thus a so-called "bugger factor" is used to correct a joint diagram analysis, to make the analysis agree, for example, with experimental results (which might show how an external tensile load actually affects the tension in a preloaded bolt). The loading plane remains a useful concept, though.

In the preceding analysis:

- The bolt was treated as a tension spring
- The upper and lower flange members were treated as compression springs

- Tensile loads applied to each end of the bolt stretched (loaded) the bolt and partially relieved (unloaded) the joint.

All of this was analysed in a joint diagram which showed how one spring was loaded and the other unloaded by the external load.

If the same tensile force, however, were applied to the interface between the upper and lower joint members, then both the bolt tension spring and the joint compression spring would be loaded by the external load.

The two flange pieces initially exert an equal and opposite force on each other – forces equal to the preload in the bolt. As a small external load is applied at the interface, the forces that the two joint members exert on each other are partially relieved. This means that the external load reduced the flange-on-flange force without increasing the total force in either the flange members or the bolt, yet. The joint diagram for this situation is shown in Figure 3.19. Note that both elastic curves are drawn on the same side of the common vertical axis (the axis that represents original preload or F_P) because both springs are loaded by the external force.

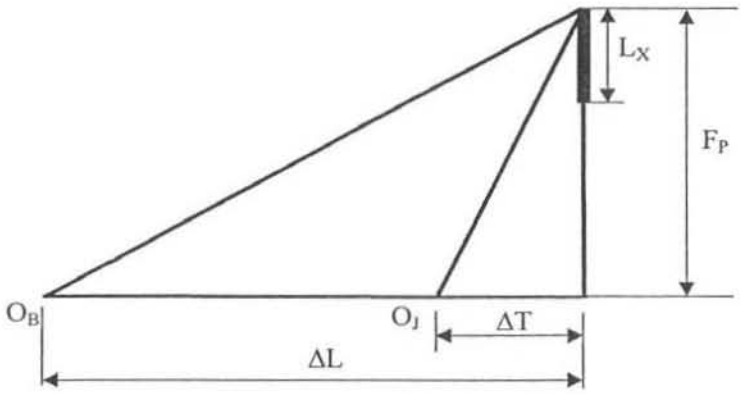

Figure 3.19 – *Joint Diagram when an external tension load is applied at the joint interface.* ΔL = elongation of the bolt; ΔT = compression of the joint; F_P = original preload

When the external load equals the original preload in the bolt, it will have replaced all of the force that each joint member was exerting on the other. Neither bolt deformation nor joint deformation has changed to this point.

Increasing the external load beyond this point will now add to the original deformation of both the bolt and the joint members. The bolt gets longer and the joint compresses more. The joint diagram merely "gets larger". (In figure 3.20, the dashed lines represent the original joint diagram; the solid lines represent then new joint diagram.) At all times, both bolt and joint see the same total load, change in load, etc.

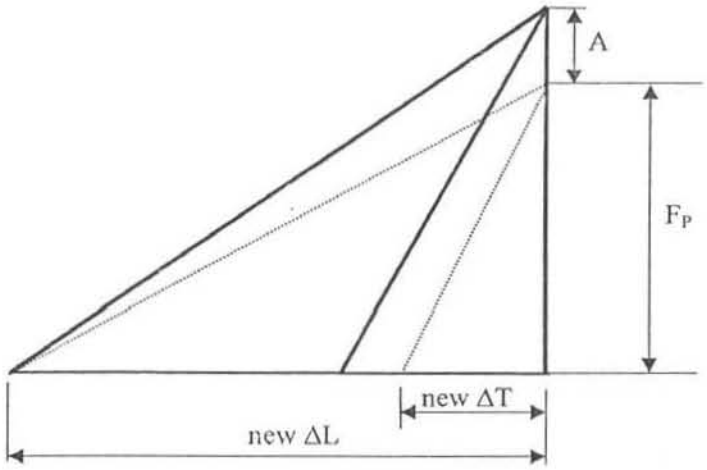

Figure 3.20 – ***The External Load Applied to the Joint Interface has Exceeded the Critical Load by an Amount A***

The mathematics of a tension load at the interface is very simple, and can be determined by inspection of the joint diagram.

The change in bolt force is:

$$\Delta F_B = 0$$

until the external load exceeds the preload, F_P, after which

$$\Delta F_B = L_X - F_P \qquad (3.52)$$

The critical external load required to cause joint separation is

$$L_{Xcrit} = F_P \tag{3.53}$$

This is true regardless of the spring constants, or spring constant ratios, of the bolt and joint members.

One of the keys of the first joint diagram was that the change in elongation of the bolt under an external load equalled the change in compression of the joint; but the changes in force in each were unequal. In the present case, where the tension load is applied at the interface, the deflections are not equal, but the force in the bolt is always equal to the force in the flange. So this present case could be called the inverse of the first.

The mathematics above indicates that there will be no change in the force seen by the bolt when tension loads are applied at the interface until the external load exceeds the original preload in the bolt. It is very desirable to be able to apply external loads to a joint in such a way.

On the other hand, interface loading gives a critical external load (the load required to cause joint separation) that is equal to the preload. This is less than the load required for separation when the tension loads are applied at joint surfaces. The load capacity of the interface joint, therefore, is less than the load capacity of the original joint (with external loads applied between the bolt head and nut).

The maximum bolt load, working change in bolt load, and critical external load are important design factors. They are different for each possible pair of loading planes, hence the importance of loading planes to the calculations.

A more complex situation can also be imagined: loading planes that are at some arbitrary point within the joint members, as suggested in Figure 3.21. Upon reflection, it is realised that:

- The bolt will still stretch when the external load is applied.
- The inner portion of each joint member – those portions nearest the interface – will unload when the external load is applied.
- The outer portions of each joint member, however, will be placed under additional compression load by the external load.

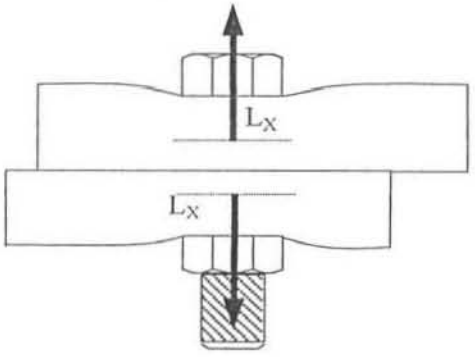

Figure 3.21 – ***External Load Applied at Some Point Within the Joint Members***

This could be plotted by placing the elastic curves for all the springs that are loaded (by the external load) on the left of the vertical F_P axis, and all of those that are unloaded on the right. This is not particularly helpful, however. It is simpler, and more meaningful, to realise that the head-to-nut and joint interface diagrams

developed earlier represent limiting conditions. In-between loading planes lead to in-between values for all factors of interest – bolt loads, joint loads, critical external load, etc. Designers can assume that the true values lie halfway between the limits; the computations will be accurate enough for virtually all applications.

One reason for avoiding calculations based on the true loading plane location is that this location is difficult to find – it is not really a true plane. A Finite Element Analysis or the like would probably be required to determine what portion of the flange members is unloaded and what portion sees added load when the external load is applied. It is complicated and unnecessary.

Note, however, that assuming the "worst case" loading of Figure 3.17, or even a loading plane halfway to the interface, can be so conservative as to seriously affect the assumptions about the amount of change in bolt load actually created by an external load.

External loads can also fluctuate. Consider a fluctuating load that is applied at the joint surface (bolt head to nut). The load applied will have a maximum value a little less than the critical load. With a static external load, the bolt sees a portion of the load and the joint sees the rest – the ratio depending on the relative stiffness of bolt and joint, at least until the external load exceeds the critical load. This fluctuating external load will cause the total tension load in the bolt and the load in the joint to fluctuate also (See Figure 3.22).

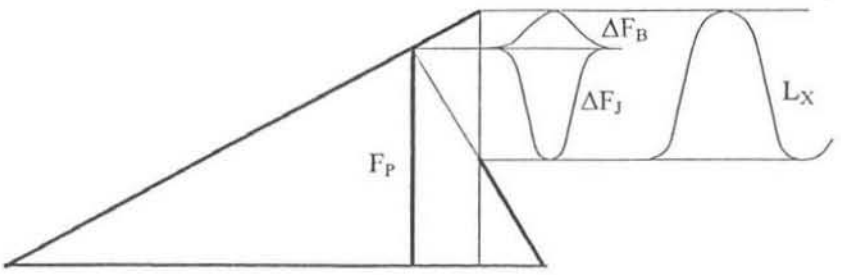

Figure 3.22 – *Bolt and Joint Loads when the External Load Fluctuates*

3.2.11 Fatigue Failure

A fastener subjected to repeated cyclic tension loads can suddenly and unexpectedly break – even if those loads are well below the yield strength of the material. The fastener fails in fatigue. Such failure, of course, is an example of gross "instability" of the clamping force. The force is lost, completely, as far as that fastener is concerned. If several fasteners fail in fatigue, and/or fatigue failure of one or a few fasteners overloads the rest, all of the clamping force on a joint can be lost. Although failures under repeated cyclic compression loads have been reported, these are rare and shall be ignored in this discussion.

Fatigue will only be a potential problem if four "essential conditions" are present:

- Cyclic tensile loads
- Stress levels above a threshold value (called the endurance limit)
- A susceptible material
- An initial flaw in the material.

If these conditions are all present, then a natural sequence of events can occur, and can lead to fatigue failure. These events are:

Crack Initiation: Many things can produce that first fatal flaw which starts the fatigue process. A tool mark can do this. So can a scratch produced when the part is mishandled. Improper heat treatment can leave cracks. Corrosion can initiate them. Inclusions in the material can also cause cracks. It is probably safe to say that no part is entirely free from tiny defects of this sort.

Crack Growth: A tiny crack creates stress concentrations. When the part is subjected to cyclic tension loads, these stress concentrations yield and/or tear the material at the root of the crack. Since most of the bolt still remains undamaged to support the load, initial crack growth is fairly slow.

Crack Propagation: As the crack grows, stress levels at the end of the crack also increase, since less and less cross section is left to support the loads. The crack grows more rapidly as stress levels increase.

Final Rupture: There comes a time when the crack has destroyed the bolt's capability to withstand additional tension cycles. Failure now occurs very rapidly. As far as the user is concerned, failure has been sudden and unexpected because, until this part of the fatigue process is reached,

there is often no visible damage or change in the behaviour of the bolt. Everything appears to be fine until suddenly, the bolt breaks.

The number of cycles required to break the bolt this way is called fatigue life. Apparently identical bolts in apparently identical applications can have, substantially different fatigue lives, depending on the location and seriousness of those initial cracks as well as on apparently minor differences in such things as bolt and joint stiffness, initial preload, alloy content, heat treat, location and magnitude of external tension loads, etc. As a result, there is a lot of scatter in the fatigue life of bolts used in a given application.

Fatigue failures are called high-cycle or low-cycle failures, depending on the number of load cycles required to break the part. High-cycle fatigue requires hundreds of thousands or even millions of cycles before rupture occurs. Low-cycle failure occurs in anything form one to a few tens of thousands of cycles. Low-cycle fatigue can be demonstrated by bending a paperclip back and forth until it breaks.

The number of cycles required to break a bolt is determined by the magnitudes of mean and alternating stresses imposed on the bolt by external cyclic loads. Low-cycle failure occurs under very large loads; high-cycle failure under lesser loads. In many applications the bolt can see some of each – lots of relatively mild loads interrupted once in a while by a sudden shock or larger load (e.g. when a tractor hits a rock). In many cases it is difficult to know whether to characterise the failure as a low-cycle or

high-cycle failure. In most well designed bolted joints, however, fatigue failure, if it occurs at all, will be high cycle.

Close examination of the broken bolt can often tell you whether or not it failed in fatigue. That portion of the break surface which failed slowly, as the crack initiated and grew, will have a relatively smooth and shiny surface. That portion which failed during crack propagation will have a rougher surface; that portion which failed during final rupture will have a very rough surface. If the entire fastener fails suddenly during tightening or the like, the entire break surface will be rough; so the smooth "beach marks" seen on a fatigue surface can be used to distinguish fatigue breaks from breaks which occur under static load.

More than one crack may be found in a bolt which has failed in fatigue. The initiation and growth of one crack may drastically increase loads in another region of the fastener, causing a second crack to grow and propagate there. Failure can occur in whichever one reduces the strength of the bolt more rapidly.

The most common places to find fatigue cracks and failures in bolts are in the regions of highest stress concentration. These are:

- Where the head joins the shank of the bolt
- The thread run-out point
- The first thread or two of engagement in the nut
- Any place where there is a change in diameter of the body or shank.

In general, the higher the cyclic loads seen by the bolt, the sooner it will fail. Whether or not, or how rapidly a fastener will fail depends on the mean stress level and the variation in stress level under cyclic loads.

There are techniques for estimating what the life of a given material and/or body will be. Accurate prediction, however, is possible only through actual experiments on the body of interest – on the bolt. Test results are usually presented in the form of S-N diagrams, where S stands for stress level and N for number of cycles of applied load. An examination of these diagrams gives considerable insight into the fatigue process.

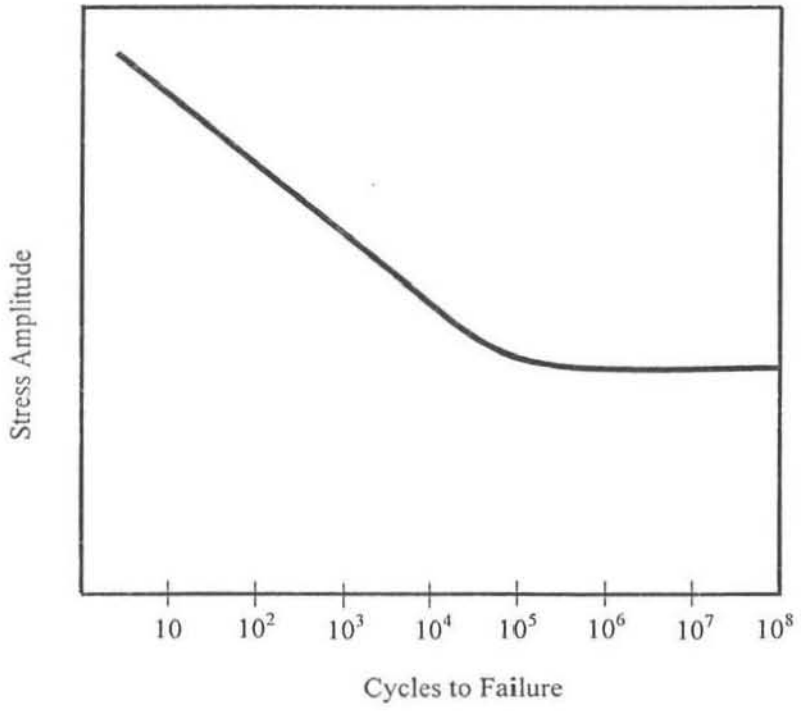

Figure 3.23 – *The Mean Life of a Group of Test Coupons Subjected to Fully Alternating Stress Cycles.* When stresses are "full alternating," maximum tension stress equals maximum compression stress and the mean stress on the part is zero.

Figure 3.23 shows one possible form of the S-N diagram. Alternating tension and compression loads have been applied to the test specimen. Maximum compression

stress equals maximum tension stress. Maximum amplitude of either stress is potted on the vertical axis of the diagram. The number of cycles required to cause failure to the test coupon is plotted on the horizontal axis. The curve shows the mean life of the test coupons.

Because the fatigue life of one test coupon may differ drastically from that of others, it is necessary to test many coupons before plotting the results shown in Figure 3.23. The statistical deviations in life can also be determined by such tests. A diagram such as that given in Figure 3.24, therefore, would show a more complete picture of the tests. Note that many of the test specimens will fail at some number of cycles less than the mean. The remainder will fail at some number of cycles greater than the mean. If the lowest line in Figure 3.24 represents the minus two standard deviation data, then 95% of the test coupons will survive more cycles before failure than the number of cycles indicated by this line. Only 5% will last longer than the number of cycles indicated by the uppermost line.

Note that either Figure 3.23 or Figure 3.24 says that cycle life will be very short when applied alternating stress levels are very high. As alternating stresses are reduced, cycle life increases. Below some stress level, in fact, the curve becomes essentially parallel to the horizontal axis, and fatigue life becomes very large. This stress level is called the endurance limit of the material or part and is defined as the completely reversing stress level below which fatigue life will be infinite. There is some such limit for any material and any part. Unfortunately, endurance stress levels are usually only a small fraction of the static yield strength or static ultimate strength of a material or body.

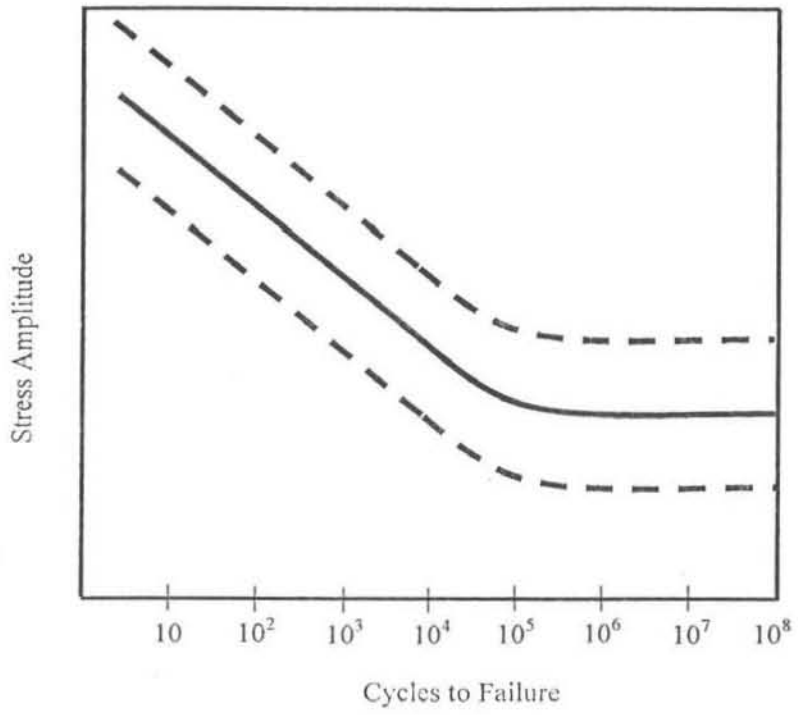

Figure 3.24 –*Mean Life Results and Statistical Deviations*

Another large number of specimens could be tested after changing the mean tension while leaving the excursion (difference between maximum and minimum tension) the same as it was in the previous tests. This would result in a family of curves such as that shown in Figure 3.25. For clarity, only the mean curves are shown.

Although all the S-N data examined thus far are based on tension (and/or compression) loading along the axis of the fastener, it must be noted that if the fastener is subjected to some other form of stress as well as tension, its fatigue life will be adversely affected. Shear stress, for example, would rob a portion of the strength of the fastener, making it more susceptible to tension fatigue.

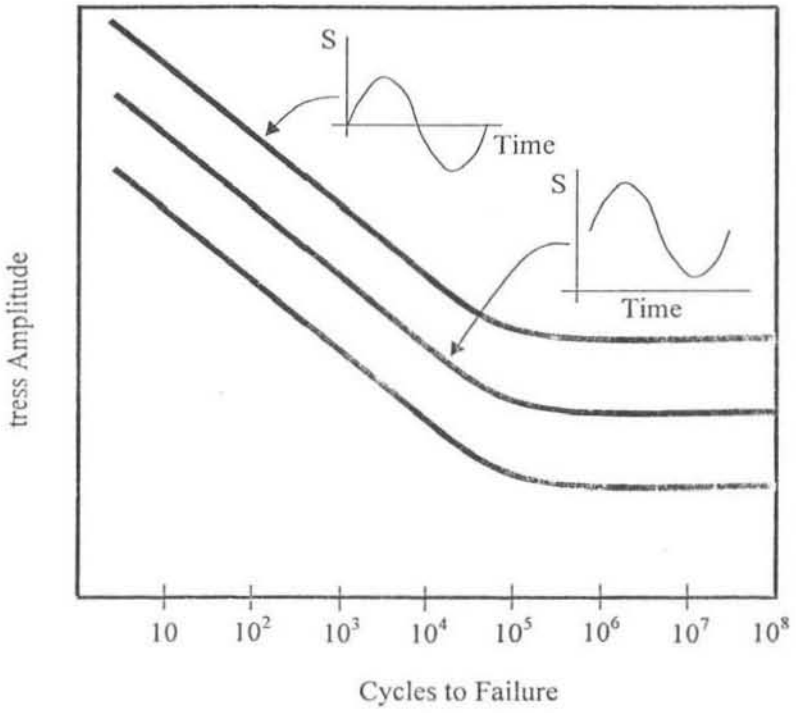

Figure 3.25 – *Effect of Changing the Mean Stress*

Fatigue life is a function of material and heat treatment. It is also a function of the shape of the part being tested because the shape of the body determines the stress levels. These vary from point to point; the behaviour of the body, therefore, varies from point to point. The gross behaviour of the body is determined by the accumulation of its point-to-point behaviour.

A bolt is a very poor shape when it comes to fatigue resistance. Although the average stress levels in the body may be well below the endurance limit of the material, stress levels in unavoidable stress concentration points such as the thread roots, heat-to-body fillets, etc., can be well over the endurance limit. As a result, the apparent endurance limit of commercial fasteners can be as little as 10% of the endurance limit of the base material.

In summary, the major factors which affect fatigue life are:

- Choice of material
- Shape of the part
- Mean stress level
- Magnitude of stress excursions or variations

Of these, the shape of the part may be the most significant, magnitude of stress excursions the next most significant, and within reason, material choice the least significant.

The bolt will see a portion of any external tension load which is imposed on the joint. The magnitude of the mean load on the bolt depends on the preload in the bolt. The magnitude of the load excursion, ΔF_B, depends on:

- The magnitude of the external tension load
- The bolt-to-joint stiffness ratio (K_B/K_J)
- Whether or not the external tension load exceeds the critical load required to separate the joint (which is determined by the magnitude of the initial preload)

The effect of the first two factors is summarised in Figure 3.26.

The triangular joint diagram can also be used to show the effects of very large external loads and/or insufficient preload. It is probably more instructive, however, to use the form of the alternative joint diagram as seen in Figures 3.27 through 3.30.

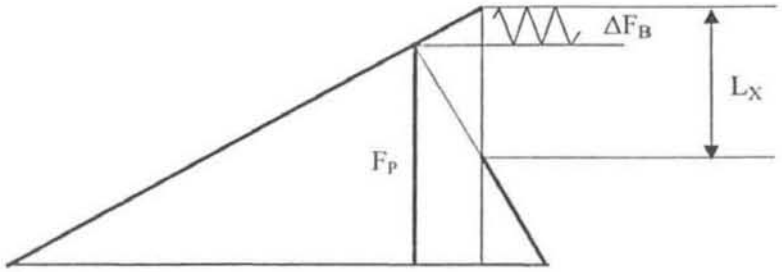

small L_X, small ΔF_B

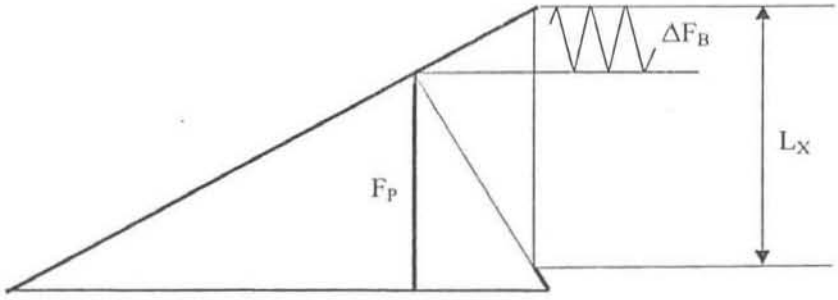

large L_X, large ΔF_B

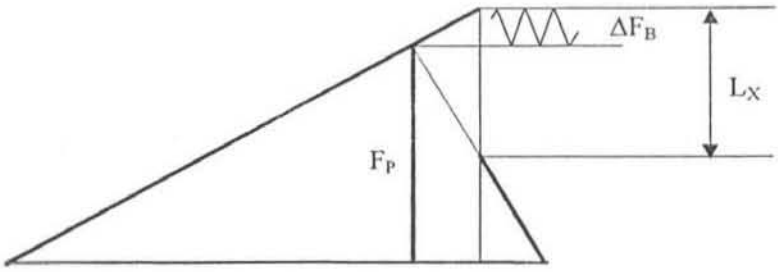

small (K_B/K_J), small ΔF_B

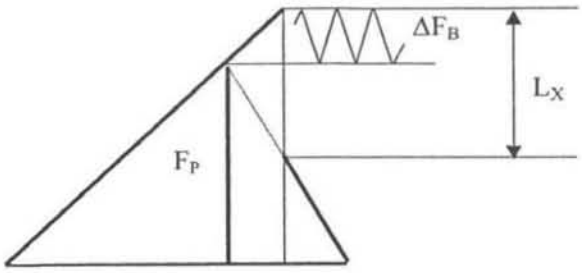

large (K_B/K_J), large ΔF_B

Figure 3.26 – *Load Variations*. The alternating loads, ΔF_B, in the bolt are increased with an increase in external load, L_X, and/or an increase in the bolt-to-joint stiffness ratio, (K_B/K_J). Note that the initial preload is the same in each case.

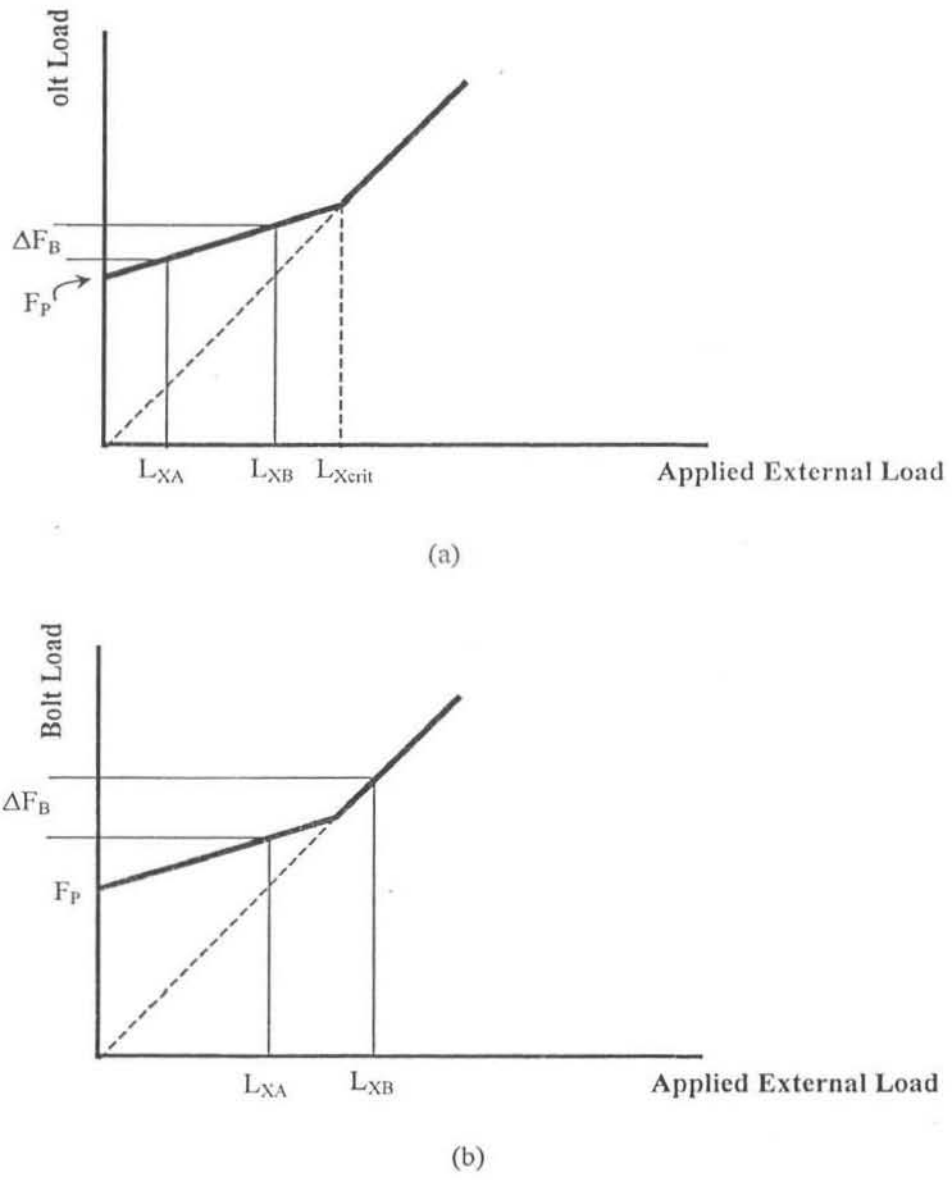

Figure 3.27 – *Alternative Bolt Diagram.* The bolt sees a far greater variation in tension, F_B, if the external load exceeds the critical load required for joint separation (as in (b)) than it does when external loads are less than the critical value (a). Note that the initial preload and joint stiffness ratio are the same in both cases

In Figure 3.27, for example, external loads are applied to two joints having the same initial preload and the same stiffness ratios as each other. Furthermore, the excursion (difference between maximum and minimum) of the external load is the same in both cases. Only the values of the maximum and minimum loads have changed. In Figure

3.27 (a), the maximum external load is less than that which would be required for joint separation. The resulting excursion in bolt load, ΔF_B, is relatively small.

In Figure 3.27 (b), however, the maximum external load exceeds the critical load. The bolt sees 100% of any external load that exceeds the critical level and so, under these circumstances, the excursion in bolt load is greatly increased.

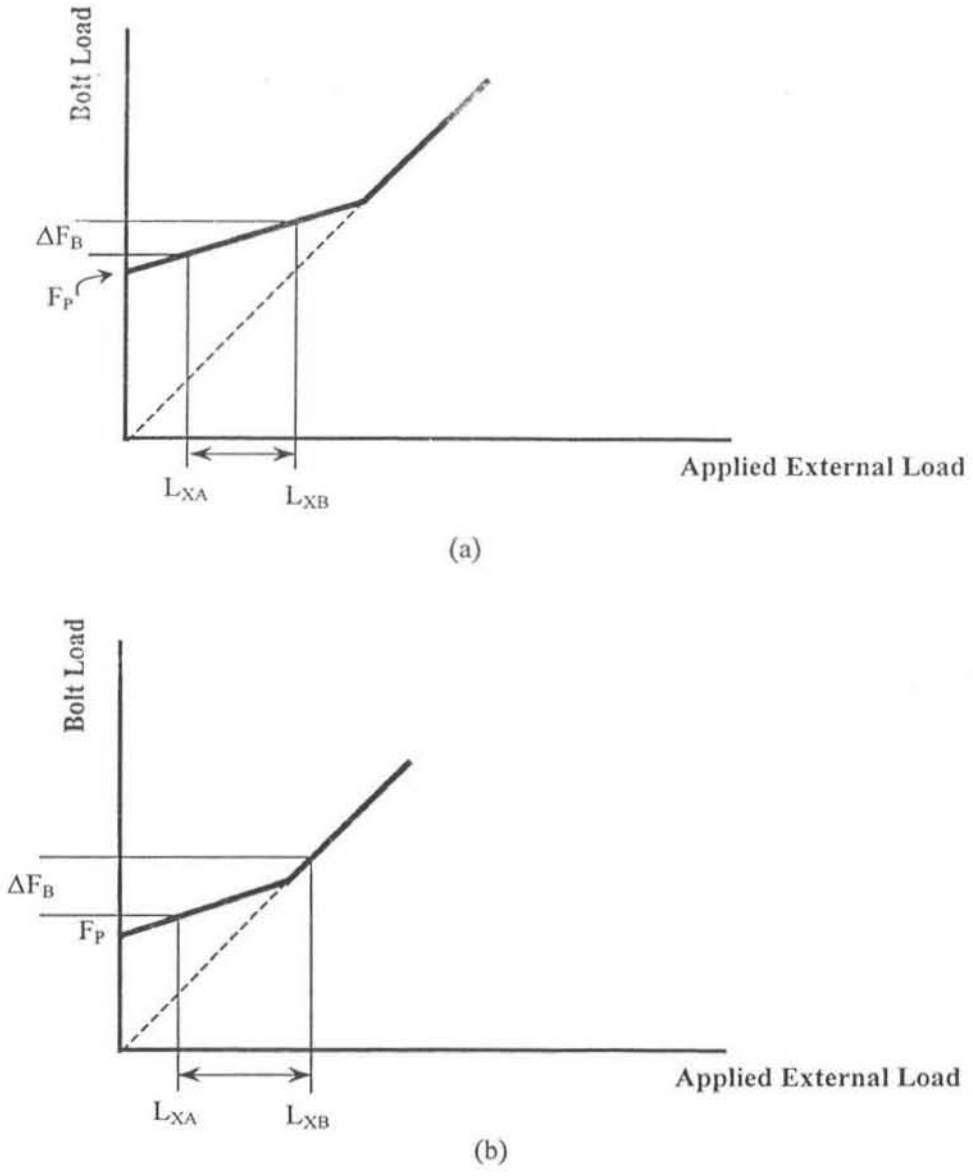

Figure 3.28 – ***Effect of Lowered Preload.*** The maximum and minimum external loads are the same in both cases here. The maximum load, however, exceeds the critical load required for joint separation in (b) because of insufficient preload, F_P. Note that the initial preload and joint stiffness ratio are the same in both cases.

The critical load depends on the initial preload. If the preload is lowered, the joint may fail too early, as shown in Figure 3.28. Conversely, of course, raising the preload in the joint can make the joint more "reliable."

The above analysis was based on the assumption that the joint will behave in a linear and fully elastic fashion. This is not always the case. If the external load, for example, is not applied along the axis of the bolt and/or the bolt is not located in the centre of the joint, prying action can increase the load seen by the bolt. This can make a substantial difference in the load excursions produced in the bolt by a given cyclic external load, as suggested in Figure 3.29.

With reference to Figure 3.27, one can sometimes reduce the load excursions seen by the bolt by increasing the preload. This only works, however, if the new, higher preload raises the critical load required for joint separation above the maximum external load seen by the joint. If the maximum external load was already below the critical level, increasing the preload does not reduce the excursion seen by the bolt, but merely increases the mean stress in the bolt, as shown in Figure 3.30.

Increasing the preload in an eccentric prying joint will also increase the mean tension seen by the bolt. This time, however, because of the non-linear nature of the joint, it is likely that increasing the preload will also reduce the load excursion seen by the bolt. Under these conditions, increasing the preload can result in a net gain in fatigue life. The increase in mean stress is detrimental but is more than offset by the reduction in excursion.

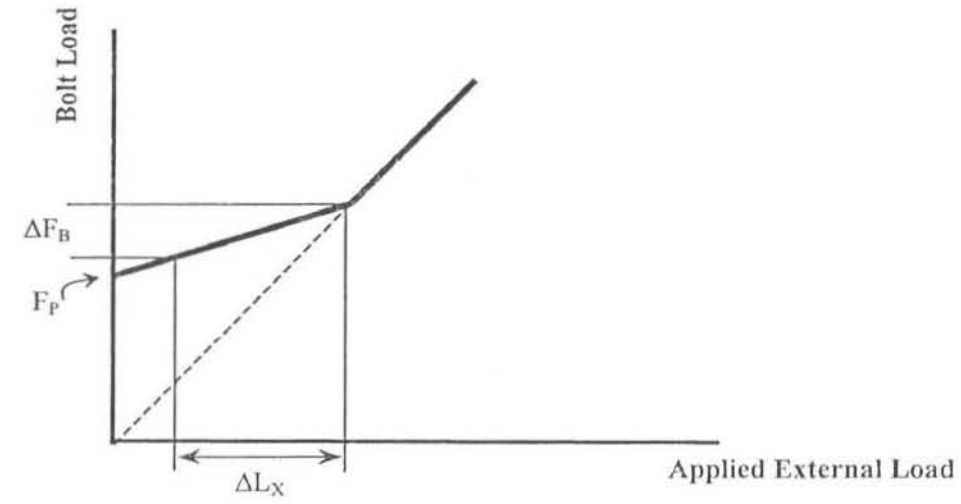

(a)

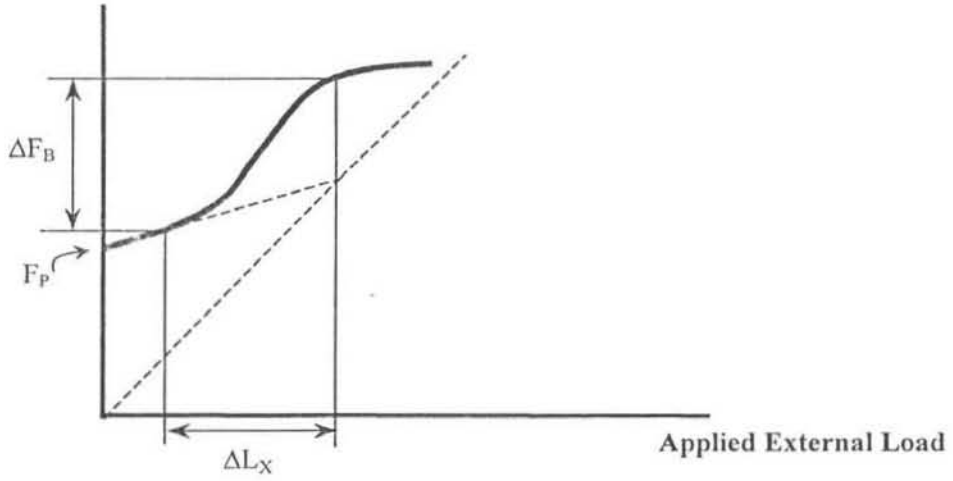

(b)

Figure 3.29 – ***Effect of Non-Linearity.*** This is a comparison of the loads seen by a bolt in a linear concentric joint (a), and an eccentric joint in which the bolt is subjected to prying action (b). Note that the initial preload, joint stiffness ratio and the maximum-minimum external loads are the same in both cases. At least apparent stiffness is the same. The fact that prying action occurs alters the stiffness of the joint.

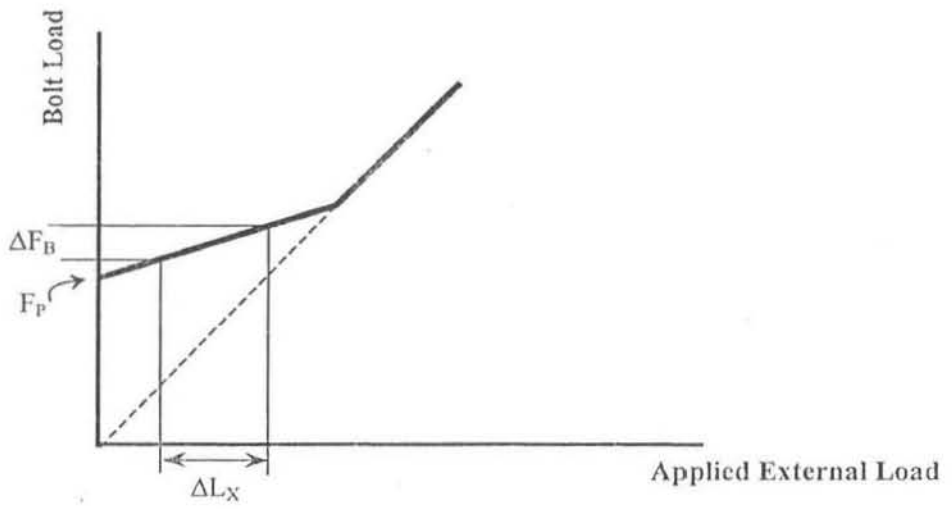

(a)

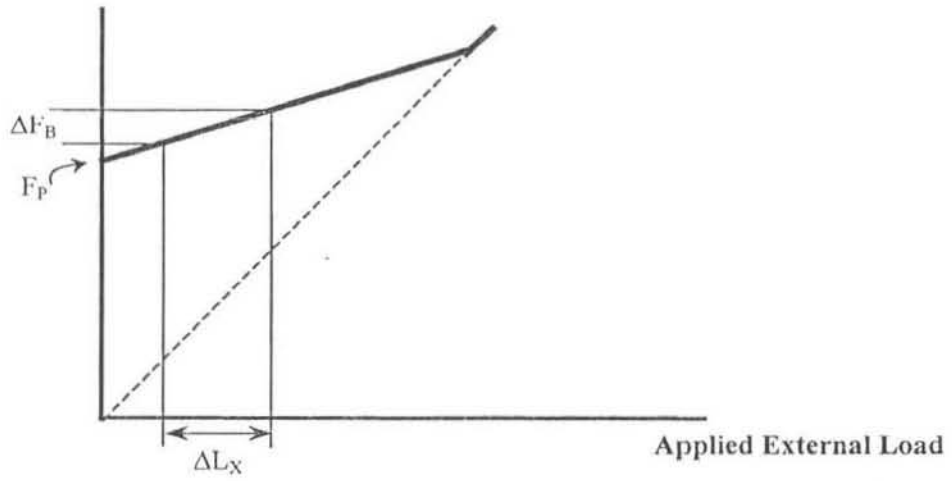

(a)

Figure 3.30 – *Effect of Higher Preload.* If the maximum external load is already below the external load required for joint separation, then raising the bolt preload will not reduce the load excursion seen by the bolt; it will merely increase the mean bolt load.

One is now in a position to answer the question, "What preload should be used for maximum fatigue life?"

In general, greater load excursions (or fluctuations) reduce fatigue life more than higher mean load – but neither is helpful. As a result, one can conclude that:

- A higher preload will help if it reduces bolt load excursions substantially. Higher preload will therefore always help if it raises the critical load required for joint separation above the maximum external load which will be seen by the joint. Higher preload will also help it if reduces the amount of prying experienced by the joint.
- A higher preload will reduce fatigue life if it makes no change in the load excursions seen by the bolt.
- A higher preload is probably neither good nor bad if it does not reduce the load excursions by very much. So, there are "grey areas" where results could go either way.

Some authorities argue that since most joints are eccentric, and since one is more likely to develop too little than too much preload as fasteners are tightened, one should operate under the assumption that more preload will always increase fatigue life [8]. Others argue that since a higher mean stress will reduce fatigue life, though not as much as a larger excursion will, a higher preload can be helpful but also might not be [9], and only a careful analysis will answer the question.

It should be realised that each of the things that can be done to reduce or eliminate a fatigue problem is an attempt to overcome one or more of the four essential conditions without which failure would not occur. Recall, these conditions are cyclic tensile loads, stresses above an endurance limit, a susceptible material, and an initial flaw. Any one of these can rarely be eliminated completely, but if one or more of these factors can be reduced, the fatigue life of bolted joints can usually be improved.

In general, most of the steps one can take are intended to reduce stress levels (including stress concentrations) and/or to reduce the load excursions seen by the bolt. Surface flaws and the susceptibility of the material will usually be the concern of the bolt manufacturer rather than the user.

The following are not listed in order of importance. They merely describe some of the many things which can be and are manipulated to limit fastener stress concentrations and/or general stress levels. Some of them are relatively obvious; others are subtle. Many are incorporated in so-called fatigue-resistant fasteners which are available from some manufacturers.

Rolled Threads: Rolling of the threads instead of cutting them provides a smoother thread finish (fewer initial cracks). Rolling provides an unbroken flow of the grain of the material in the region of the threads, partially overcoming their notch effect, and it builds compressive stress into the surface of the bolt. This compressive "preload" must be overcome by tension force before the thread roots will be in net tension. A given tension load on the bolt, therefore, will result in a smaller tension excursion at this critical point (point of stress concentration).

Threads can be rolled either before or after heat-treating. After is better but is also more difficult. Rolling before heat-treating is possible on larger diameters.

Fillets: A generous fillet between head and shank will reduce stress concentrations at this critical point. The exact shape of the fillet is also important; an elliptical fillet, for example is better than a circular one.

Increasing the radius of a circular fillet will help. So will pre-stressing the fillet (akin to thread rolling).

Perpendicularity: If the face of the nut, the underside of the bolt head, and/or joint surfaces are not perpendicular to thread axes and bolt holes, the fatigue life of the bolt can be severely affected. A two-degree error reduces fatigue life by 79% [10].

Overlapping Stress Concentrations: Bolts normally have stress concentrations at thread run-out, first threads to engage the nut, and head-to-shank fillet. Anything which imposes additional load or concentration of load at these points is particularly damaging. For best performance, for example, there should be at least two full bolt threads above and below the nut. Thread run-out should not coincide with the joint interface, where shear loads exist.

Thread Run-Out: Thread run-out should be gradual rather than abrupt.

Thread Stress Distribution: Most of the tension in a conventional bolt is supported by the first two or three nut threads. Anything which increases the number of active threads will reduce stress concentrations and increase fatigue life.

Modifying the nut pitch so that it is slightly different to the pitch of the bolt threads can also make a substantial improvement in fatigue life.

Another way to smooth stress distribution in the threads is to use a nut that is slightly softer than that bolt. The nut will be able to conform to the bolt more readily. Standard nuts are softer than the bolts they're used with, for this reason; still softer nuts are possible if the loss in proof load capability can be tolerated.

A helical thread insert in a tapped hole also "conforms" to the male threads, because the insert is flexible; but the insert does not reduce static strength the way a soft nut will.

A lock nut improves thread stress distribution too, by pre-loading the threads in a direction opposite to that of the final load.

A final way to improve thread stress distribution is to taper them slightly.

Bending: Bending increases the stress levels on one side of the fastener. This is one of the reasons why nut angularity hurts fatigue life. One way to reduce bending is to use a spherical washer.

Corrosion: Anything done to minimise corrosion will reduce the possibilities of crack initiation and/or crack growth and will therefore extend fatigue life. This is confirmed by the fact that running bolts in a strong vacuum results great improvement in fatigue life because it completely eliminates corrosion.

Surface Condition: Any surface treatment which reduces the number or size of incipient cracks can improve fatigue life substantially. Polished surfaces, for example, will make a big difference. Shot peening the surfaces also helps – not only because it smoothes out beginning cracks, but also because it puts the surfaces in compressive stress (as much as thread rolling does).

Nothing can help extend the fatigue life of a bolt or joint more dramatically than a reduction in load excursions. The following are some ways of doing this:

Proper Selection of Preload: Correctly identify the maximum safe preload that the joint can withstand, estimating fastener strength, joint strength,

and external loads, analysing them carefully with the help of a suitable joint diagram.

Control of Bolt-to-joint Stiffness Ratios: One should do whatever is required to minimise the bolt-to-joint stiffness ratio, so that most of the excursion and external load will be seen by the joint and not by the bolt. The use long, thin bolts, for example, instead of short, stubby ones, even if it means using more bolts in a given joint, helps significantly.

Achieving the Correct Preload: Poor quality tools and/or controls will increase the preload scatter and force one to work to a lower mean preload.

Techniques for predicting the endurance limit or fatigue life of bolts have been widely researched. Some experts say that the endurance limit of bolts is only about one tenth the endurance limit of the base materials [1]. Others say that the cyclic loads imposed on a joint should be kept below 4% of the ultimate tensile strength of the fasteners if infinite life is desired [13]. Yet another source says that a guess of the endurance limit can be achieved by experimentally determining the endurance limit of a polished, notch-free specimen of bolt material, then dividing that limit by a suitable stress concentration factor [14].

The following is a more carefully though-out way to estimate the endurance limit of a bolt. Typical automotive companies estimate the endurance limit, $S_n{}'$, by multiplying

the endurance limit of a standard test specimen by a series of "correction factors" using the following equation:

$$S_n^1 = S_n(C_1 \times C_2 \times C_3) \tag{3.54}$$

where

S_n = the endurance limit of a standard test coupon (normally taken as one-half of the ultimate tensile strength for wrought ferrous metals, or 0.4 of the ultimate tensile strength for stainless steels)

C_1 = the loading factor (0.85 for axial loading, 0.58 for torsional loading)

C_2 = the size vs. type of stress effect factor (0.85 for bending or torsional loads in fasteners 0.5" to 2" in diameter, 1.0 for axial loads of any diameter)

C_3 = the stress concentration factor (0.3 for rolled threads in quenched and tempered fasteners)

Other correction factors are added if the fastener is to be exposed to a corrosive environment or if the consequences of failure are great and a safety or reliability factor is added.

To guarantee that 98% of the fasteners will exceed the predicted life, for example, a reliability factor $C_4 = 0.8$ is included in the equation.

The multipliers need not all be less than 1.0. If the fastener has been cold-worked, or surface-hardened and plated, correction factor C_5, greater than 1.0 can also be included.

4. Strength of Trip Steels

4.1 Background

The TRIP (transformation induced plasticity) effect was observed in high alloyed austenitic steels about 30 years ago. The excellent combination of strength and ductility of these steels is attributable to the irreversible strain-induced austenite-to-martensite phase transformation during plastic straining. An austenite-to-martensite phase transformation also implies a change from a non-magnetic to magnetic material. The high content of expensive alloying elements, however, limits industrial applications.

Through a special two-step heat treatment it became possible to stabilise significant amounts of austenite at room temperature even in low alloyed steels. The typical chemical composition is in the range of 0.2 wt.% carbon, 1.0-2.5 wt.% silicon and 1.0-3.0 wt.% manganese. The high silicon content of such steels leads to undesirable hot rolling properties. This one disadvantage of the application of TRIP steels for the SmartBolt as rolled threads will increase fatigue life.

The steels display a solid-state, strain dependent phase transformation from a metastable, austenitic (face-centred-cubic crystal structure) parent phase to the thermodynamically stable, martensitic product phase.

The strain-induced phase transformation is responsible for the incredible values of ductility and strain hardening that are observed in these steels. As the material begins to yield or enter into the plastic deformation regime, the phase transformation is triggered. The extent of transformation increases with the applied strain so that more and more strain-induced martensite forms as strain increase. The transformation occurs inhomgeneously along the gauge length of a tensile specimen such that the regions where martensite has formed become stronger than the rest of the

gauge length and so necking is delayed. Once the transformation occurs to a significant extent along the entire gauge length, the specimen deforms homogeneously throughout the gauge length until failure, typically with very little or no necking associated with final fracture.

Specimen elongations (at ambient temperature) of 40% to 60% were observed for materials with yield strengths over 1379MPa. Typical elongations for conventional high strength steels are 10% to 15%.

Early work in this topic was centred on understanding the nature of the phase transformation and the associated changes in mechanical behaviour accompanying the phase transformation. There was also much attention directed at ausforming, a method of thermomechanical fabrication treatment whereby metastable austenite is warm-rolled to produce a high dislocation density to increase the yield strength of the materials. This warm-rolling process was performed at a temperature above that necessary to cause any strain-induced phase transformations. Research related to the phase transformations in austenitic stainless steel was also conducted. Much of the understanding of the behaviour of austenitic stainless steels applied either directly or indirectly to understanding TRIP steels, which themselves are austenitic.

4.2 Mechanical Behaviour of TRIP Steels

The delay of necking and the resultant, dramatic increases in energy absorption during fracture can best be appreciated by considering the nature of the simple, uniaxial tension stress-strain behaviour. The tensile properties of high-strength and low-strength variants of TRIP steels are compared with those of structural steels and the high-strength, low-alloy (HSLA) steels in Figure 4.1. While the strongest TRIP steels are stronger than the HSLA steels, the ductilities and energy absorption capacities of TRIP materials make them impressive candidates for many

applications requiring high-strength. Figure 4.2 compares representative stress-strain curves for TRIP steels to the HSLA steels and structural steels.

While the areas under the engineering curves provide an indication of toughness, it is necessary to consider the true stress-strain curves to calculate the energy absorbed during fracture:

$$E_V = \int_0^{\varepsilon_f} \sigma(\varepsilon) d\varepsilon$$

where, E_V = energy absorbed per unit volume

ε = true strain

ε_f = true failure strain

$\sigma(\varepsilon)$ = the true stress expresses as a function of true strain

Type II materials, which include the metastable Fe-Mn-Cr alloys, have received less attention for a variety of reasons. They are not as strong, but they have also not been evaluated in a condition other than as-austenitised using the simplest in heat-treating processing schemes. In order to obtain the highest yield strengths depicted in Figure 4.1 for the type I TRIP steels it is necessary to process the material thermomechanically using complicated and expensive schemes. The type II materials were simply austenitised and either air-cooled or quenched to room temperature. The type I TRIP steels have much lower yield strengths if not thermomechanically processed to produce the high strength levels, but still retain extraordinary levels of uniform elongation. Type I TRIP steels in this weaker condition are referred to as low strength type I TRIP steels. The lower yield strengths of the type II TRIP steels, more typical of those in standard structural grade steels, also reflect the lack of thermomechanical processing. High strain hardening rates and elongations are observed with ultimate tensile strength to yield strength ratios in the range of three to four being quite common. The corrosion resistance of the type II TRIP steels is superior

to that of the type I materials due to the higher levels of chromium added to their chemical formulations. In addition, both the type I and type II TRIP steels experience the strain-induced phase transformations responsible for delaying mechanical instability and necking in uniaxial tensile testing. The increased uniform plastic deformation observed in these alloys corresponds to increased levels of energy absorption capacity.

Whereas the energy absorbed per unit volume is generally much greater after the neck forms, the actual volume of material participating in the deformation process must be taken into account. TRIP steels display uniform elongations, i.e., non-localised deformation throughout the entire gauge length, and in so doing, the entire gauge length is contributing to energy absorption. Indeed, in many TRIP steels there is little, if any, necking and localised deformation behaviour prior to failure. Thus, the maximum amount of energy absorption occurs.

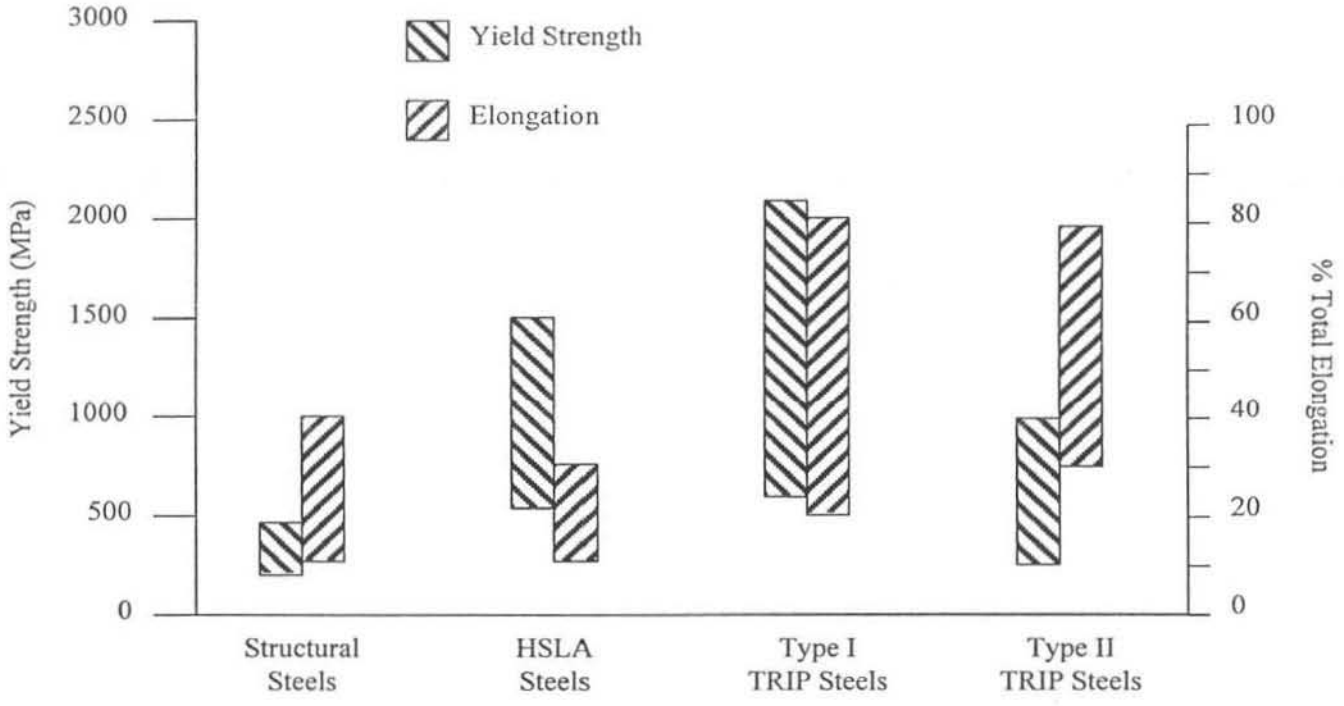

Figure 4.1 – ***A Comparison Of The Tensile Properties For Structural Steel Materials***. For illustrative purposes only – not drawn to scale.

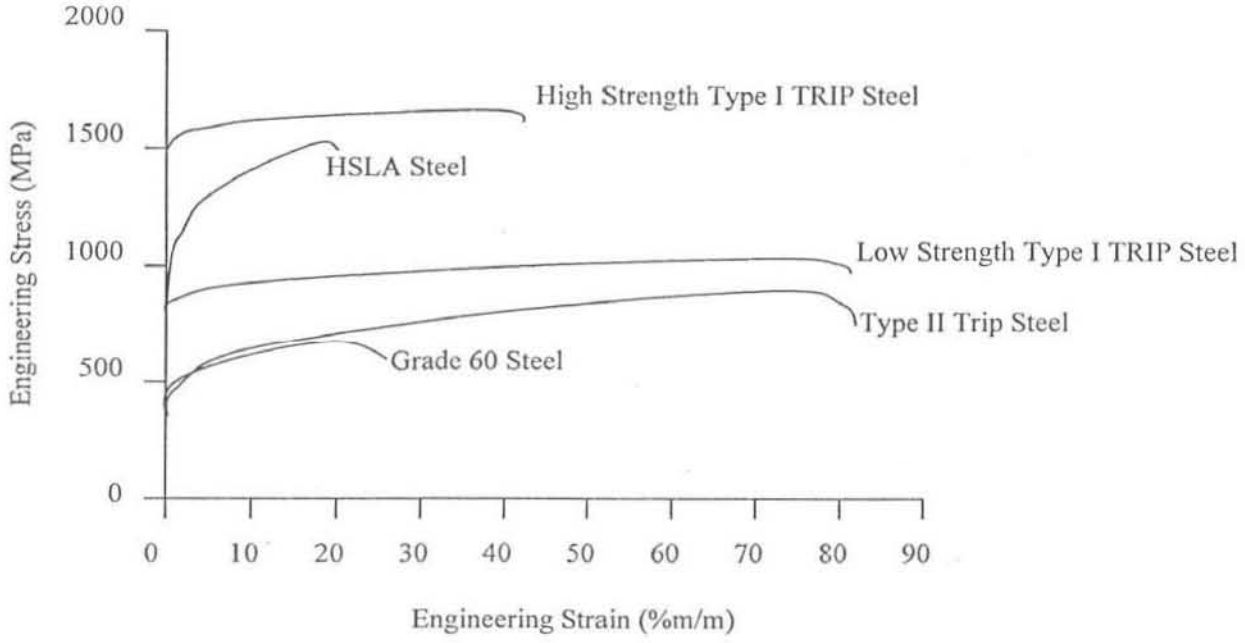

Figure 4.2 – ***Representative Engineering Stress-Strain Curves for Structural Materials.*** For illustrative purposes only – not drawn to scale.

Figure 4.3 shows the true stress-strain curves for a TRIP steel processed in three different ways and those for two different tempers of 4340 steel. The necking point for each test is shown by a circle on the respective curve. Any further deformation beyond the necking strain is locally concentrated within the necked region of the tensile specimen gauge length. The true strain at necking represents the point at which the gauge volume deformation begins to concentrate in the localised region to become the neck. So, at strains below the necking strain the entire volume (either gauge or component) is absorbing energy. Beyond the necking strain, only the neck volume is actually absorbing energy. The true strain at necking, sometimes called the strain hardening exponent, n, is therefore a useful parameter in modelling the deformation response of a material.

The fracture energy absorption capacity of a material is directly related to the strain hardening exponent, i.e., to maximise fracture energy, high values of n are desirable. TRIP steels have a combination of high strength and high ductility, thus accounting for their fracture resistance.

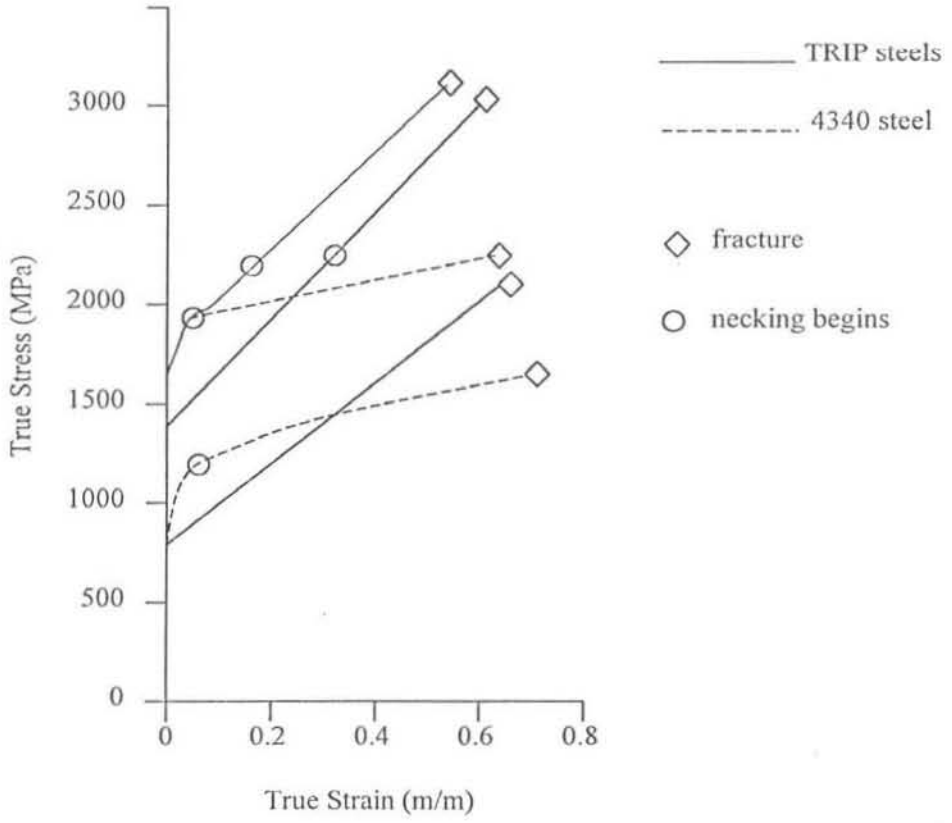

Figure 4.3 – ***True Stress-Strain Curves for a HSLA Steel (AISI 4340) and a Type I TRIP Steel.*** Different curves represent different processing conditions for the materials. For illustrative purposes only – not drawn to scale

The total fracture energy per unit volume, E_V, is the sum of energy absorbed per unit volume prior to and after necking:

$$E_V = \int_0^{\varepsilon_{uts}} \sigma(\varepsilon)d\varepsilon + \int_{\varepsilon_{uts}}^{\varepsilon_f} \sigma(\varepsilon)d\varepsilon$$

where, ε_{uts} = true strain at the ultimate tensile strength

(all other symbols have been defined previously)

Total energy absorption during fracture is then obtained by multiplying the respective integrals by the corresponding volumes participating in deformation before (V_0)and after (V_n) necking:

$$E = V_0 \int_0^{\varepsilon_{uts}} \sigma(\varepsilon)d\varepsilon + V_n \int_{\varepsilon_{uts}}^{\varepsilon_f} \sigma(\varepsilon)d\varepsilon$$

The low-cycle and high-cycle fatigue properties of TRIP steels have also been evaluated. Figure 4.4 shows high-cycle fatigue data for a type I TRIP steel compared with those of three high performance structural alloys. Again, the combination of strength and fatigue resistance displayed by the TRIP steel is superior to that of the other materials. The electro-slag remelt 4340 HSLA steel displayed much better fatigue properties as compared to the conventionally melted material due to the lower density of non-metallic inclusions, but the combinations of fatigue and ultimate strengths for the high-strength TRIP steels were unequalled.

Table 4.1 compares the energy absorption characteristics of the materials for which properties are displayed in Figure 4.3. The volume of material associated with necking is assumed to be one-tenth of the total gauge length volume, i.e., $0.1V_0$. For the sake of the calculations, V_0 is assumed to be $1m^3$. The true strain at necking is sometimes referred to as the strain hardening exponent, n. The entire gauge volume absorbs energy during the uniform plastic deformation at true strain levels grater than n. The three TRIP steel variants absorb considerably more energy during fracture than the two variants of HSLA steels. Both types of steels can be processed to achieve a range of stress-strain behaviour, but the effectiveness in delaying necking of the deforming gauge section is readily apparent in the levels of energy absorbed. One interesting aspect of the data is that the lower strength TRIP steel variant, which had a true strain at necking equal to 0.6, absorbs considerably more energy than all of the high-strength steels including the high-strength TRIP steels. These estimates of energy absorption indicate the enhanced structural

safety that could be realised through selective utilisation of TRIP steels as structural components. The additional energy absorption would be particularly beneficial in structures subjected to earthquake-induced cyclic deformation where the energy absorption would delay structural collapse, thereby enhancing structural safety. It is also interesting to note that while the yield strength of the materials can be raised to impressive levels, the energy absorption is actually much higher in the lower yield strength TRIP steel as compared to the other materials. This is one of the points that remains largely unappreciated as far as selective use of TRIP steels in structural applications is concerned.

Steel	σ_{yield} (MPa)	n value	$E_v(\varepsilon<n)$, (MJ/m^3)	$E_v(\varepsilon>n)$, (MJ/m^3)	E_{total} (MJ/m^3)
TRIP	760	0.60	858	N/A	858
TRIP	1400	0.35	433	56	489
TRIP	1600	0.25	395	104	499
4340	800	0.10	100	85	185
4340	1600	0.08	138	104	242

Table 4.1 – *Energy Absorption Characteristics for TRIP Steels and HSLA 4340 Steels.* $V_0 = 1m^3$ and $V_n = 0.1m^3$.

The TRIP steels have the inherent capacity to delay necking as a result of the strain-induced phase transformation. If a mechanical instability initiates within the deforming section during plastic deformation, any further straining is concentrated within the unstable region. This would lead to the formation a true neck in the conventional steel materials. The unstable region in a TRIP steel component transforms from the weaker austenitic phase to the stronger martensitic phase thereby making the local region stronger than the surrounding material so that deformation continues without the formation of a true neck. This process is repeated throughout the deforming gauge section of a tensile specimen or deforming region of a component. A true

strain of 0.60 corresponds to an engineering strain of 0.82, i.e., a uniform elongation of 82% which is truly phenomenal for a material with an yield strength above 700 MPa. This compares with an engineering strain at necking of 10.5% for the low-strength 4340 and 8.3% for the high-strength 4340 variant. Figure 4.4 shows a comparison between the fatigue properties of TRIP steels with those of conventionally melted 4340 steel, electro-slag remelted (ESR) 4340, high-strength alloy 300M (currently used in aircraft landing gear applications) and high performance alloy HP9-4. The ultimate tensile strengths and fatigue endurance limits for 10^7 cycles are plotted for fatigue tests where the minimum-to-maximum load ratio, R, is 0.1. Again, the TRIP steels display excellent fatigue properties, particularly in the higher strength materials where their combinations of tensile strength and fatigue endurance limits are unequalled by the other materials which are currently considered as superior, commercially available, structural materials.

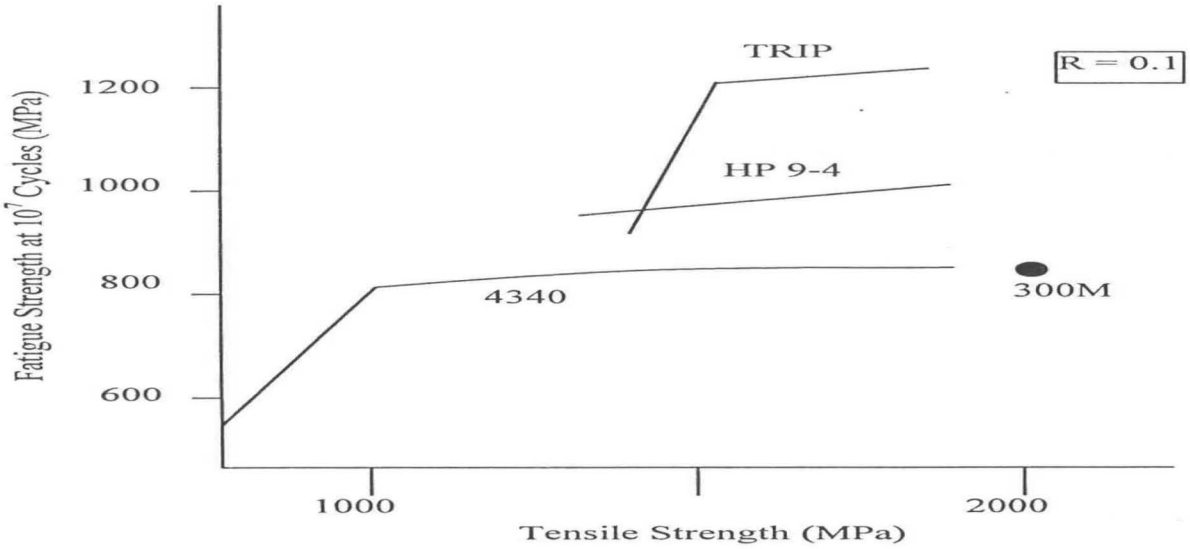

Figure 4.4 — ***High-Cycle Fatigue Properties of a TRIP Steel and High Performance Structural Steels.*** For illustrative purposes only — not drawn to scale.

5. Smart Bolt Analysis

5.1 Objectives of the Analysis

The objective of the analysis is to observe the effect of a small, hole drilled through the centre of the bolt, on the bolt strength. This hole would be used to insert an electronic sensing device which would indicate the presence of plastic strains by sensing the presence of magnetic material. The modified bolt will still operate under the same conditions as the old one, thus it is desired that the analysis shows adequate strength of the modified bolt for effective service. The relative amount by which the stresses in the bolt change is analysed.

Only the most critical bolts on the aircraft wing (the larger, bottom ones) have been analysed.

5.2 Design Philosophy

After careful consideration of all the possible approaches to the analysis and evaluation of all the data available (most of the Aircraft's design data was classified), the following approach was selected:

Step 1: *Determine the load(s) applied to the bolt.* This load would be approximated conservatively from the available data, and using guidelines from Section 3.

Step 2: *Analyse the existing (old) bolt.* The analysis inputs would comprise the theoretical geometry of the existing bolt (simplified for modelling purposes), applicable material data, and the load(s) as determined in

Step 1. Some of the concepts discussed in Section 2 were used to build an appropriately reliable model, e.g. imposed load.

Step 3: *Analyse the bolt with a "small" centrally-drilled hole.* The size of the hole would be varied up to 5mm and a stress trend for the different sized holes would be established. The applied load would be as determined in Step 1.

At first thought, one might be tempted to use the following simple tensile stress formula to find the bolt stress:

$$\sigma = \frac{F}{A} \qquad (5.1)$$

where, F = applied force

A = cross sectional area

σ = tensile stress

The analysis, however, is much more complex. The fact that the bolt is in fatigue service cannot be ignored. Because the bolt has already been designed (or selected) based on its expected fatigue service, the actual tensile strength of the body of the bolt would be much smaller than that required for simple tensile failure. Fatigue failure is anticipated at the stress concentrations, and as discussed in Section 3, stress concentrations are expected at:

- The root of the first engaged thread
- The thread run out point
- The fillet between the shank and head

The South African Airforce workshop and inspection personnel report that failures occur at the root of the first engage thread.

The distribution of stresses (occurring at stress concentrations) through the bolt must also be observed. For these reasons, Finite Element Analysis was performed.

The primary function of the aircraft bolt presently under consideration, is to clamp the outer wing to the inner wing (See Section 5.3). This implies that the primary stress in the bolt is tension. Bolts are generally designed to operate in tension. Thus, the analysis only addresses pure tension loads applied to the bolt.

5.3 Design Data

The first step to design data procurement constituted visits to the South African Airforce Waterkloof air base. This opportunity offered valuable experience and understanding of the operational environment of the bolt, its actual location in the wing structure, the shape of the structure, etc. In addition, the visits presented an opportunity to establish contacts with the aircraft maintenance and inspection personnel. This facilitated valuable data exchange.

Figure 5.1 shows a picture of a C-130 aircraft and the arrows indicate the location of the bolts whose design is considered here. There is one "row" of bolts on the top of the wing ($^3/_4$"), and another at the bottom ($^7/_8$"). These bolts are located underneath an easily removable panel which protects the bolt from corrosive mediums and also provides some insulation against extremely low temperatures (reducing the risk of brittle fracture).

Figure 5.1 – *The C-130 Aircraft*. The arrows show the location of the bolts under consideration: one row at the top, and another at the bottom.

Figure 5.2 shows a picture of another C-130 aircraft in the workshop undergoing complete maintenance and inspection. The particular aircraft had been out of service for a long time, so the maintenance and inspection work could almost be called a refurbishment.

For the purpose of this investigation, the panel covering the row of bolts on the top of one wing was removed, revealing the location of the bolts in the structure. This is shown in Figure 5.3.

Figure 5.2 – ***A C-130 Aircraft Undergoing Full Maintenance And Inspection In The Workshop***

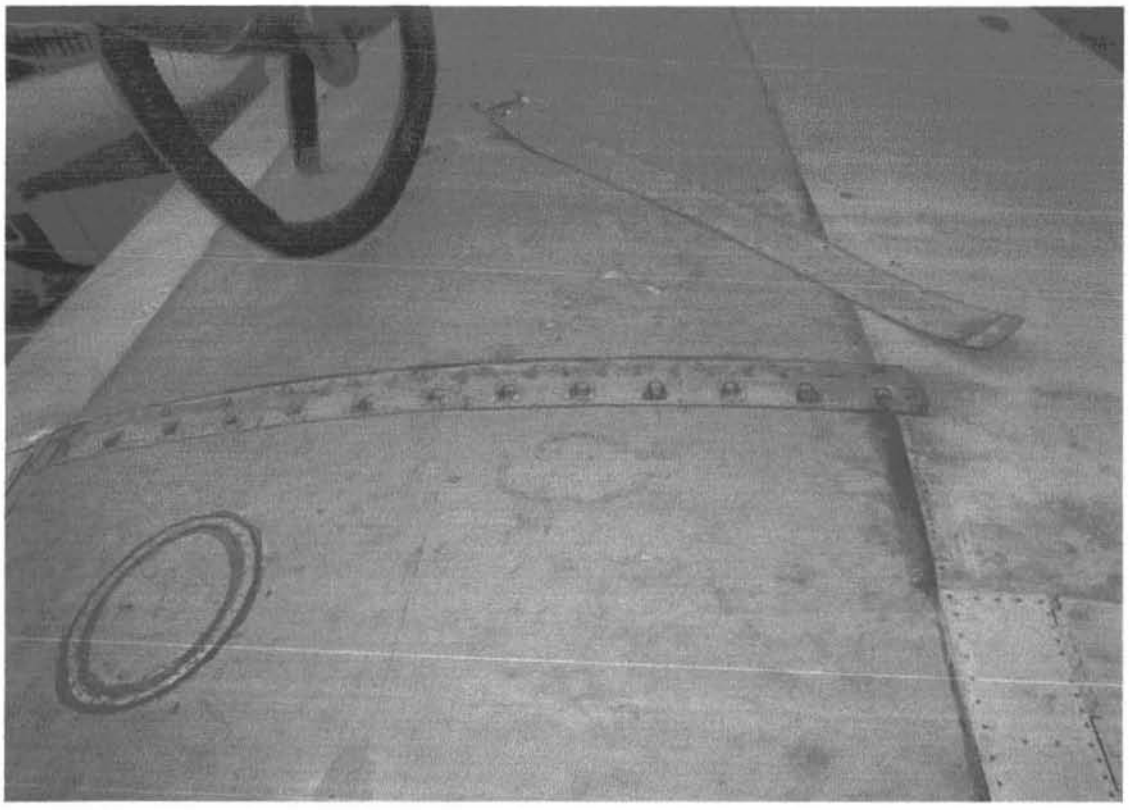

Figure 5.3 – ***Location Of The Bolts In The Wing Structure.*** This picture was taken from the top of the wing.

Figure 5.4 shows a close-up picture of one bolt located in the structure. Note that this is taken from the top of the wing where the bolts are smaller ($^3/_4$") than the ones at the bottom ($^7/_8$").

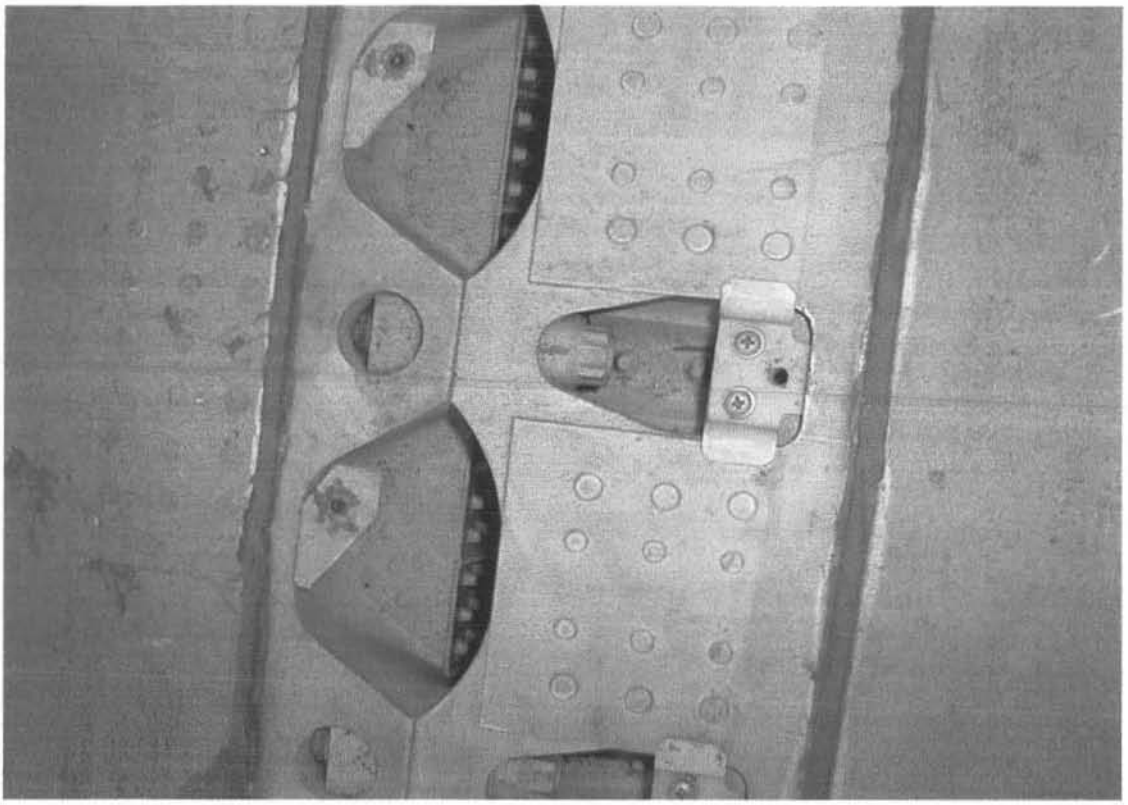

Figure 5.4 – ***A Close-Up View Of A Bolt Located In The Wing Structure***

Figure 5.5 shows a picture of two new bolts obtained from the air base store.

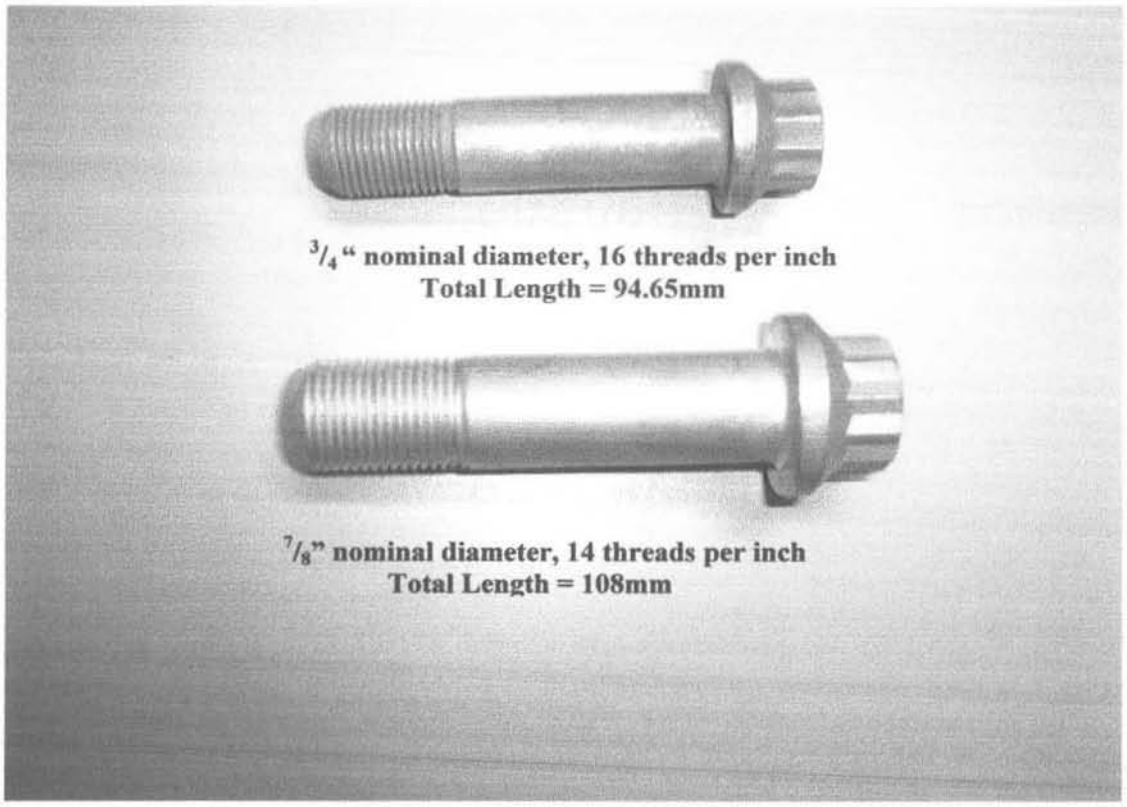

Figure 5.5 – *New Top And Bottom Wing Bolts*

As these aircraft were built several decades ago, one would expect that due to technology advances, replaceable part (like bolts and nuts) specifications (e.g. materials, thread dimensions) would not necessarily be the same as originally specified at the time of manufacture.

The bolt data (dimensions and material properties) used in the present analysis were obtained from the bolt manufacturer, SPS Technologies, and is applicable to new items available today. The data is contained in Appendix A. Some dimensions were measured directly from the new bolts.

5.4 Calculation of the Applied Load

Information regarding the geometry of the bolt is contained in Appendix A. The following calculations address the applied load.

The torque applied to the bottom bolts, according to workshop personnel, is 220 lb.ft (or 298 Nm). The preload, F_P of the bolt can be estimated using the formula:

$$T_{in} = F_P(KD) \qquad (2.27)$$

where T_{in} = input torque = 298 Nm

F_P = achieved preload

D = nominal diameter of the bolt = $^7/_8$" or 22.225 mm

K = "nut factor" (dimensionless)

As discussed in Section 3, the nut factor, K, is determined experimentally, but usually ranges from 0.15 to 0.25. Its mean value is 0.199, with a standard deviation of 0.05. K = 0.199 is used here:

$$F_P = \frac{T_{in}}{KD} \qquad (5.2)$$

$$F_P = \frac{298 \times 10^3}{0.199 \times 22.225}$$

$$\mathbf{F_p = 67303\ N}$$

When an external load is applied to the tightened joint, part of the external load will be "absorbed" by the joint, and the balance will add to the tension in the bolt (Refer to Section 3). The load applied to the bolt which would cause joint separation is estimated as:

$$L_{Xcrit} = F_p\left(1+\frac{K_B}{K_J}\right) \qquad (2.51)$$

where, L_{Xcrit} = The critical external load required for joint separation

K_B = stiffness of the bolt

K_J = stiffness of the joint

Design data of the joint (wing attachments) was not available. Thus, the ratio, K_B/K_J is conservatively estimated. Discussion in Section 3, indicated that the bolt to joint stiffness ratio ranges from one third to one fifth. A conservative value (which yields a higher external load) of one third is used:

$$L_{Xcrit} = 67303\left(1+\frac{1}{3}\right) \qquad (5.3)$$

$$\mathbf{L_{Xcrit} = 89\ 737\ N}$$

89 737 N is the conservative tensile load to be applied to the bolt.

5.5 The Finite Element Model

Simplifications in a finite element model are almost always necessary, especially in an analysis as complex as a bolt. Many variables are unknown. Furthermore, the analysis must be performed within the limitations of the available software. A full solid model of the bolt with 'exact' geometric characteristics was not possible as the model would require very fine meshing to capture the geometry of the thread – this would be beyond the limits of the academic Nastran software available. Furthermore, such "accuracy" is unnecessary considering the simplifications (in loading) already made and the enormity of unknown properties, e.g., friction constants. Also, there are always manufacturing tolerances, which would make an attempt at "exactness" futile.

For the reasons stated above, the analysis was simplified to represent the bolt as an axisymmetric finite element model. This implies that the helical geometry of the threads was ignored. Considering the high ratio of the bolt diameter to thread depth, it is reasonable to assume that the effects of the helical thread would not affect the through-thickness stress distribution of the bolt significantly.

Non-linear static analysis was used which incorporated only geometric nonlinearity. Material nonlinearity was not considered (although yielding can be expected in the threads) because the actual stresses are not the subject of this investigation – only the stress distribution is – as is the relative change in stress for different hole sizes. It is emphasised that the original bolt would have been designed or selected based on the fatigue service of the component.

Only a normal force was applied to the bolt (at the bolt head), as calculated in paragraph 5.4.

Initially, fixed constraints were applied directly to the thread, on the side that would make contact with the nut. This was not very representative of the real situation and a high stress concentration occurred in the model at the first fixed node of the first engaged thread. Thus, the barrel nut was also modelled and gap elements were used between the bolt and nut. This yielded much more realistic results, and is more representative of the real operation of the bolt.

The following material properties, which correspond to high strength steel, were used:

Elastic Modulus, E = 200 GPa

Poisson's Ratio, ν = 0.32

The strength of the original bolts used on the aircraft could go up to 280 ksi (or 1930 MPa), as published in the aircraft manual available at the South African Air Force depot.

5.6 Finite Element Analysis Of The Bolt.

The following plots were extracted from the analysis to illustrate some facts already discussed, and the finite element analysis results achieved. A description of each plot and the rational behind its use is presented after each figure. Note that the stresses, especially at stress concentrations are very high: in excess of yield. More discussion on these high stresses is included later. Deformations are in metres and stresses are in Pascal.

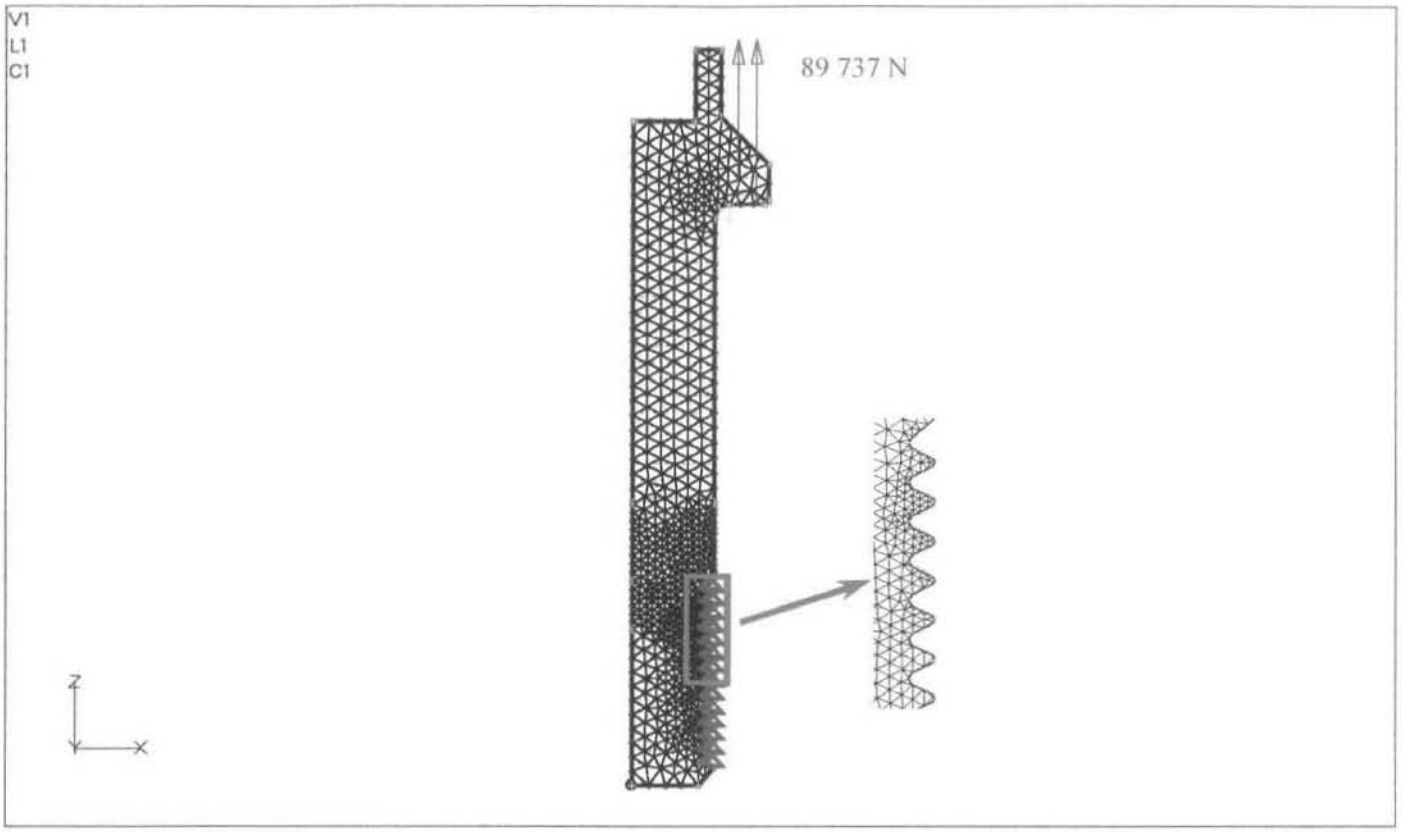

Figure 5.6 – ***Finite Element Model Of The Bolt With Fixed Constraints At The Thread Contact Points***

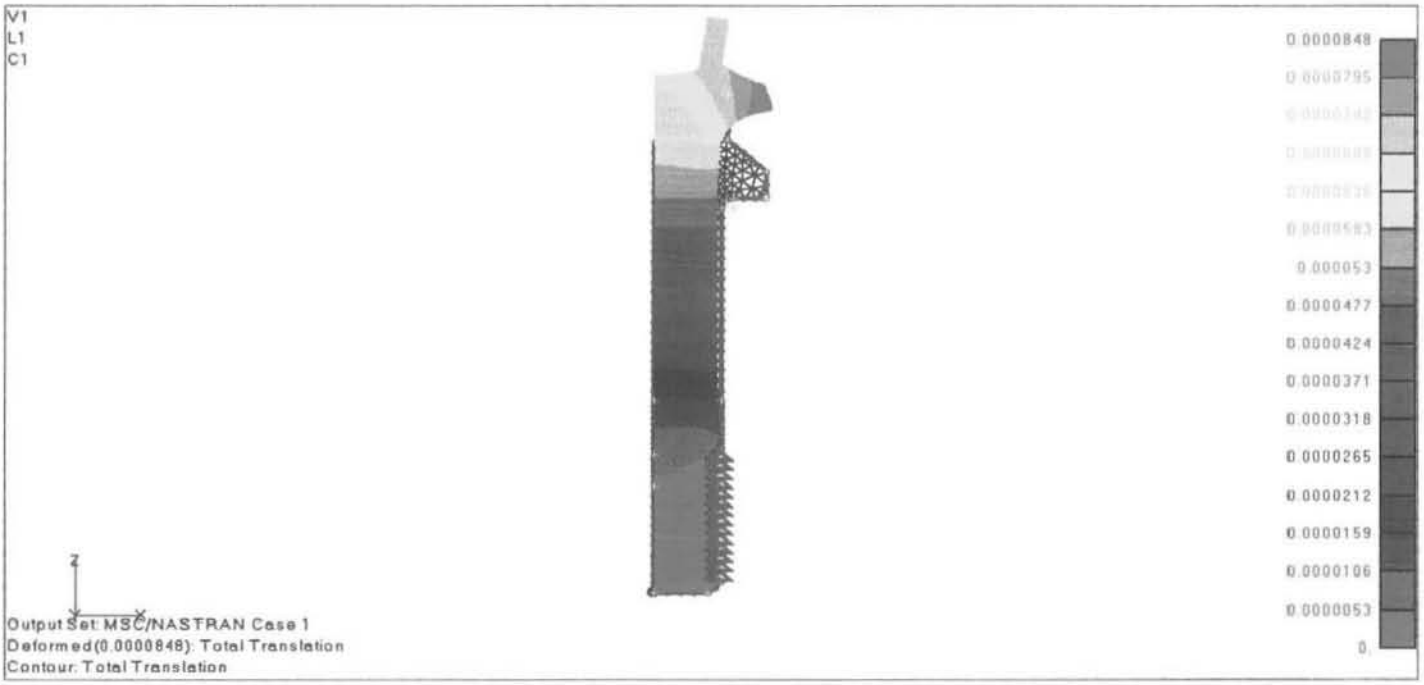

Figure 5.7 – ***Exaggerated Deformed Shape.*** No deformation is allowed at the threads. Values are in metres.

Deformation plots are very useful in checking the "engineering sense" of a model, yet it is very easy to obtain in most software. Figure 5.7 shows that the bolt deforms under the load as one would expect. Note that the plot is exaggerated for clarity. The actual deformations (in metres) are listed on the right.

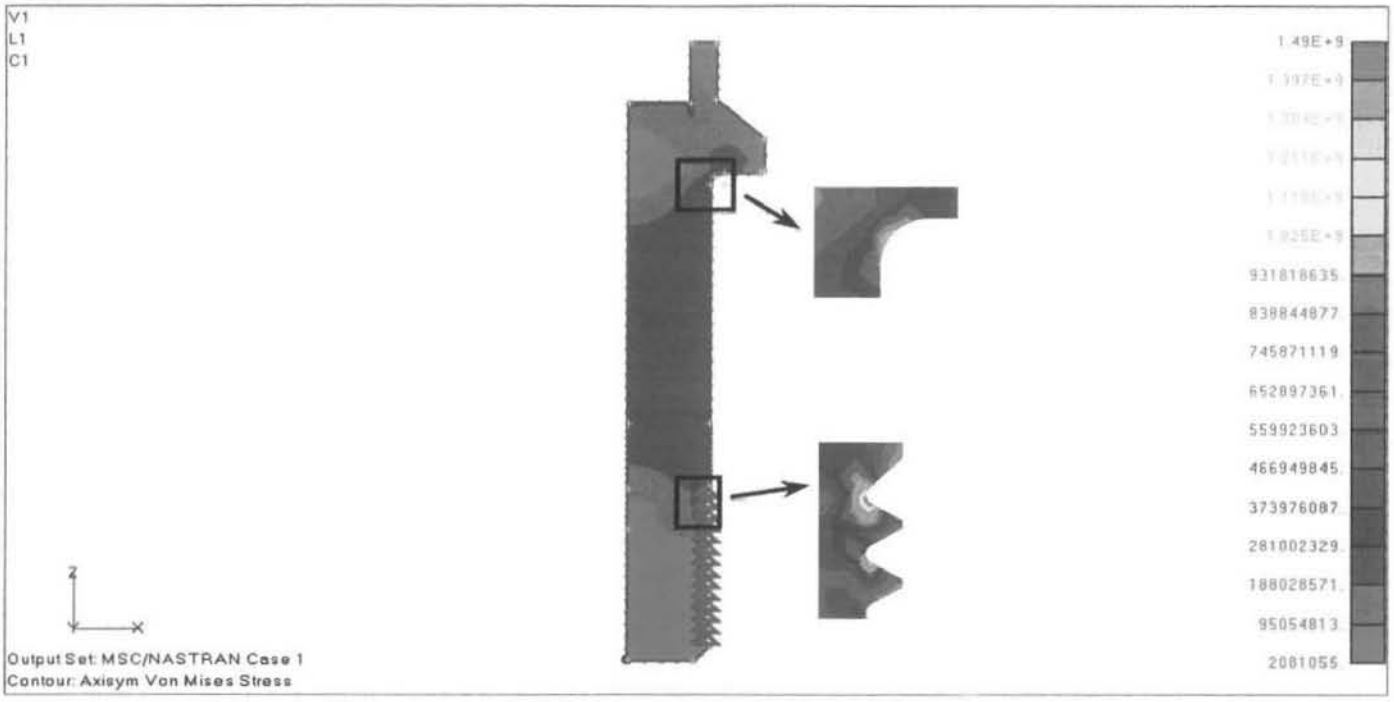

Figure 5.8 – *Stress Results of the Bolt Model with Fixed Constraints at the Thread Contact Points.* Stresses are in Pascal.

Figure 5.8 shows that a high stress concentration occurs at the first fixed. This is the first restraint against movement that the bolt experiences.

Due to the critical nature of thread root stress, i.e. the point where most failures occur, and considering that this stress would most probably govern the analysis, it was decided to use a more accurate model instead of fixing the thread contact points.

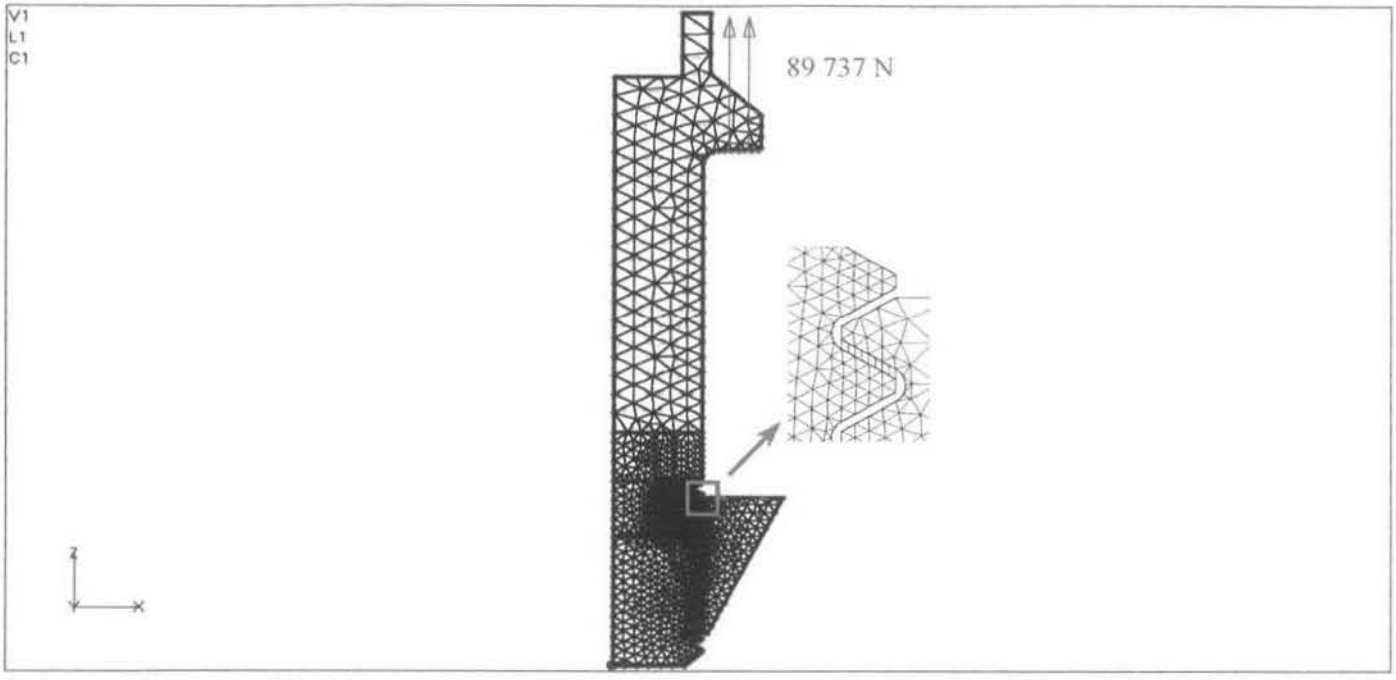

Figure 5.9 – *Bolt and Nut Model.* Gap elements are used to join the bolt threads to the nut threads.

Figure 5.9 shows a more representative model of the bolt and nut configuration than the fixed thread model. The bolt and thread contact points are joined by gap elements which have a coefficient of friction of 0.2 – typical of steel-to-steel static friction. The first bolt thread is not engaged, as was observed from the bolt and nut samples obtained from the South African Air Force. The top face of the nut was constrained against movement.

Various meshing zones were created in order to achieve the best possible mesh, with acceptable refinement at the points of interest within the limits of the available software. Parabolic elements were used because 3-noded triangular elements did not produce acceptable convergence. However, the use of the 6-noded triangular axisymmetric element implied a less uniform mesh in order to maintain the limitations

of the software. Their use is justified by the convergence analysis and the calculations illustrated later.

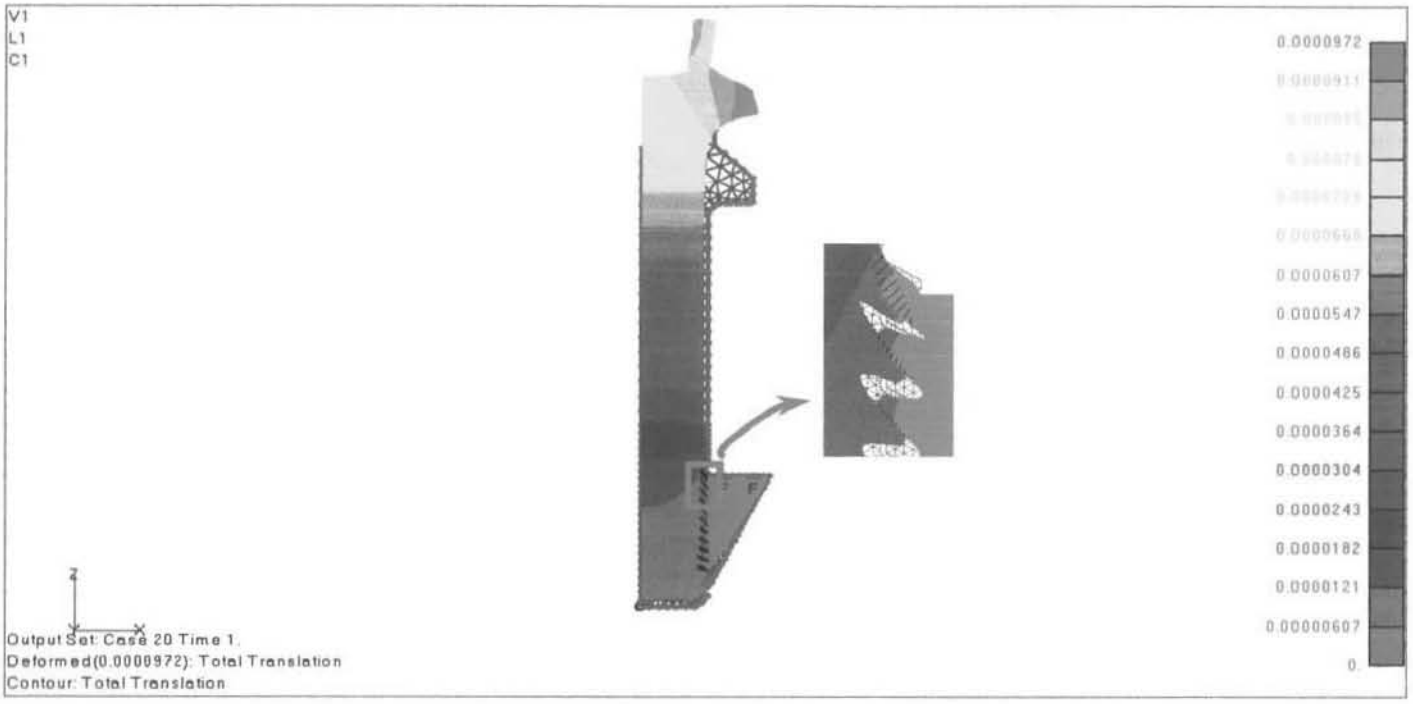

Figure 5.10 – *Exaggerated Deformation Plot Of The Bolt And Nut Model.* Deformation values are in metres.

The model deforms as expected, illustrating the "sense" of the model. The overlap observed at the threads is a consequence of the exaggerated view. The actual deformations are very small.

The stress plots in Figure 5.11 show a similar stress pattern as the fixed thread model shown in Figure 5.8. However, the actual stresses are more reliable due to the more representative nut contact (ignoring yielding of the material – note, non-linear material analysis could not be performed as the material for the SmartBolt is not selected yet). Proof that the model is converged follows.

5.7 Proof of Convergence of the Model

The first check to verify the reliability of the model was to compare the stress in the shank of the bolt (far from discontinuities) to stresses calculated from simple strengths of materials formulas.

The tension stress in the bolt shank can be expressed as:

$$\sigma = \frac{F}{A} \tag{5.4}$$

where, σ = tensile stress

F = applied tensile force = L_{Xcrit} = 89 737 N

A = cross sectional area

$= \frac{\pi d^2}{4}$, where d = nominal diameter of the bolt, so

$$A = \frac{\pi \times 0.022225^2}{4}$$

Thus, the tensile stress in the shank of the bolt is:

$$\sigma = \frac{4 \times 89737}{\pi \times 0.022225^2}$$

$$\sigma = \mathbf{231.3\ MPa}$$

The stress obtained from the finite element analysis, averaged across the thickness is 232.02 MPa, i.e. within 0.3%. The stresses near the centre of the bolt are higher than those at the edge. This is explained by the fact that the centre of the bolt is furthest from the constraint (in the cross-axial direction).

Verifying adequate mesh density at the root of the first engaged thread (the highest stress concentration) proved to be much more difficult, especially because of the model size limit of the software. The limit is 5000 nodes, and the model already analysed contains 4977 nodes, which leaves almost no room for mesh refinement. Thus, a smaller model – more focused on the threads – was built, utilising Saint Venant's Principle discussed in Section 2. This allowed a finer mesh to be used at the first three engaged threads. The model is shown in Figure 5.12.

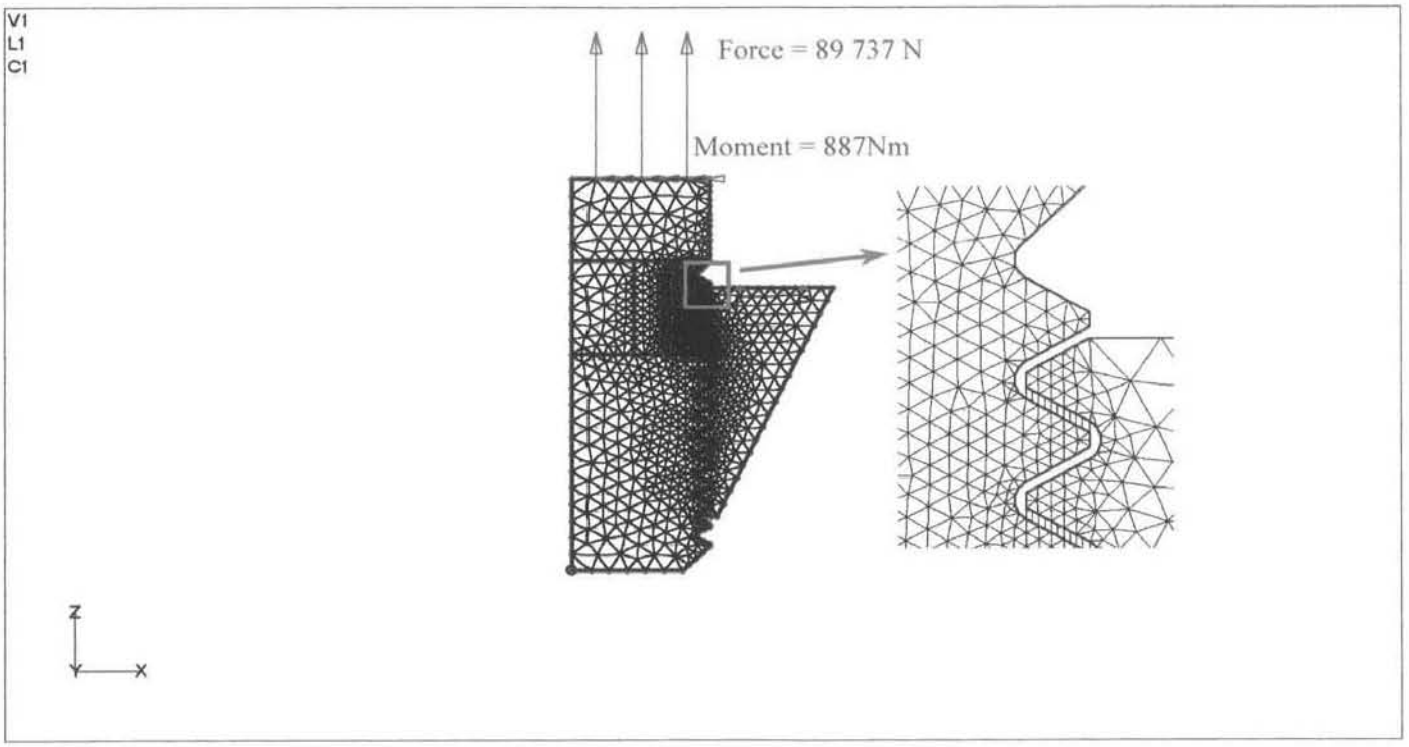

Figure 5.11 - ***The Refined Thread Finite Element Model***

The separating force in the actual bolt acts under the head of the bolt. Thus, it was not sufficient to apply only a tensile force to the model in Figure 5.12. A moment, calculated as follows was also applied, about the y-axis:

$$M = F \times L \qquad (5.5)$$

where, F = the separating force applied at the bolt head = 89 737 N

L = the distance from the centre of the load application region to the centre of the modelled shank. = 9.8838 mm

(or 0.0098838 m)

Therefore, the applied moment is:

$$M = 89737 \times 0.0098838$$

$$M = 887 \text{ Nm}$$

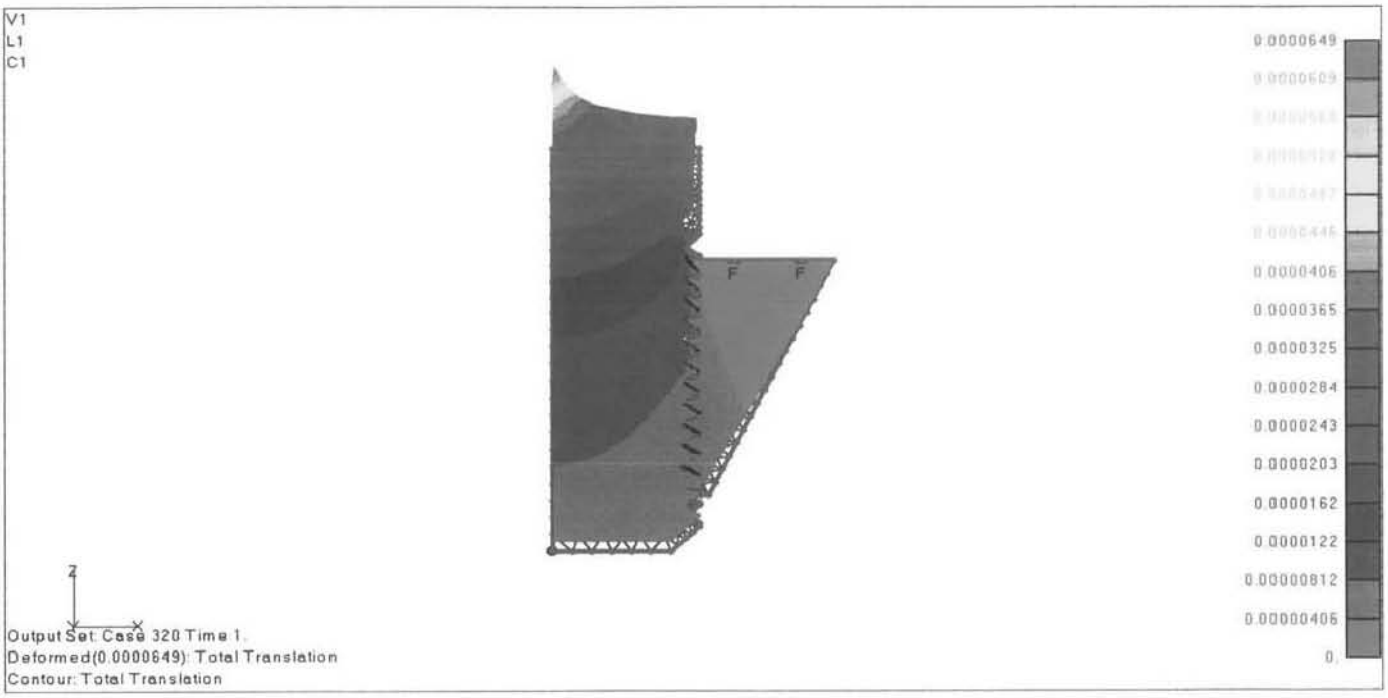

Figure 5.12 - *Exaggerated Deformation Plot.* The actual values of the deformations are listed on the right, in metres.

The centre of the bolt is furthest form the constraints – this explains the high deformation at the top-centre of the shortened bolt in Figure 5.13 – note, only half of the bolt cross-section is modelled in this axisymmetric model. The loads are applied to the topmost curve.

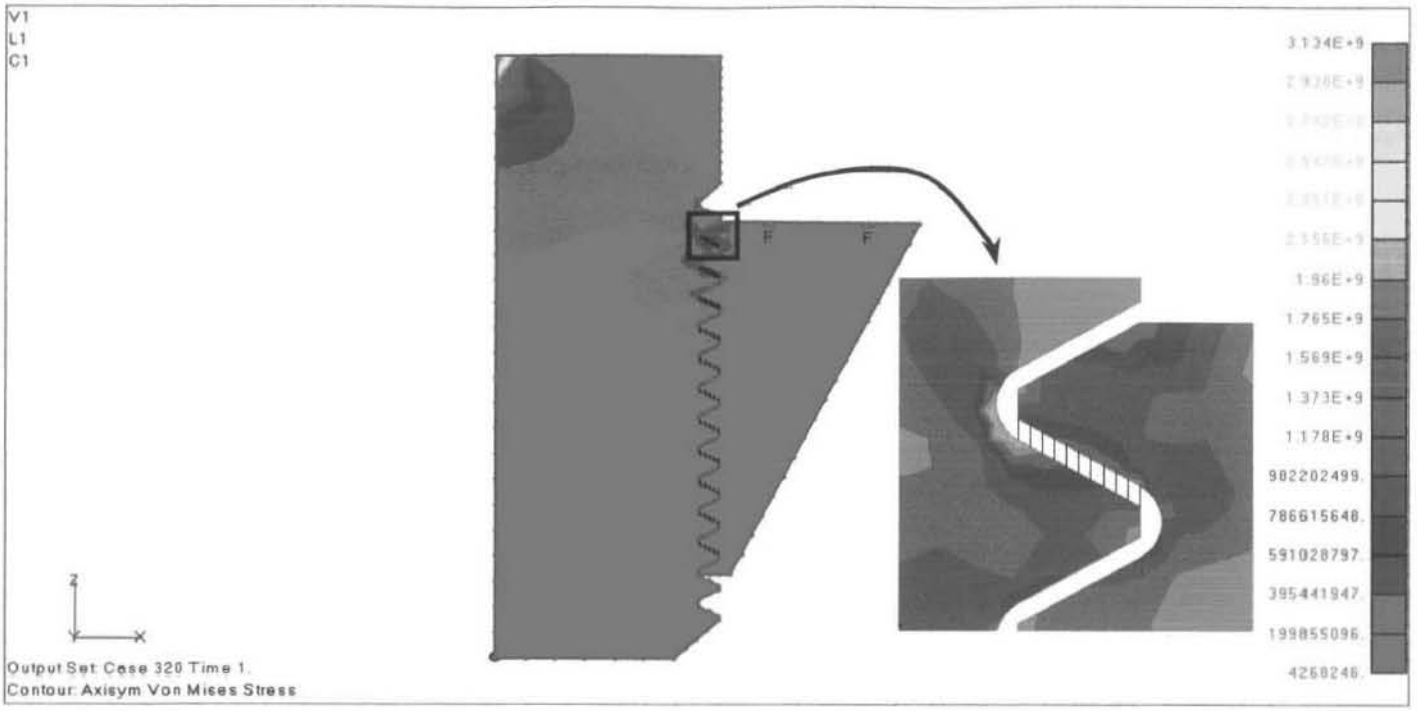

Figure 5.13 - ***Stress Plot of the Refined Thread Model.*** Stresses are in Pascal.

The stress plot of the thread-focused model in Figure 5.14 shows a stress concentration at the top-centre of the "shortened" bolt. This agrees with the deformation plot in Figure 5.13, and the same explanation applies. The effect of this concentration, however, is insignificant compared to the magnitude of the stresses in the first engaged thread root: the region on which this model is focused. The stress concentration at the thread root is between 1373 MPa and 1569 MPa. This compares well to the 1435 MPa observed in Figure 5.11: within 10%.

The above indicates adequate reliability of the model in Figures 5.9 to 5.11. The actual values of the stresses are not of particular concern for the approach used in investigation. The greatest concern is the effect of a hole through the centre of the

bolt on the **stress distribution** and the relative **change** in peak stresses, as discussed in following paragraphs.

5.8 Bolt Models With Small Holes Through The Centre

Several axisymmetric bolt models were constructed with different hole sizes through the centre. The mesh used at the threads was the same as used in Figures 5.9 to 5.11 as the reliability of the mesh has been proven to be adequate for its purpose in paragraph 4.7.

The largest hole size considered is 5mm. As the stress distribution did not change significantly for all the hole sizes analysed, only the model with the 5mm hole is plotted in Figure 5.15. Table 5.1 presents a list of the variation in peak stresses for different hole sizes.

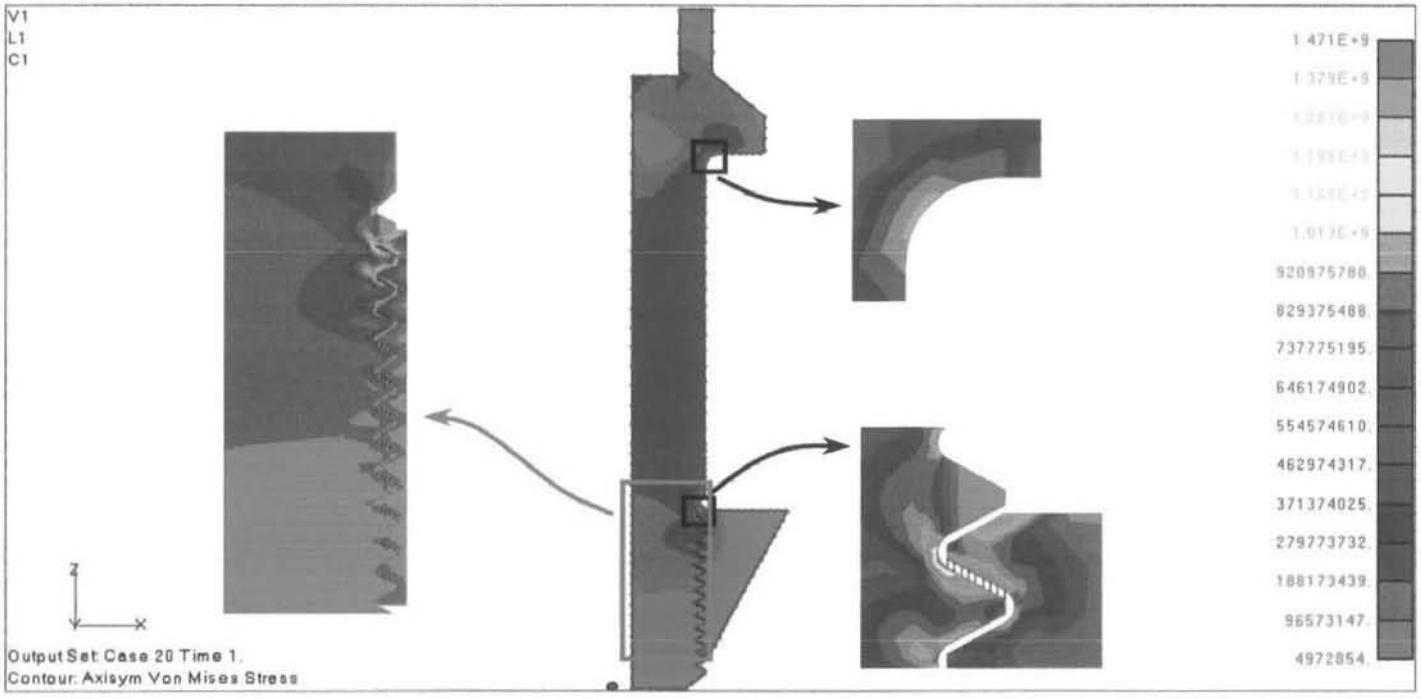

Figure 5.14 – ***Bolt And Nut Model With 5mm Hole Through The Centre Of The Bolt***

Hole Size (mm)	Calculated Nominal Bolt Stress (MPa)	Peak Stress (MPa)	% Difference From Original Peak Stress
0 - original	231.3	1435	N/A
1	231.8	1438	0.2
2	233.2	1441	0.4
3	235.6	1448	0.9
4	239.1	1458	1.6
5	243.6	1471	1.5

Table 5.1 – ***Comparison of Peak Stresses for Varying Hole size***

The nominal bolt stress was calculated using Equation 5.4 – the area of the bolt was reduced by the area of the hole.

6. Discussion and Recommendation

In order to maintain continuity of the presentation, detailed discussion was included after each plot, hence this section is only a summary.

The results show that weakening of the bolt by drilling a hole right through the centre of the bolt does affect the stresses in the thread, but by a small amount. The overall stress pattern, or stress distribution does not change significantly, but the relative change in magnitudes must be noted for fatigue purposes.

Drilling a hole through the centre of the bolt will only be a viable option if the fatigue strength of the new material is slightly higher than the existing one, at least by the percentage shown in Table 5.1, i.e. 1.5% for a 5mm hole. This is easily achievable for certain TRIP steels discussed in Section 4. Should the actual peak stresses be required, it is suggested that a conservative 10% be added to the values in Table 5.1 in order to account for the convergence of the model.

Considering Figure 4.4, a bolt made with an appropriate TRIP steel with a 5mm centrally drilled hole is actually expected to have better fatigue life than the existing bolt (without a hole).

Considerations during the material selection phase of the project should include:

- A comparison of Young's Modulus and Poisson's Ratio of the selected material to the values used in the analysis
- brittle fracture assessment, as the bolt sees sub-zero temperatures

- the corrosion resistance of the new material should be equal or superior to that of the existing material.

During the development of the sensing devices, attention must be paid to detecting plastic strains at the root of the first engaged thread, i.e. the most highly stressed region. A second area of interest (as can be seen in the Finite Element Analyses) is the shank-to-body transition.

The whole concept of manufacturing the aircraft bolts from TRIP steels with a centrally drilled hole is not only a viable option, but is likely to produce a more reliable structure, as the selected material is likely to have superior mechanical properties. The hole does not weaken the bolt significantly, as it is located in the least stressed area of the bolt body. Furthermore, the centrally drilled hole will make the bolt accessible for the insertion of a sensing device, which would detect the presence of magnetic material (i.e. a martensitic microstructure, in the case of THRIP steels), indicating that plastic strain has been induced.

This technology will certainly contribute to faster, cheaper and more reliable (depending on the sensitivity of the sensors) monitoring of the highly stressed bolts. Considering that the loading conditions addressed in the thesis for the bolt operation in the aircraft wing are common to highly stressed bolts, it can be stated that the research is applicable to most bolted joints.

7. Conclusion

For the conservative load applied to the model, the stress distribution at the most highly stressed areas does not change significantly when a small centrally-drilled hole is introduced to the bolt structure. The relative change in the peak stresses however, must not be ignored in the material selection process, i.e., the fatigue strength of the new SMART material must be higher than that of the existing bolt material, but only by a small percentage (See Sections 5 and 6 for details). This is very convenient as the envisaged THRIP steels demonstrate superior fatigue strength properties.

The results obtained and presented in this thesis prove that the concept of a SMART bolt with a small hole drilled through the centre for the insertion of a sensing device remains a viable concept from a structural strength point of view.

In addition to its application in aircraft bolting, the technology would be viable for most high strength bolted joints as the primary loading pattern in almost all bolted joints is tension (as in the aircraft bolt). Furthermore, the mechanical properties of THRIP steels are superior, by far, to common bolting materials.

The total proposition to detect plastic strains by sensing the presence of magnetic material, which results from strain-induced phase transformation of the component from austenite to martensite, is unmistakably leading-edge technology.

APPENDIX A

Aircraft Bolt Data

FED. SUP CLASS
5306

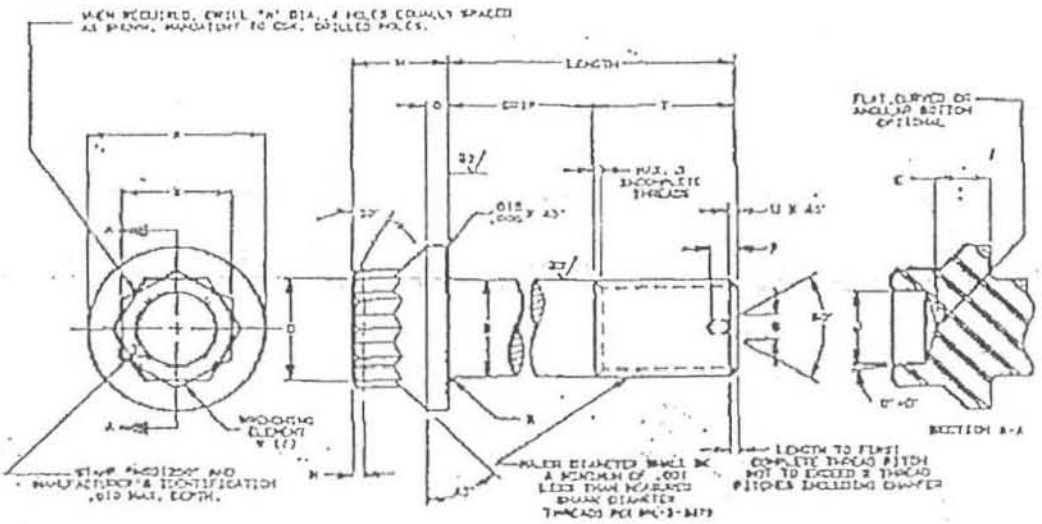

REQUIREMENTS:

1. MATERIAL: STEEL ALLOY, MIL-S-5626 (AISI 4140) MIL-S-5000 (AISI 4340) MIL-S-6049 (AISI 8740) MIL-S-8503 (AISI 8150).
2. (L) PLATING: CADMIUM PLATE IN ACCORDANCE WITH QQ-P-416, TYPE II, CLASS 2. ~~CLASS 3 MAY BE USED UNTIL 1 JAN 1974.~~
3. SURFACE TEXTURE IN ACCORDANCE WITH ANSI (USA) B46.1. UNLESS OTHERWISE SPECIFIED, THE SURFACE TEXTURE SHALL NOT EXCEED 125 MICROINCHES.
4. DIMENSIONS ARE IN INCHES, UNLESS OTHERWISE SPECIFIED. TOLERANCES: DECIMALS ±.010, ANGLES ±2°.
5. DIMENSIONS TO BE MET AFTER PLATING.
6. TENSILE STRENGTH TO BE 180,000 TO 200,000 PSI.
7. (L) DIAMETER DASH NO. AT TOP OF TABLE, SHEET 3, PLUS GRIP DASH NO. FIRST COLUMN IN LEFT OF TABLE CONSTITUTE A COMPLETE DASH NO. IDENTIFYING SPECIFIED LENGTHS OF A GIVEN SIZE OF BOLT. GRIP EQUALS LAST THREE DASH NUMBERS TIMES .0625.
8. (L) ADD LETTER R BEFORE DASH NO. TO DESIGNATE DRILLED HEAD. FIRST TWO DASH NUMBERS DESIGNATE DIAMETER IN SIXTEENTHS. LAST THREE DASH NUMBERS DESIGNATE GRIP LENGTH IN SIXTEENTHS. UNASSIGNED INTERMEDIATE OR LONGER GRIP LENGTHS NOT INCLUDED IN TABLE MAY BE SPECIFIED BY THE USE OF MIDDLE DASH NUMBERS ONLY.

(L) EXAMPLES OF PREFERRED PART NUMBER: MS21250-04006 = BOLT, UNDRILLED HEAD, .2500-28, .500 GRIP LENGTH
MS21250H04008 = BOLT, DRILLED HEAD, .2500-28, .500 GRIP LENGTH

(L) EXAMPLES OF UNASSIGNED PART NUMBER: MS21250-04009 = BOLT, UNDRILLED HEAD, .2500-28, .562 GRIP LENGTH
MS21250H04009 = BOLT, DRILLED HEAD, .2500-28, .562 GRIP LENGTH
(THREADS PER INCH, DIAMETER OF THREAD)

(L) SEE TABLE ON SHEET 3 FOR PREFERRED GRIP DASH NUMBERS.
GRIP LENGTH OF BOLT SHALL BE MEASURED FROM UNDERSIDE OF HEAD TO THE END OF FULL CYLINDRICAL PORTION OF THE SHANK.

9. HARDNESS: 39-43 RC.

FOR DESIGN FEATURE PURPOSES, THIS STANDARD TAKES PRECEDENCE OVER PROCUREMENT DOCUMENTS REFERENCED HEREIN. REFERENCED DOCUMENTS SHALL BE OF THE ISSUE IN EFFECT ON DATE OF INVITATIONS FOR BID.

(L) INACTIVE FOR NEW DESIGN AFTER 4 DEC 1990.

(L) DENOTES CHANGES

AMSC N/A

P.A. NAVY — AS Other Govt USAF - 99 ARMY - AV	TITLE (L) BOLT, TENSION, STEEL, EXTERNAL WRENCHING, FLANGED, 12-POINT, 180 KSI Fsu, 450°F	MILITARY STANDARD MS21250
PROCUREMENT SPECIFICATION MIL-H-83131	SUPERSEDING MS21250(USC)	SHEET 1 OF 3

DD FORM 672-1

PROJECT NO. 5306-0710

REVISED (L) 30 JAN 89 (K) 17 JUNE 1982 APPROVED 13 NOV 80

AMSC N/A

DISTRIBUTION STATEMENT A. APPROVED FOR PUBLIC RELEASE; DISTRIBUTION IS UNLIMITED.

This military standard is approved for use by all Departments & Agencies of the Department of Defense. Selection for all new engineering and design applications and for repetitive use shall be made from this document.

"Review/user information is current as of the date of this document. For future coordination of changes to this document, draft circulation should be based on the information in the current DODISS."

REVIEWER ACTIVITIES: DLA-IS, ARMY-AR, AIR FORCE-82

USER ACTIVITIES:

TABLE I

DIA DASH NO.	THREAD MIL-S-8879	A DIA	B DIA	NOM SIZE W (f)(L)	D DIA	E MIN	H	J +.010 -.030	M	N DIA ±.005	(e) P MAX	Q	R	(e) S MAX	(d) T MIN REF	U ±.016	DRILL SIZE REF	CONCENTRICITY FIM (a) X	CONCENTRICITY FIM (b) Y	CONCENTRICITY FIM (c) Z	DOUBLE SHEAR LBS MIN	ULT TENSILE LBS MIN
02	.1640-32 UNJC-3A	.300 .290	.1635 .1625	.2188	.219 .204	.076	.250	.100			-	.050		-	.385		-	.004	.003	.003	4,600	2,550
03	.1900-32 UNJF-3A	.350 .340	.1895 .1885	.2500	.250 .235	.092	.265	.125	.062	.037	-	.055		-	.470	.031	-				6,100	3,910
04	.2500-28 UNJF-3A	.438 .428	.2495 .2485	.3125	.312 .297	.135	.300	.180			-	.069	.042 .031	-	.492		-	.005	.004	.0045	10,600	6,980
05	.3125-24 UNJF-3A	.531 .521	.3120 .3110	.3750	.375 .360	.162	.348	.215			-	.082		-	.579		-	.006	.005		16,600	11,100
06	.3750-24 UNJF-3A	.649 .639	.3745 .3735	.4375	.437 .422	.197	.388	.260	.070		-	.091		-	.625	.047	-	.008	.006		23,900	17,100
07	.4375-20 UNJF-3A	.750 .740	.4370 .4360	.5000	.500 .485	.228	.455	.320			-	.099	.057 .047	-	.721		-	.009	.008		32,500	23,200
08	.5000-20 UNJF-3A	.828 .818	.4995 .4985	.5625	.562 .547	.234	.504	.380			-	.123		-	.768		-	.010			42,400	30,900
09	.5625-18 UNJF-3A	.938 .928	.5615 .5605	.6250	.625 .610	.287	.557	.440			-	.135		-	.852		-	.011	.009	.005	53,700	39,200
10	.6250-18 UNJF-3A	1.050 1.040	.6240 .6230	.6875	.687 .672	.327	.618	.500	.094		-	.150		-	.899	.062	-	.012	.010		66,300	49,000.
12	.7500-16 UNJF-3A	1.230 1.220	.7490 .7480	.8125	.812 .797	.380	.711	.570		.055	.200	.178		.187	1.036		2	.015	.012		95,400	71,100
14	.8750-14 UNJF-3A	1.438 1.428	.8740 .8730	.9375	.937 .922	.438	.803	.650			.280	.198	.073 .063		1.244	.078		.018	.014		129,900	97,100
16	1.0000-12 UNJF-3A	1.625 1.615	.9990 .9980	1.0625	1.062 1.047	.493	.923	.740				.222		.250	1.479		3	.020	.016	.009	169,600	126,000
18	1.1250-12 UNJF-3A	1.875 1.863	1.1240 1.1225	1.2500	1.250 1.235	.556	1.051	.840	.125			.258			1.650			.022	.019		214,700	162,000
20	1.2500-12 UNJF-3A	2.125 2.113	1.2490 1.2475	1.3125	1.312 1.297	.636	1.155	.950			.320	.269			1.760	.094		.025	.021		265,100	202,000
22	1.3750-12 UNJF-3A	2.313 2.303	1.3740 1.3725	1.4375	1.437 1.422	.698	1.266	1.070				.274	.089 .077	.312	1.885		4	.028	.023	.012	320,700	247,000
24	1.5000-12 UNJF-3A	2.500 2.490	1.4990 1.4975	1.6250	1.625 1.610	.750	1.434	1.200	.188			.335			2.010			.030	.025		381,700	296,000

(a) DIMENSIONS A, B AND J SHALL BE CONCENTRIC TO EACH OTHER WITHIN VALUES SPECIFIED FOR X FIM.
(b) DIMENSIONS W AND J SHALL BE CONCENTRIC TO EACH OTHER WITHIN VALUES SPECIFIED FOR Y FIM.
(c) DIMENSIONS N AND THREAD PITCH DIAMETER SHALL BE CONCENTRIC TO EACH OTHER WITHIN VALUES SPECIFIED FOR Z FIM.
(d) REFERENCE DIMENSIONS ARE FOR DESIGN PURPOSES ONLY AND ARE NOT AN INSPECTION OR MANUFACTURING REQUIREMENT.
(e) ON BOLTS 3/4 INCH OR LARGER, CENTER DRILLING OF SHANK IS OPTIONAL FOR MANUFACTURER.
ONLY BOLTS FOR WHICH THERE ARE QUALIFIED PRODUCTS LISTED IN QPL8831 SHALL BE USED FOR DESIGN.
(f) WRENCHING ELEMENT SHALL BE IN ACCORDANCE WITH AS 870.

FED. SUP CLASS 5306

P.A. NAVY-AS
Other Cust USAF-99 ARMY-AV

PROCUREMENT SPECIFICATION MIL-B-8831

SPECIFICATIONS MS21250(ASG)

TITLE BOLT, TENSION, STEEL, 180 KSI FTU, 450°F, 12 POINT, EXTERNAL WRENCHING FLANGED

MILITARY STANDARD MS21250

SHEET 2 OF 3

APPROVED 23 NOV 60 REVISED (L) FOR CHANGES SEE SHEET 1 AND 2

DD FORM 672-1

FED. SUP CLASS 5306

GRIP DASH NO.	GRIP ±.010	DIAMETER DASH NUMBERS															
		02	03	04	05	06	07	08	09	10	12	14	16	18	20	22	24
		LENGTH															
004	.250	.655	.690	.762	.849	.895	.951	1.038									
006	.375	.780	.815	.887	.974	1.020	1.116	1.163	1.247	1.294	1.431						
008	.500	.905	.940	1.012	1.099	1.145	1.241	1.288	1.372	1.419	1.556	1.764	1.999	2.170			
010	.625	1.030	1.065	1.137	1.224	1.270	1.366	1.413	1.497	1.544	1.681	1.889	2.124	2.295	2.405	2.530	2.655
012	.750	1.155	1.190	1.262	1.349	1.395	1.491	1.538	1.622	1.669	1.806	2.014	2.249	2.420	2.530	2.655	2.780
014	.875	1.280	1.315	1.387	1.474	1.520	1.616	1.663	1.747	1.794	1.931	2.139	2.374	2.545	2.655	2.780	2.905
016	1.000	1.405	1.440	1.512	1.599	1.645	1.741	1.788	1.872	1.919	2.056	2.264	2.499	2.670	2.780	2.905	3.030
018	1.125	1.530	1.565	1.637	1.724	1.770	1.866	1.913	1.997	2.044	2.181	2.389	2.624	2.795	2.905	3.030	3.155
020	1.250	1.655	1.690	1.762	1.849	1.895	1.991	2.038	2.122	2.169	2.306	2.514	2.749	2.920	3.030	3.155	3.280
022	1.375	1.780	1.815	1.887	1.974	2.020	2.116	2.163	2.247	2.294	2.431	2.639	2.874	3.045	3.155	3.280	3.405
024	1.500	1.905	1.940	2.012	2.099	2.145	2.241	2.288	2.372	2.419	2.556	2.764	2.999	3.170	3.280	3.405	3.530
026	1.625	2.030	2.065	2.137	2.224	2.270	2.366	2.413	2.497	2.544	2.681	2.889	3.124	3.295	3.405	3.530	3.655
028	1.750	2.155	2.190	2.262	2.349	2.395	2.491	2.538	2.622	2.669	2.806	3.014	3.249	3.420	3.530	3.655	3.780
030	1.875	2.280	2.315	2.387	2.474	2.520	2.616	2.663	2.747	2.794	2.931	3.139	3.374	3.545	3.655	3.780	3.905
032	2.000	2.405	2.440	2.512	2.599	2.645	2.741	2.788	2.872	2.919	3.056	3.264	3.499	3.670	3.780	3.905	4.030
034	2.125	2.530	2.565	2.637	2.724	2.770	2.866	2.913	2.997	3.044	3.181	3.389	3.624	3.795	3.905	4.030	4.155
035	2.187					2.833											
036	2.250	2.655	2.690	2.762	2.849	2.895	2.991	3.038	3.122	3.169	3.306	3.514	3.749	3.920	4.030	4.155	4.280
038	2.375	2.780	2.815	2.887	2.974	3.020	3.116	3.163	3.247	3.294	3.431	3.639	3.874	4.045	4.155	4.280	4.405
039	2.437							3.225									
040	2.500	2.905	2.940	3.012	3.099	3.145	3.241	3.288	3.372	3.419	3.556	3.764	3.999	4.170	4.280	4.405	4.530
042	2.625	3.030	3.065	3.137	3.224	3.270	3.366	3.413	3.497	3.544	3.681	3.889	4.124	4.295	4.405	4.530	4.655
044	2.750	3.155	3.190	3.262	3.349	3.395	3.491	3.538	3.622	3.669	3.806	4.014	4.249	4.420	4.530	4.655	4.780
046	2.875	3.280	3.315	3.387	3.474	3.520	3.616	3.663	3.747	3.794	3.931	4.139	4.374	4.545	4.655	4.780	4.905
048	3.000	3.405	3.440	3.512	3.599	3.645	3.741	3.788	3.872	3.919	4.056	4.264	4.499	4.670	4.780	4.905	5.030
050	3.125	3.530	3.565	3.637	3.724	3.770	3.866	3.913	3.997	4.044	4.181	4.389	4.624	4.795	4.905	5.030	5.155
052	3.250	3.655	3.690	3.762	3.849	3.895	3.991	4.038	4.122	4.169	4.306	4.514	4.749	4.920	5.030	5.155	5.280
054	3.375	3.780	3.815	3.887	3.974	4.020	4.116	4.163	4.247	4.294	4.431	4.639	4.874	5.045	5.155	5.280	5.405
056	3.500	3.905	3.940	4.012	4.099	4.145	4.241	4.288	4.372	4.419	4.556	4.764	4.999	5.170	5.280	5.405	5.530
058	3.625	4.030	4.065	4.137	4.224	4.270	4.366	4.413	4.497	4.544	4.681	4.889	5.124	5.295	5.405	5.530	5.655
060	3.750	4.155	4.190	4.262	4.349	4.395	4.491	4.538	4.622	4.669	4.806	5.014	5.249	5.420	5.530	5.655	5.780
062	3.875	4.280	4.315	4.387	4.474	4.520	4.616	4.663	4.747	4.794	4.931	5.139	5.374	5.545	5.655	5.780	5.905
064	4.000	4.405	4.440	4.512	4.599	4.645	4.741	4.788	4.872	4.919	5.056	5.264	5.499	5.670	5.780	5.905	6.030
066	4.125	4.530	4.565	4.637	4.724	4.770	4.866	4.913	4.997	5.044	5.181	5.389	5.624	5.795	5.905	6.030	6.155
068	4.250	4.655	4.690	4.762	4.849	4.895	4.991	5.038	5.122	5.169	5.306	5.514	5.749	5.920	6.030	6.155	6.280
070	4.375	4.780	4.815	4.887	4.974	5.020	5.116	5.163	5.247	5.294	5.431	5.639	5.874	6.045	6.155	6.280	6.405
072	4.500	4.905	4.940	5.012	5.099	5.145	5.241	5.288	5.372	5.419	5.556	5.764	5.999	6.170	6.280	6.405	6.530
074	4.625	5.030	5.065	5.137	5.224	5.270	5.366	5.413	5.497	5.544	5.681	5.889	6.124	6.295	6.405	6.530	6.655
076	4.750	5.155	5.190	5.262	5.349	5.395	5.491	5.538	5.622	5.669	5.806	6.014	6.249	6.420	6.530	6.655	6.780
078	4.875	5.280	5.315	5.387	5.474	5.520	5.616	5.663	5.747	5.794	5.931	6.139	6.374	6.545	6.655	6.780	6.905
080	5.000	5.405	5.440	5.512	5.599	5.645	5.741	5.788	5.872	5.919	6.056	6.264	6.499	6.670	6.780	6.905	7.030
082	5.125	5.530	5.565	5.637	5.724	5.770	5.866	5.913	5.997	6.044	6.181	6.389	6.624	6.795	6.905	7.030	7.155
084	5.250	5.655	5.690	5.762	5.849	5.895	5.991	6.038	6.122	6.169	6.306	6.514	6.749	6.920	7.030	7.155	7.280
086	5.375	5.780	5.815	5.887	5.974	6.020	6.116	6.163	6.247	6.294	6.431	6.639	6.874	7.045	7.155	7.280	7.405
088	5.500	5.905	5.940	6.012	6.099	6.145	6.241	6.288	6.372	6.419	6.556	6.764	6.999	7.170	7.280	7.405	7.530
090	5.625	6.030	6.065	6.137	6.224	6.270	6.366	6.413	6.497	6.544	6.681	6.889	7.124	7.295	7.405	7.530	7.655
092	5.750	6.155	6.190	6.262	6.349	6.395	6.491	6.538	6.622	6.669	6.806	7.014	7.249	7.420	7.530	7.655	7.780
094	5.875	6.280	6.315	6.387	6.474	6.520	6.616	6.663	6.747	6.794	6.931	7.139	7.374	7.545	7.655	7.780	7.905
096	6.000	6.405	6.440	6.512	6.599	6.645	6.741	6.788	6.872	6.919	7.056	7.264	7.499	7.670	7.780	7.905	8.030
098	6.125								6.997	7.044	7.181	7.389	7.624	7.795	7.905	8.030	8.155
100	6.250								7.122	7.169	7.306	7.514	7.749	7.920	8.030	8.155	8.280
102	6.375								7.247	7.294	7.431	7.639	7.874	8.045	8.155	8.280	8.405
104	6.500								7.372	7.419	7.556	7.764	7.999	8.170	8.280	8.405	8.530
106	6.625								7.497	7.544	7.681	7.889	8.124	8.295	8.405	8.530	8.655
108	6.750								7.622	7.669	7.806	8.014	8.249	8.420	8.530	8.655	8.780
110	6.875								7.747	7.794	7.931	8.139	8.374	8.545	8.655	8.780	8.905
112	7.000								7.872	7.919	8.056	8.264	8.499	8.670	8.780	8.905	9.030
114	7.125													8.795	8.905	9.030	9.155
116	7.250													8.920	9.030	9.155	9.280
118	7.375													9.045	9.155	9.280	9.405
120	7.500													9.170	9.280	9.405	9.530
122	7.625													9.295	9.405	9.530	9.655
124	7.750													9.420	9.530	9.655	9.780
126	7.875													9.545	9.655	9.780	9.905
128	8.000													9.670	9.780	9.905	10.030

APPROVED 23 NOV 60 REVISED (L) FOR CHANGES SEE SHEET 1 AND 2

P.A. NAVY - AS Other Cust USAF - 99 ARMY - AV	TITLE BOLT, TENSION, STEEL, 180 KSI FTU, 450°F, 12 POINT, EXTERNAL WRENCHING FLANGED	MILITARY STANDARD MS21250
PROCUREMENT SPECIFICATION MIL-B-8831	SUPERSEDES: MS21250(ASG)	SHEET 3 OF 3

DD FORM 672-1 (Continued)

USER SYMBOLS

REVIEWER SYMBOLS
DLA-IS
ARMY-AR
AIR FORCE-82

"Revision/Page information is current as of the date of this document. For future applications of changes to this document, draft revisions should be based on the information in the current revision."

AMSC N/A

DISTRIBUTION STATEMENT A: APPROVED FOR PUBLIC RELEASE; DISTRIBUTION IS UNLIMITED.

This military standard is approved for use by all Departments & Agencies of the Department of Defense. Selection for all new engineering and design applications and for repetitive use shall be made from this document.

U.S. GOVERNMENT PRINTING OFFICE:1969 604-033/11958

SPS TECHNOLOGIES

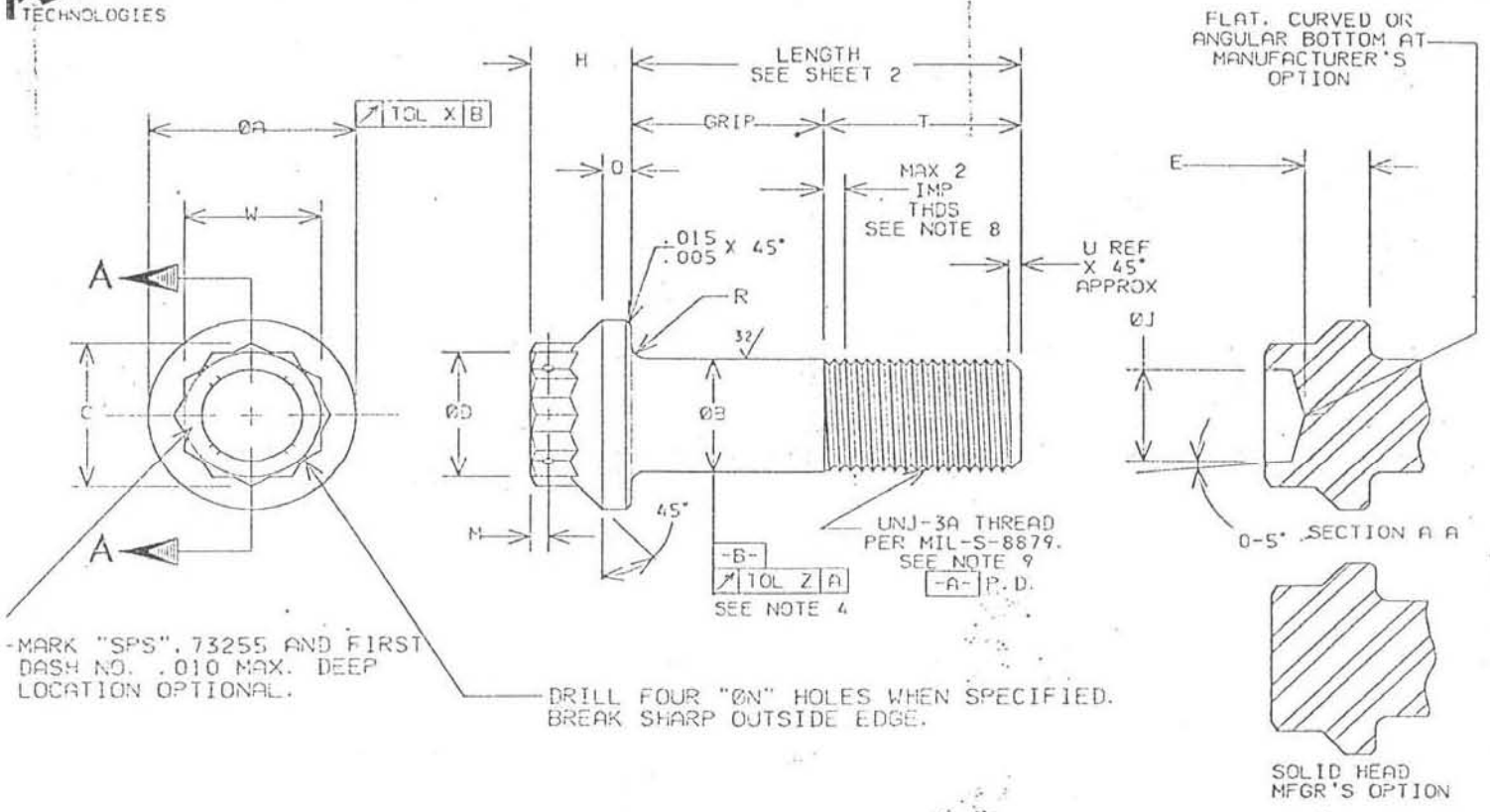

BASIC PART NUMBER	THREAD	A	B	C MIN	D	E MIN	H	J	M	N	O	R	T REF	W	X	Z
73255-428	.250-28	.438	.2500	.347	.312	.135	.310	.190	.072	.042	.079	.041	.492	.313	.005	.0045
73255-420	.250-20	.428	.2435		.297		.290	.150	.052	.032	.059	.031		.304		
73255-524	.3125-24	.532	.3125	.419	.375	.162	.358	.225	.080	.060	.092	.041	.579	.376	.006	.0045
73255-518	.3125-18	.520	.3053		.360		.338	.185	.060	.050	.072	.031		.367		
73255-624	.3750-24	.650	.3750	.491	.437	.197	.396	.270	.080	.060	.101	.057	.625	.439	.008	.0045
73255-616	.3750-16	.638	.3678		.422		.378	.230	.060	.050	.081	.047		.430		
73255-720	.4375-20	.752	.4375	.561	.500	.228	.445	.330	.080	.060	.109	.057	.721	.502	.009	.006
73255-714	.4375-14	.738	.4294		.485		.425	.290	.060	.050	.089	.047		.492		
73255-820	.5000-20	.830	.5000	.631	.562	.254	.514	.390	.104	.060	.133	.057	.768	.564	.010	.006
73255-813	.5000-13	.816	.4919		.547		.494	.350	.084	.050	.113	.047		.553		
73255-918	.5625-18	.941	.5625	.703	.625	.287	.567	.450	.104	.060	.143	.057	.852	.627	.011	.006
73255-912	.5625-12	.925	.5538		.610		.547	.410	.084	.050	.123	.047		.616		
73255-1018	.6250-18	1.053	.6250	.775	.687	.327	.628	.510	.104	.060	.160	.073	.899	.690	.012	.006
73255-1011	.6250-11	1.037	.6163		.672		.608	.470	.084	.050	.140	.063		.679		
73255-1216	.7500-16	1.234	.7500	.917	.812	.380	.721	.580	.104	.060	.188	.073	1.036	.814	.015	.008
73255-1210	.7500-10	1.216	.7406		.797		.701	.540	.084	.050	.168	.063		.803		
73255-1414	.8750-14	1.442	.8750	1.059	.937	.438	.818	.660	.135	.060	.208	.073	1.244	.940	.018	.009
73255-1409	.8750-9	1.424	.8647		.922		.798	.620	.115	.050	.188	.063		.928		
73255-1614	1.0000-14	1.630	1.0000	1.200	1.062	.493	.933	.750	.135	.060	.232	.073	1.479	1.064	.020	.009
73255-1612	1.0000-12	1.610	.9886		1.047		.913	.710	.115	.050	.213	.063		1.052		
73255-1608	1.0000-8															
73255-1812	1.1250-12	1.881	1.1250	1.414	1.250	.556	1.061	.850	.135	.060	.268	.073	1.650	1.252	.022	SEE NOTE 4
73255-1807	1.1250-7	1.859	1.1086		1.235		1.041	.810	.115	.050	.248	.063		1.239		
73255-2012	1.2500-12	2.131	1.250	1.484	1.312	.636	1.165	.960	.135	.060	.279	.089	1.760	1.314	.025	
73255-2007	1.2500-7	2.109	1.2336		1.297		1.155	.920	.115	.050	.259	.077		1.360		
73255-2212	1.3750-12	2.320	1.3750	1.626	1.437	.698	1.276	1.080	.198	.060	.284	.089	1.885	1.440	.028	
73255-2206	1.3750-6	2.296	1.3568		1.421		1.258	1.040	.178	.050	.264	.077		1.427		
73255-2412	1.5000-12	2.508	1.5000	1.842	1.625	.750	1.444	1.210	.198	.060	.345	.089	2.010	1.627	.030	
73255-2406	1.5000-6	2.482	1.4880		1.609		1.424	1.170	.178	.050	.325	.077		1.614		
73255-2812	1.750-12	2.824	1.750	2.484	1.938	.848	1.660	1.302	.188	.050	.350	.073	2.278	1.940	.030	
73255-285	1.750-5	2.796	1.7295							.050		.058		1.926		
73255-3212	2.000-12	3.170	2.000	2.839	2.188	.993	1.997	1.500	.188	.060	.419	.111	2.573	2.190	.030	
73255-324.5	2.000-4.5	3.140	1.9780							.050		.091		2.176		
73255-3612	2.250-12	3.706	2.250	2.769	2.437	1.111	2.114	1.688	.188	.060	.486	.114	23778	23440	.030	
73255-364.5	2.250-4.5	3.676	2.2280							.050		.099		2.426		
73255-4012	2.500-12	4.071	2.500	3.124	2.750	1.227	2.341	1.875	.188	.060	.583	.122	3.034	2.752	.030	
73255-404	2.500-4	4.039	2.4762							.050		.107		2.737		
73255-4412	2.750-12	4.441	2.7500	3.409	3.000	1.343	2.567	2.062	.188	.060	.637	.131	3.290	3.002	.030	
73255-444	2.750-4	4.407	2.7262							.050		.116		2.987		
73255-4812	3.000-12	4.806	3.000	3.695	3.250	1.457	2.794	2.250	.188	.060	.689	.139	3.546	3.252	.030	
73255-484	3.000-4	4.770	2.9762							.050		.124		3.237		

ERANCES ± .010 AND ±2°
FACE ROUGHNESS 125√
ESS OTHERWISE NOTED
N: KATHY SCHWARTZ DATE: 05/20/97
ROVED: L.KLINE DATE: 2/26/98
ROVED: S. HUTCHINSON

SPS TECHNOLOGIES

FSCM NO. 56878
CUSTODIAN: JENKINTOWN, PA.

STANDARDS AND SPECIFICATIONS
SPS-B-645

TITLE
BOLT, TENSION, EXTERNAL WRENCHING
DOUBLE HEXAGON ALLOY STEEL, 180 KSI, 450°F.,
COMMERCIAL APPLICATIONS

PART NUMBER: 73255-( )( )( )

SHEET 1 OF 2 PROJECT 6A854

GRIP TOLERANCES	LENGTH TOLERANCES			
.010 THRU 1.000 DIA .031 OVER 1.000 DIA	BOLT LENGTH	NOMINAL BOLT DIAMETERS		
		THRU .375 DIA.	.4375 THRU .7500 DIA.	.8750 THRU 1.500 DIA.
THRU 6.000 GRIP	UP TO 1.000	-.030	-.030	-.050
.062 GRIP 6.000	1.000 THRU 2.500	-.040	-.060	-.100
THRU 16.000	OVER 2.500 THRU 6.000	-.060	-.080	-.140
.125 OVER 16.000 GRIP	OVER 6.000 BOLT LENGTH	-.120	-.120	-.200

GRIP TOLERANCES FOR DIAMETERS OVER 1.500	LENGTH TOLERANCES FOR DIAMETERS OVER 1.500
±.031 THRU 6.000 OF GRIP LENGTH	+.000 FOR LENGTHS UP TO 6.000 INCLUSIVE -.200
±.062 - 6.000 THRU 16.000 GRIP LENGTH	
±.125 OVER 16.000 GRIP LENGTH	+.000 FOR LENGTHS OVER 6.000 -.240

1. MATERIAL: ALLOY STEEL.
2. HEAT TREATMENT: 180,000 PSI MINIMUM.
3. FINISH: CADMIUM PLATE PER QQ-P-416, TYPE II, CLASS 3.
4. THE RUNOUT OF BODY AND PITCH DIAMETER OF BOLTS OVER 1.000 SHALL BE WITHIN .005 PER INCH OF BODY LENGTH, .060 MAX.
5. PART NUMBER: 73255 - ( ) ( ) ( )
   - = GRIP LENGTH IN SIXTEENTHS
   - ADD "H" TO DESIGNATE DRILLED HEAD
   - ADD "-" TO DESIGNATE UNDRILLED HEAD
   - DIAMETER IN SIXTEENTHS AND THREADS PER INCH.
   - = BASIC PART NUMBER

   LENGTH = NOMINAL GRIP PLUS "T" REF.

   EXAMPLE: 73255-524H20 = .3125-24 BOLT, DRILLED HEAD, 1.250 GRIP LENGTH, CADMIUM PLATED.
6. BREAK ALL SHARP EDGES .003-.006.
7. REFERENCE DIMENSIONS ARE FOR DESIGN PURPOSES ONLY AND ARE NOT INSPECTION REQUIREMENTS.
8. MAX. OF THREE INCOMPLETE THREADS FOR 1.000 AND OVER DIAMETER BOLTS.
9. BOLTS OVER 1.000 DIAMETER SHALL HAVE UNJ-2A THREADS PRIOR TO PLATE.
10. CHAMFER "U" X 45° PLUS INCOMPLETE THREADS ARE NOT TO EXCEED TWO PITCHES.
11. DIMENSIONS ARE IN INCHES.

TABLE I. Basic thread data

Threads per inch	Pitch	Truncation of internal thread crest	Flat at internal thread root and external thread crest	Height of sharp V thread	Truncation of internal thread root and external thread crest	Minimum root radius	Height from sharp "V" to external thread root and max. root radius	Half addendum of external thread	Flat at internal thread crest
n	p= 1/n	$\frac{5H}{16}$ = 0.27063p	$\frac{P}{8}$ = 0.125p	H= 0.866025p	$\frac{H}{8}$ = 0.108225p	0.14011p	$\frac{5H}{24}$ = 0.18042p	$\frac{3H}{16}$ = 0.16238p	$\frac{5p}{16}$ = 0.3125p
1	2	3	4	5	6	7	8	9	10
80	0.012500	0.00338	0.00156	0.010825	0.00135	0.0018	0.00226	0.00203	0.00391
72	0.013889	0.00376	0.00174	0.012028	0.00150	0.0021	0.00251	0.00226	0.00434
64	0.015625	0.00423	0.00195	0.013532	0.00169	0.0023	0.00282	0.00254	0.00488
56	0.017857	0.00483	0.00223	0.015465	0.00193	0.0027	0.00322	0.00290	0.00558
48	0.020833	0.00564	0.00260	0.018042	0.00226	0.0031	0.00376	0.00338	0.00651
44	0.022727	0.00615	0.00284	0.019682	0.00246	0.0034	0.00410	0.00369	0.00710
40	0.025000	0.00677	0.00312	0.021651	0.00271	0.0038	0.00451	0.00406	0.00781
[illegible]								[illegible]	0.00977
20	0.050000	0.01353	0.00625	0.043301	0.00541	0.0075	0.00902	0.00812	0.01562
18	0.055556	0.01504	0.00694	0.048113	0.00601	0.0083	0.01002	0.00902	0.01736
16	0.062500	0.01691	0.00781	0.054127	0.00677	0.0094	0.01128	0.01015	0.01953
14	0.071429	0.01933	0.00893	0.061859	0.00773	0.0107	0.01289	0.01160	0.02232
13	0.076923	0.02082	0.00962	0.066617	0.00833	0.0115	0.01388	0.01249	0.02404
12	0.083333	0.02255	0.01042	0.072169	0.00902	0.0125	0.01503	0.01353	0.02604
11	0.090909	0.02460	0.01136	0.078730	0.00984	0.0136	0.01640	0.01476	0.02841
10	0.100000	0.02706	0.01250	0.086603	0.01083	0.0150	0.01804	0.01624	0.03125
9	0.111111	0.03007	0.01389	0.096225	0.01203	0.0167	0.02005	0.01804	0.03472
8	0.125000	0.03383	0.01562	0.108253	0.01353	0.0188	0.02255	0.02030	0.03906
7	0.142857	0.03866	0.01786	0.123718	0.01546	0.0214	0.02577	0.02320	0.04464
6	0.166667	0.04510	0.02083	0.144338	0.01804	0.0250	0.03007	0.02706	0.05208
5	0.200000	0.05413	0.02500	0.173205	0.02165	0.0300	0.03608	0.03248	0.06250
4.5	0.222222	0.06014	0.02778	0.192450	0.02406	0.0334	0.04009	0.03608	0.06944
4	0.250000	0.06766	0.03125	0.216506	0.02706	0.0375	0.04510	0.04059	0.07812

TABLE I. Basic thread data - (Continued)

Addendum of external thread $\frac{3H}{8}$ = 0.32476p	Height of internal thread and depth of thread engagement $\frac{9H}{16}$ = 0.48714p	Height of external thread $\frac{2H}{3}$ = 0.57735p	Twice the external thread addendum $\frac{3H}{4}$ = 0.649519p	Difference between max-major and pitch diameters of internal thread $\frac{11H}{12}$ = 0.79386p	Double Height of internal thread $\frac{9H}{8}$ = 0.97428p	Double Height of external thread $\frac{4H}{3}$ = 1.1547p	Difference between max pitch dia. and max. minor diameter external thread $\frac{7H}{12}$ = 0.50518p	Difference between min. pitch dia. and min. minor diameter of external thread .6533H= 0.56580p	Maj Dia Tolerance $.06\sqrt[3]{p^2}$
11	12	13	14	15	16	17	18	19	20
0.00406	0.00609	0.00722	0.008119	0.00992	0.01218	0.01443	0.00631	0.00707	0.0032
0.00451	0.00677	0.00802	0.009021	0.01103	0.01353	0.01604	0.00702	0.00786	0.0035
0.00507	0.00761	0.00902	0.010149	0.01240	0.01522	0.01804	0.00789	0.00884	0.0038
0.00580	0.00870	0.01031	0.011599	0.01418	0.01740	0.02062	0.00902	0.01010	0.0041
0.00677	0.01015	0.01203	0.013532	0.01654	0.02030	0.02406	0.01052	0.01179	0.0045
[illegible]	[illegible]	[illegible]	[illegible]	[illegible]	[illegible]	[illegible]	[illegible]	[illegible]	[illegible]
[illegible]	[illegible]	[illegible]	[illegible]	[illegible]	[illegible]	[illegible]	0.01804	[illegible]	0.0065
0.01353	0.02030	0.02406	0.027063	0.03308	0.04060	0.04811	0.02105	0.02358	0.0072
0.01624	0.02436	0.02887	0.032476	0.03969	0.04871	0.05774	0.02526	0.02829	0.0081
0.01804	0.02706	0.03208	0.036084	0.04410	0.05413	0.06415	0.02807	0.03143	0.0087
0.02030	0.03045	0.03608	0.040595	0.04962	0.06089	0.07217	0.03157	0.03536	0.0094
0.02320	0.03480	0.04124	0.046394	0.05670	0.06959	0.08248	0.03608	0.04041	0.0103
0.02498	0.03747	0.04441	0.049963	0.06107	0.07494	0.08882	0.03886	0.04352	0.0108
0.02706	0.04059	0.04811	0.054127	0.06615	0.08119	0.09622	0.04210	0.04715	0.0114
0.02952	0.04429	0.05249	0.059047	0.07217	0.08857	0.10497	0.04593	0.05144	0.0121
0.03248	0.04871	0.05774	0.064952	0.07939	0.09743	0.11547	0.05052	0.05658	0.0129
0.03608	0.05413	0.06415	0.072169	0.08821	0.10825	0.12830	0.05613	0.06287	0.0139
0.04059	0.06089	0.07217	0.081190	0.09923	0.12178	0.14434	0.06315	0.07072	0.0150
0.04639	0.06959	0.08248	0.092788	0.11341	0.13918	0.16496	0.07217	0.08083	0.0164
0.05413	0.08119	0.09623	0.108253	0.13231	0.16238	0.19245	0.08420	0.09430	0.0182
0.06495	0.09743	0.11547	0.129904	0.15877	0.19486	0.23094	0.10104	0.11316	0.0205
0.07217	0.10825	0.12830	0.144338	0.17641	0.21651	0.25660	0.11226	0.12573	0.0220
0.08119	0.12178	0.14434	0.162380	0.19846	0.24357	0.28868	0.12630	0.14145	0.0238

39C

TABLE III. Fine thread series.

BASIC SIZE			EXTERNAL THREAD - UNJF CLASS 3A								INTERNAL THREAD - UNJF CLASS 3B				
			MAJOR DIAMETER		PITCH DIAMETER		MINOR DIAMETER		ROOT RADIUS		MINOR DIAMETER		PITCH DIAMETER		MAJOR DIA
PRI-MARY	SEC OND-ARY	THDS PER INCH	MIN	MAX	MIN	MAX	MIN	MAX	MIN	MAX	MIN	MAX	MIN	MAX	MIN
1	2	3	4	5	6	7	8	9	10	11	12	13	14	15	16
0.0600		80	0.0568	0.0600	0.0506	0.0519	0.0435	0.0456	0.0019	0.0023	0.0479	0.0511	0.0519	0.0536	0.0600
	0.0730	72	0.0695	0.0730	0.0626	0.0640	0.0547	0.0570	0.0021	0.0025	0.0595	0.0631	0.0640	0.0659	0.0730
0.0860		64	0.0822	0.0860	0.0744	0.0759	0.0658	0.0680	0.0023	0.0028	0.0708	0.0749	0.0759	0.0779	0.0860
	0.0990	56	0.0949	0.0990	0.0858	0.0874	0.0757	0.0784	0.0027	0.0032	0.0816	0.0862	0.0874	0.0895	0.0990
0.1120		48	0.1075	0.1120	0.0967	0.0985	0.0849	0.0880	0.0031	0.0038	0.0917	0.0971	0.0985	0.1008	0.1120
0.1250		44	0.1202	0.1250	0.1083	0.1102	0.0954	0.0987	0.0034	0.0041	0.1029	0.1088	0.1102	0.1126	0.1250
0.1380		40	0.1329	0.1380	0.1198	0.1218	0.1057	0.1092	0.0038	0.0045	0.1137	0.1202	0.1218	0.1243	0.1380
0.1640		36	0.1585	0.1640	0.1439	0.1460	0.1282	0.1320	0.0042	0.0050	0.1370	0.1442	0.1460	0.1487	0.1640
0.1900		32	0.1840	0.1900	0.1674	0.1697	0.1497	0.1539	0.0047	0.0056	0.1596	0.1675	0.1697	0.1726	0.1900
	0.2160	28	0.2095	0.2160	0.1904	0.1928	0.1702	0.1748	0.0054	0.0064	0.1812	0.1896	0.1928	0.1959	0.2160
0.2500		28	0.2435	0.2500	0.2243	0.2268	0.2041	0.2088	0.0054	0.0064	0.2152	0.2229	0.2268	0.2300	0.2500
0.3125		24	0.3053	0.3125	0.2827	0.2854	0.2591	0.2644	0.0063	0.0075	0.2719	0.2799	0.2854	0.2890	0.3125
0.3750		24	0.3678	0.3750	0.3450	0.3479	0.3214	0.3268	0.0063	0.0075	0.3344	0.3418	0.3479	0.3516	0.3750
0.4375		20	0.4294	0.4375	0.4019	0.4050	0.3736	0.3797	0.0075	0.0090	0.3888	0.3970	0.4050	0.4091	0.4375
0.5000		20	0.4919	0.5000	0.4643	0.4675	0.4360	0.4422	0.0075	0.0090	0.4513	0.4591	0.4675	0.4717	0.5000
0.5625		18	0.5538	0.5625	0.5230	0.5264	0.4916	0.4983	0.0083	0.0100	0.5084	0.5166	0.5264	0.5308	0.5625
0.6250		18	0.6163	0.6250	0.5854	0.5889	0.5540	0.5608	0.0083	0.0100	0.5709	0.5788	0.5889	0.5934	0.6250
0.7500		16	0.7406	0.7500	0.7056	0.7094	0.6702	0.6778	0.0094	0.0113	0.6892	0.6977	0.7094	0.7143	0.7500
0.8750		14	0.8647	0.8750	0.8245	0.8286	0.7841	0.7925	0.0107	0.0129	0.8055	0.8152	0.8286	0.8339	0.8750
1.0000		12	0.9886	1.0000	0.9415	0.9459	0.8944	0.9038	0.0125	0.0150	0.9189	0.9298	0.9459	0.9516	1.0000
1.1250		12	1.1136	1.1250	1.0664	1.0709	1.0192	1.0288	0.0125	0.0150	1.0439	1.0559	1.0709	1.0768	1.1250
1.2500		12	1.2386	1.2500	1.1913	1.1959	1.1442	1.1538	0.0125	0.0150	1.1689	1.1789	1.1959	1.2019	1.2500
1.3750		12	1.3636	1.3750	1.3162	1.3209	1.2690	1.2788	0.0125	0.0150	1.2939	1.3039	1.3209	1.3270	1.3750
1.5000		12	1.4886	1.5000	1.4411	1.4459	1.3940	1.4038	0.0125	0.0150	1.4189	1.4289	1.4459	1.4522	1.5000

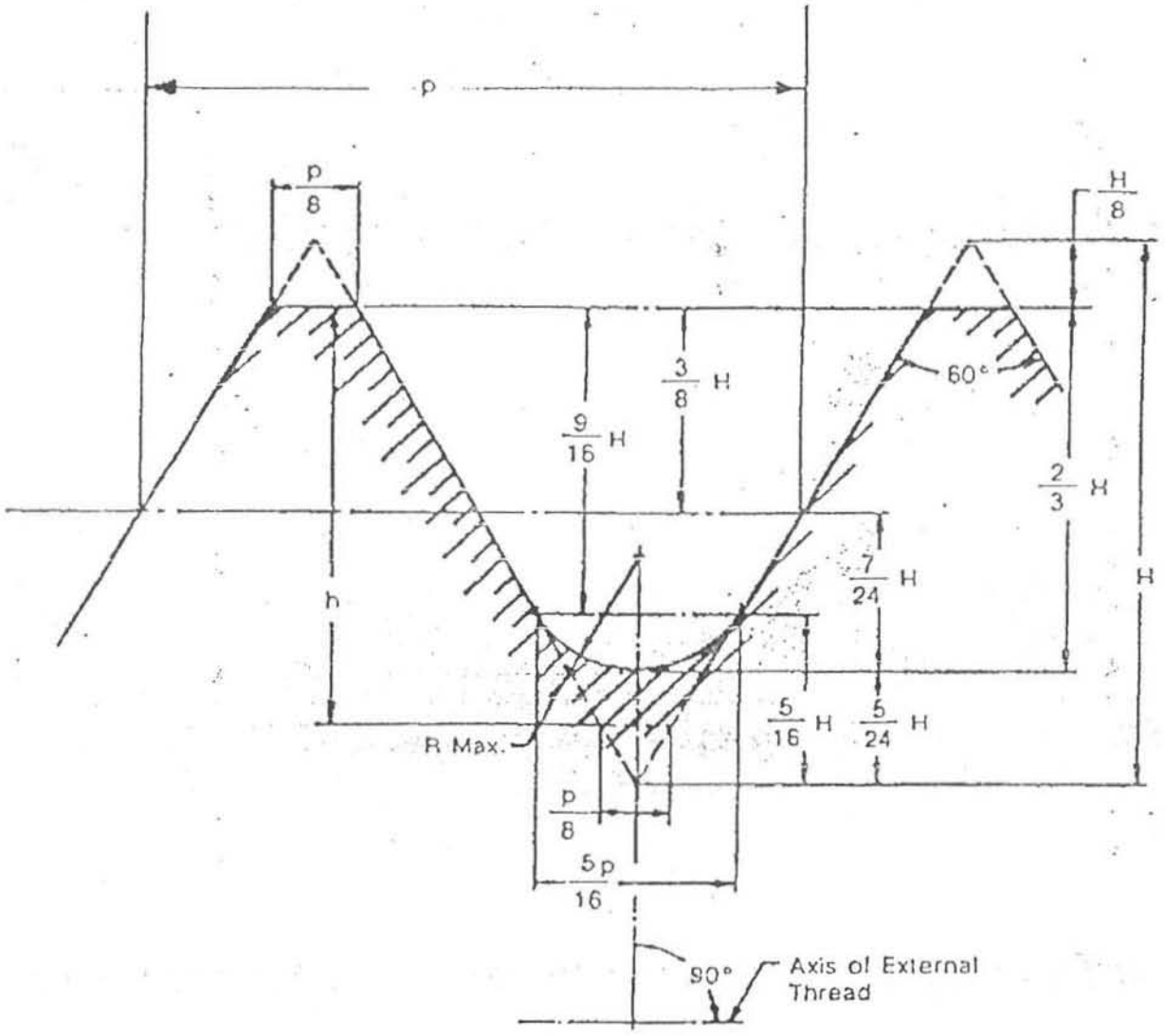

p = Pitch = 1/n
n = number of threads per inch
H = 0.866025p
h = 0.649519p

FIGURE 2. External thread maximum material condition.

is based on the effective datum of the thread

APPENDIX B

Finite Element Method Examples

Example B-1

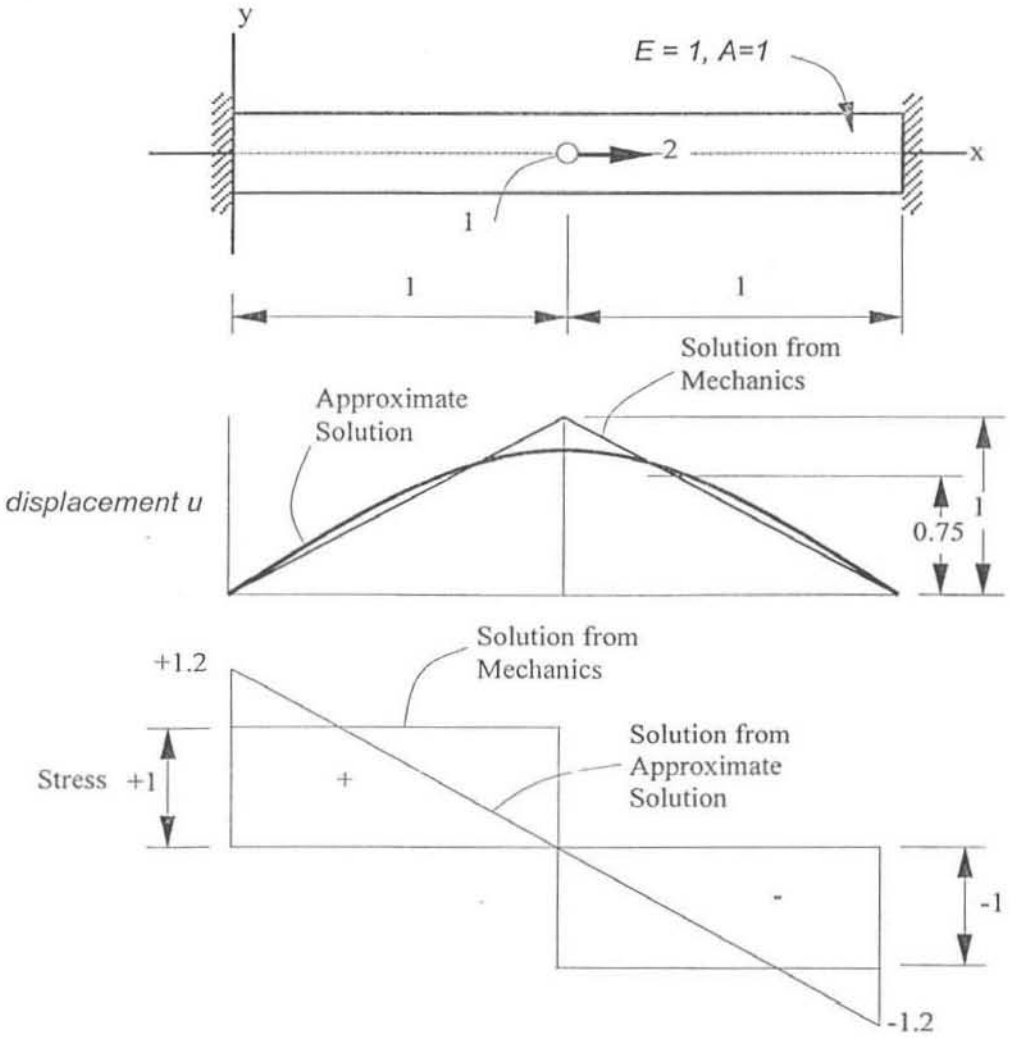

Figure B-1.1 – ***Liner Elastic One-dimensional Rod***

The potential energy of the linear elastic one-dimensional rod (Figure B-1.1), with body force neglected, is:

$$\Pi = \frac{1}{2}\int_0^l EA\left(\frac{du}{dx}\right)^2 dx - 2u_1 \qquad \text{(B-1.1)}$$

where $u_1 = u(x=1)$.

Consider a polynomial function:

$$u = a_1 + a_2 x + a_3 x^2$$

This must satisfy $u = 0$ at $x = 0$ and $x = 2$. Thus,

$$0 = a_1$$

$$0 = a_1 + 2a_2 + 4a_3$$

Hence,

$$a_2 = -2a_3$$

$$u = a_3(-2x + x^2) \qquad u_1 = -a_3$$

Then, $^{du}/_{dx} = 2a_3(-1 + x)$ and

$$\Pi = \frac{1}{2}\int_0^2 4a_3^2(-1+x)^2\,dx - 2(-a_3)$$

$$= 2a_3^2\int_0^2(1-2x+x^2)dx + 2a_3$$

$$= 2a_3^2\left(\frac{2}{3}\right) + 2a_3$$

Setting $\frac{\partial \Pi}{\partial a_3} = 2a_3\left(\frac{2}{3}\right) + 2 = 0$ gives:

$$a_3 = 0.75 \qquad u_1 = -a_3 = 0.75$$

The stress in the bar is given by:

$$\sigma = E\frac{du}{dx} = 1.5(1-x)$$

Note, the finite element method provides a systematic way of constructing the basis functions ϕ_I used in Equation 2.20.

Example B-2

Solving the problem in Example B-1 using Galerkin's approach, we get the equilibrium equation:

$$\frac{d}{dx}EA\frac{du}{dx}=0 \qquad \ldots\ u=0 \text{ at } x=0 \text{ and at } x=2$$

Multiplying the differential equation above by ϕ, and integrating by parts, we get:

$$\int_0^2 -EA\frac{du}{dx}\frac{d\phi}{dx}dx+\left(\phi EA\frac{du}{dx}\right)_0^1+\left(\phi EA\frac{du}{dx}\right)_1^2=0$$

where ϕ is zero at $x = 0$ and $x = 2$. *EA(du/dx)* is the tension in the rod, which takes a jump of magnitude 2 at $x = 1$ (from Figure B-1.1). Thus,

$$\int_0^2 -EA\frac{du}{dx}\frac{d\phi}{dx}dx+2\phi_1=0$$

Using the same polynomial (basis) for u and ϕ, if u_1 and ϕ_1 are the values at $x = 1$, we have:

$$u=(2x-x^2)u_1$$

$$\phi=(2x-x^2)\phi_1$$

Substituting these and E = 1, A = 1 in the above integral yields

$$\phi_1\left[-u_1\int_0^2(2-2x)^2dx+2\right] \qquad =0$$

$$\phi_1\left(-\frac{8}{3}u_1+2\right) \qquad =0$$

This is to be satisfied for every ϕ_1. We get:

$$u_1=0.75$$

APPENDIX C

Summary of Common Types of Elements

Truss Elements

Truss structures such as mechanical linkages, roof frames, and bridges can be modelled with truss elements. In general, a structural member can be modelled with truss elements if it fulfils the following three requirements:

- its length is much grater than its width and depth (the loosely defined term "much greater" can be quantified from 8 to 10 times greater for most applications)
- it is connected with the rest of the structure with hinges that do not allow transfer of moments
- it is loaded with external loads applied only at the joints.

Truss elements can only undertake tension or compression. Thus, the only cross-sectional property that needs to by specified is their axial area. The geometrical profiles of truss elements are identical to beam elements.

Beam Elements

Beam elements are probably the most commonly used elements. Besides their obvious application in frame structures, many other systems such as mechanical linkages, piping systems, conduits, and bridge girders can be modelled with beam elements.

For a structural member to be modelled with beam elements, one of its dimensions must be much greater, as a general rule at least 10 times greater, than the other two. Contrary to truss elements, beam elements can undertake shear and moment in addition to tension and compression.

Common beam profiles include I-sections, T-sections, box, circular, and channel sections. The cross-sectional properties that must be specified for a beam element include the axial area, the shear area, the torsional resistance, the flexural moments of inertia, and the section moduli.

Unless the beam cross-section area is axisymmetric, e.g. a circular or square cross section, the orientation of the beam element with respect to the global system XYZ is critical. Most finite element programs orient a beam element with the aid of an additional node, which together with the two end nodes specify the local co-ordinate system.

It is recommended that the appropriate non-zero value for the shear areas is used in the analysis, since accounting for shear deformations improves the solution accuracy. Usually, non-zero values for shear areas must be assigned if L<10D, where L and D are the longest and shortest dimensions of the beam, respectively.

The torsional constant is equal to the polar moment of inertia only for circular sections. Use of the wrong torsional constant is a common source of error in frame analysis.

Plane Stress Elements

When a structural system is under conditions of plane stress, all stress components normal to the YZ plane vanish:

$$\sigma_{xx} = \tau_{yx} = \tau_{zx} = 0 \qquad (2.34)$$

A representative example of a plane stress problem is a thin plate loaded along its edges with a uniform load in the YZ plane. Due to the small thickness of the plate, the stresses that develop along its thickness are very small compared with the stresses in the YZ plane and they can be ignored in the analysis. Most commonly used plane stress elements are either quadrilateral or triangular. In either case, every node has two transitional degrees-of-freedom.

As a general rule, quadrilateral elements are preferred over triangular elements for reasons of geometric isotropy. However, it is suggested that triangular elements be used to better model irregular boundaries as well as areas around crack tips.

Depending on the approximation of stresses within the element, two different plane stress elements are commonly used: elements with a constant stress variation within the element (CST) also known as compatible, and elements with a linear stress variation (LST) known as incompatible. Incompatible elements are usually effective in modelling regions with significant changes in stress gradient. A more refined mesh is required if compatible elements are used in the analysis. As the best modelling approach that combines the computational efficiency of compatible elements with the computational accuracy of incompatible elements, it has been suggested to use incompatible elements only in those regions of the structure where good solution accuracy is desired, for example, in areas of high variation in stress gradient, e.g., around holes and cracks. In practice, however, incompatible elements are used for the whole model. An effort should also be made to keep the aspect ratio, i.e., the ratio between the element's longest to shortest dimensions, close to one.

In plane stress analysis, one should strive to:

- keep the aspect ratio as close to unity as possible, i.e., strive for either equilateral triangular elements or square elements
- keep internal angles close to 90° in quadrilateral elements.

Plane Strain Elements

A system is considered to be under conditions of plane strain if one of its dimensions is much greater than the other two and is subjected to a load that does not vary along the long dimension. Typical examples are dams, tunnels, retaining walls, but also small scale systems such as rollers and bars compressed by forces normal to their cross section. If the structure fulfils conditions of plane strain, and in addition is restrained to deform along its longest dimension, say the x-axis, then the strain, ε_{xx}, is zero. Note, however, that σ_{xx} is not zero. If the structure is not restrained along the x-axis, then the value of ε_{xx} is a non-zero constant. The latter case is known as generalised plane strain. In either case, however, the stresses can be determined by simply modelling and analysing a typical cross section in the YZ plane that carries the load applied on a unit length along the x-axis.

The most commonly used plane strain elements are either triangular or quadrilateral with two translational degrees-of-freedom per node. They have the same geometry and degrees-of-freedom as plane stress elements, their difference being that plane strain elements have unit thickness, while the thickness of plane stress elements is variable. The remarks made on compatible and incompatible as well as the use of a proper aspect ration for plane stress elements are also valid for plane strain elements.

Plate and Shell Elements

Use of plate and shell structures is extensive. It includes architectural structures, containers, aeroplanes, ships, missiles, and machine parts. Plates are plane, flat surface structures with thickness that is very small compared to their other dimensions.

The load-carrying behaviour of plates resembles that of beams. In fact, plate behaviour can be approximated by a grid-work or beams running in two perpendicular directions on the same plane. The two-dimensional load-carrying action of plates results in light and economical structures. In finite element modelling of a plate, the mid-surface, which is a plane parallel to the two plate surfaces that divides the thickness into equal halves, is modelled.

Modelling of plate structures is usually done with either triangular or quadrilateral plate elements. Each nodal point of either elements type possesses five degrees-of-freedom in the element or local system xyz: three displacements along the x, y, and z-axes and two rotations about the x and y-axes. No rotational degree-of-freedom is specified about the direction z normal to the plate element. Nevertheless, a very small value of the rotational stiffness is assigned about the local z-axis to eliminate numerical instability. It should be noted that plate and shell elements used in finite element programs combine bending and membrane actions.

Quadrilateral elements exhibit higher accuracy than triangular elements, and thus they should be preferred. Use of triangular elements should be limited to the part of the structure that is close to irregular boundaries.

Thin shells can be "viewed" as plates with a curved surface. Shell elements are generally understood as flat plate elements used to model curved surfaces. In fact, most commercial finite element programs rely on plate elements to model shells and curved surface structures. As for thin plates, the mid-surfaces of thin shell structures are modelled with plate elements.

The following two points are important when modelling thin shells with plate elements:

- for good accuracy, it is recommended that the plate elements should be approximating the shell surface at angles between 4° and 10°.
- the lack of a rotational degree-of-freedom about the local z-axis may cause numerical instability. Such cases could appear when plate elements intersect at an angle less than 4°. The numerical instability might not allow processing of the model and could be reported by the processor as an "error message." A remedy of this problem is to use rotational elastic elements with very small stiffness about the axes parallel to the common sides of the elements.

Brick Elements

Thick plates, thick cylindrical or spherical components, thick joints, and gear housing are a few examples where solid elements can be used to perform a finite elements

analysis. In general, structures or structural components with a thickness comparable to the other two dimensions can be modelled with brick elements.

Solid elements are three-dimensional elements with three translational degrees-of-freedom per node. They can be viewed as membrane elements that an also account for variation of stresses along the thickness. Nodes are usually introduced at either the intersections of three planes or the mid-sides of the intersection of two planes.

The advantage of using solid or brick elements instead of plate or beam elements to model components with large thickness is that solid elements can provide information about the three-dimensional variation of stresses and deformations within the component. Plate and beam elements cannot provide such information and should be used with caution only for a preliminary analysis of systems having comparable sizes in all three dimensions.

When solid elements are interconnected with beam or plate and shell elements, attention should be paid to preserve the rotational degrees-of-freedom at the common nodes. This can be achieved easily by artificially extending the beam and plate elements into the solid elements.

Tetrahedral and Hexahedral Elements

Instead of brick elements, tetrahedral and hexahedral elements can be used to model three-dimensional structures. The tetrahedron can be viewed as an extension of the triangle to a point in the third dimension, while the hexahedron can be considered as the counterpart of the planar quadrilateral extended in the third dimension. It should

be noted that the hexahedral element has the same geometric shape as the eight-node brick element. They differ, however, in their theoretical formulation and computational accuracy. Commonly used tetrahedral and hexahedral elements have only three translational degrees-of-freedom per node. The accuracy of tetrahedral and hexahedral elements is increased by introducing additional nodes at mid-sides.

Automatic mesh generation techniques favour tetrahedral and hexahedral elements over brick elements to create detailed models of three-dimensional systems with complex geometries. In practical applications, use of tetrahedral elements requires some caution to develop models without leaving any "holes" in them. In general, hexahedral elements are more accurate than tetrahedral elements and should be preferred. Nevertheless, tetrahedral elements are more versatile since they allow modelling of intricate geometries and facilitate transition form coarsely meshed regions to finely meshed regions in a model. In most cases, combination of tetrahedral and hexahedral provides the optimum mesh.

Boundary Elements

Boundary elements are used to model boundary conditions and links between structural components. As such, they can be useful in either evaluating reactions at rigid, flexible supports, and elastic links or specifying non-zero displacements and rotations to nodes. Boundary elements are two-node elements. The line defined by the two nodes indicates the direction along or about which the reaction (force or moment) is evaluated or the displacement (translation or rotation) is specified.

Boundary elements that are used to obtain reaction forces (rigid or boundary elements) or specify translational displacements (displacement boundary elements) can be considered as truss elements with only one non-zero translational stiffness. When they are employed to either evaluate reaction moments or specify rotations, they resemble beam elements with only one non-zero stiffness, that is, the rotational stiffness about the user specified axis.

Elastic boundary elements are used to model flexible supports and to calculate reactions at skewed boundaries. The stiffness of elastic boundary elements is defined by the user. Caution is needed when one wants to model skewed supports. In this case, the user should employ either translational or rotational elastic boundary elements and assign moderately high stiffness values to the elastic boundary elements.

References

1. Bickford, J.H., *An Introduction to the Design and Behaviour of Bolted Joints*, Marcel Dekker, 1990

2. Fastener preload indicator, Contract no. F33615-76-C-5151, Report prepared for Air Force Materials Laboratory, Air Force Systems Command, Wright-Patterson Air Force Base, Ohio, by General Dynamics - Ft. Worth, June 15, 1978.

3. Fisher, John W., and J. H. A. Struik, *Guide to Design Criteria for Bolted and Riveted Joints*, Wiley, New York, 1974.

4. *Unified Inch Screw Threads,* ANSI Standard B1.1-1974, ASME, New York, 1974

5. Motosh, N., *Development of design charts for bolts preloaded up to the plastic range*, J. Eng. Ind., August 1976.

6. Shigley, J.E., *Mechanical Engineering Design*, 3rd ed., McGraw-Hill, New York, 1977.

7. Meyer, G., and D. Strelow, *Simple diagrams aid in analyzing forces n bolted joints,* Assembly Eng., January 1972.

8. Junker, G.H., *Principle of the calculation of high duty bolted joints*; interpretation of directive VDI 2230, Unbrako technical thesis, published by SPS, Jenkintown, PA.

9. Fazekas, G.A., *On optimal bolt preload*, Trans. ASME, J. Eng., August 1976.

10. *High strength bolted joints,* SPS Fastener Fats, Standard Presses Steel Co., Jenkintown, PA.

11. Transactions of the ASME, *Journal of Pressure Vessel Technoloogy*, Volume 122, Number 2, May 2000.

12. Robert Finkelston, SPS Laboratories, Jenkintown, PA.

13. Bickford, JH., Fatigue failure of threaded fasteners, J. Japan Res. Institute for Screw Threads and Fasteners, Vol. 14, No. 10, 1983.

14. Considerations for the design of bolted joints, Industrial Fastener Institute, Cleveland, OH, undated.

15. Spyrakos C. C., *Finite Element Modelling in Engineering Practice*, West Virginia University Press, Morgantown, WA, 1994.

16. Kwon, Y. W. and Bang, H., *The Finite Element Method Using MATLAB*, CRC Press LLC, Florida, 1997.

17. Chandrupatla, T. R and Belegundu, A. D., *Introduction to Finite Elements in Engineering*, Prentice Hall, New Jersey, 1991.

18. Segerlind, L. J., *Applied Finite Element Analysis*, 2nd edition, Wiley, New York, 1984.

19. Yang, T. Y., *Finite Element Structural Analysis*, Prentice Hall, New Jersey, 1986.

20. Spyrakos C. C., *Linear and Nonlinear Finite Element Analysis in Engineering Practice*, Algor Inc., Pittsburgh, PA, 1997.

21. Juvinall, C. R. and Marshek K. M., *Fundamentals of Machine Component Design*, 2nd edition, John Wiley and Sons, 1991.

22. Gere, J. M. and Timoshenko, S. P., *Mechanics of Materials*, 3rd edition, PWS, Boston, 1990.